"Marginal Detonation of Gases and the Effects of Additives"

A Thesis

submitted for the degree of

Doctor of Philosophy

in the

Faculty of Engineering

of the

University of London

by

Ian Frederick Wood.

Department of Chemical Engineering
and Chemical Technology,

Imperial College of Science and Technology,

London, S.W.7.

September, 1967.

ABSTRACT.

In order to investigate the factors contributing to detonation failure, the velocity-composition relationships of the following gaseous mixtures near the limiting concentrations were investigated in a one inch diameter cylindrical tube:

System $S_H = 2H_2 + O_2$ separately diluted with H_2, O_2, He, A, CO_2 and NH_3;

System $S_D = 2D_2 + O_2$ diluted with D_2, O_2, He and A; and

System $S_C = C_2N_2 + O_2$ diluted with C_2N_2, O_2, He and A.

In all cases, detonations were initiated by passing a detonation in a stoichiometric (2:1) hydrogen-oxygen mixture into the test mixture. Velocities were determined by measuring the time taken for the detonation front to pass between successive detection stations, a known distance apart.

For these mixtures the limiting concentrations, given as a percentage of diluent added, were found to be:

$S_H + H_2$, 78.73%; $S_H + O_2$, 76.74%; S_H + He, 89.1%; S_H + A, 91.91%; $S_H + CO_2$, 40.00%; $S_H + NH_3$, 41.1%;

$S_D + D_2$, 72.1%; $S_D + O_2$, 74.48%; S_D + He, 88.76%; S_D + A, 91.50%;

$S_C + C_2N_2$, 51.9%; $S_C + O_2$, 72.0%; S_C + He, 82.20%; S_C + A, 90.4%.

In addition, several hitherto unobserved phenomena were noted:

(i) Mixtures diluted with argon showed considerably wider detonation limits than when diluted with helium despite the fact that they should be hydrodynamically similar. In the same way, mixtures containing hydrogen showed wider detonation limits than corresponding mixtures containing deuterium. These mass effects could only be partly explained by existing theories for detonation failure. Other explanations are examined.

(ii) Reproducible fluctuations in the detonation velocity-composition relationships were found near the limiting concentrations. These were found to be substantially due to a spin head following the same path down the detonation tube on successive occasions, thereby causing a displacement in the measured time intervals.

(iii) In some mixtures containing hydrogen or deuterium, a second, lower velocity regime was found to co-exist with the "normal" detonation velocity regime which alone prevailed throughout the entire composition range. The measured velocities in the lower velocity regime were generally about 30% lower than in the "normal" regime. There were strong indications that this was due to the formation of hydrogen (deuterium) peroxide in the detonation front.

Possible explanations for, and implications of, these novel phenomena are discussed.

ACKNOWLEDGEMENTS.

I wish to convey my sincere thanks to the following people for their invaluable assistance in the preparation of this thesis:

My supervisors, Professor A.R.Ubbelohde and Dr.G.Munday, for their constructive advice and criticism, and help in the design of additional experiments;

Messrs A.Alger and J.Oakley (workshops), L.Tyley (electronics), A.Jones (glass-blowing), L.Cripps (stores) and the personnel of their respective departments for their help in fabricating the experimental apparatus;

Professors A.Gaydon and F.Weinberg and Dr.J.Lawton for their helpful suggestions during the progress of these researches;

The National Coal Board for making a stipend available to the author; and

My wife for lending a sympathetic, if not scientific, ear whenever the need arose.

TABLE OF CONTENTS.

TABLE OF FIGURES.

CHAPTER 1.

INTRODUCTION.

1.1. Introductory remarks:

Gaseous detonation can be regarded as a planar shock wave propagating through a combustible gas, closely followed by a region of intense chemical reaction. These two zones are interdependent inasmuch as the shock starts chemical reaction which, in turn, supplies the energy needed to sustain the shock. When a steady state has been reached the velocity of propagation of the detonation wave is constant, and can be accurately predicted by consideration of the conservation relationships across the detonation front (Lewis and von Elbe, 1961; p.517).

However, recent work has shown that detonation can only occur within certain limiting fuel concentrations; these being referred to as the "detonation limits". These limits are known to differ for various initial conditions. A quantitative description of the factors leading to the occurrence of limits is not yet available, although several possible mechanisms have been proposed.

At the limits, the energy liberated by the chemical reaction might be insufficient to sustain the shock, especially if heat losses to the containing walls are

considered. Also, the higher proportion of non-reacting molecules would lead to a lower reaction temperature, which could appreciably lengthen the reaction time, thereby affording more time for energy to be lost to the surroundings. It would appear, then, that a detailed knowledge of the chemical kinetics of the reacting species would be an essential part of any attempt to predict detonation limits.

It has been observed that, as the limits are approached, the detonation loses its one-dimensional character, and becomes unstable. This instability can take several forms; in most cases, the detonation front displaying either a helical or a pulsating mode of propagation. It appears likely that the processes resulting in this instability are closely related to those leading to the occurrence of limits. Therefore, significant information about the nature of these processes may be ascertained by the study of the instability phenomenon.

Before any quantitative description of the factors governing detonation failure can be attempted, it is helpful to review the work that has already been done in the field of steady state detonation.

1.2. Historical background of detonation:

Both Mallard and Le Chatelier (1881) and Berthelot and Vieille (1881), whilst observing the propagation of flames in tubes, found that under certain conditions the velocity of propagation increases very rapidly, and then stays constant (1.5 - 3 Km/sec.). This phenomenon is referred to as detonation. Berthelot and Vieille found that the velocity is a function of the composition of the mixture, but is independent of the method of ignition and the tube diameter, provided a limiting diameter is exceeded. Dixon (1893, 1896, 1903) studied the properties of the phenomenon in detail.

1.2.1. Classical theory of detonation:

Michelson (1893) and later Chapman (1899) and Jouguet (1899) developed a theory for the phenomenon based on the hydrodynamic theory of shocks previously developed by Rankine (1870) and Hugoniot (1887, 1889). At that time, work in Russia was virtually unknown to the western world, and this theory is usually referred to as the Chapman - Jouguet (C-J) theory. It considers a detonation wave to be a shock wave sustained by the energy of chemical reaction of the gas.

For each detonation velocity compatible with both the equation of state of the detonation products and the

conservation relationships across the discontinuity, there exist two possible states in which the burnt gas can occur; one with a higher pressure and density than the other. The C-J theory postulates that the propagation velocity for a stable detonation is the minimum value possible, this value occurring where the two states coincide. It follows that the detonation velocity is equal to the sum of the particle velocity of the products and the speed of sound in the burnt gas. Details of the theory are given by Lewis and von Elbe (1961).

It was, perhaps, unfortunate that a theory that predicts detonation velocities with such accuracy (Lewis and Friauf, 1930; Berets et al. 1950 a) should have been formulated at such an early stage, as very little constructive work was done to improve the theory for nearly 50 years. During this period, though, several justifications for the C-J theory were offered.

Jouguet (1905, 1906, 1917) pointed out that a rarefaction wave with a velocity equal to the predicted detonation velocity would overtake the front and slow it down if the pressure of the burnt gas were for any reason to rise above the C-J pressure. This rarefaction wave must occur as there is no piston to contain the explosion. Becker (1922) showed that the entropy of the burnt gas for

pressures greater than the C-J value is greater than that for lower pressures, so detonation is thermodynamically more probable for pressures greater than or equal to the C-J value. Scorah (1935) investigated the Gibb's free energy function along the Rankine - Hugoniot curve, and found that the C-J point corresponds to the maximum degradation of free energy, and therefore maximum stability. These considerations lead to the conclusion that, if a stable detonation occurs, it will occur such that the condition of the burnt gases corresponds to the C-J state. A critical review of the C-J theory is given by Paterson (1958).

It must be noted that this theory assumes that the detonation front is similar to a shock front in that all reaction is completed instantaneously. This is not the case. A finite time is required for the reaction to go to completion, and therefore a reaction zone of finite width with corresponding temperature and pressure gradients will exist in the front.

Zeldovich (1940), von Neumann (1942) and Doering (1943) independently considered the detonation front to consist of a shock followed by a finite reaction zone, the reaction being initiated by the high temperature and pressure generated by the shock. The energy required to sustain the shock is transferred from the reaction zone to

the shock front by a compression wave. A family of Rankine- Hugoniot (R-H) curves can then be drawn for planes with different degrees of completion of reaction, the C-J plane being that at which the reaction is complete.

This theory treats detonation as being a one-dimensional steady state process. For simplicity, the detonation front is regarded as being stationary, the unburnt gas entering the front at the detonation velocity, u_1, and the burnt gas leaving at a velocity u_2. The conservation relationships for unit mass of gas passing through unit area of the detonation front can then be written:

$$\frac{u_1}{V_1} = \frac{u_2}{V_2} \qquad (1)$$

$$P_1 + \frac{u_1^2}{V_1} = P_2 + \frac{u_2^2}{V_2} \qquad (2)$$

$$H_1 + \frac{u_1^2}{2} = H_2 + \frac{u_2^2}{2} - \theta Q \qquad (3)$$

The subscript 1 refers to the initial state of the gas, and 2 refers to the state of the gas after the reaction has proceeded to the degree θ. Definitions of the symbols used are given in section 7, page 129.

The enthalpy terms in equation (3) can be related to the temperature by

$$H_2 - H_1 = \bar{C}_p (T_2 - T_1) \qquad (4)$$

Substitution of equations (1), (2) and (4), together with the equations of state,

$$P_1 V_1 = RT_1/M_1 \qquad (5)$$

into equation (3) gives

$$c(pvm - 1) = (v + 1)(p - 1) + \varsigma q \qquad (6)$$

where

$$c = 2\bar{C}_p M_1/R; \quad q = 2QM_1/RT_1; \quad p = P_2/P_1;$$
$$v = V_2/V_1; \quad \text{and} \quad m = M_2/M_1 .$$

This is the equation for the Rankine-Hugoniot (R-H) curve for any particular value of ς. A family of such curves is shown in figure 1.1.* Each curve represents a plane in the reaction zone, the curve $\varsigma = 1$ referring to the plane at which thermodynamic equilibrium has been reached.

u_2 can be eliminated from equations (1) and (2) giving

$$u_1^2 = \frac{v_1^2 (P_2 - P_1)}{V_1 - V_2}$$

or

$$\frac{p - 1}{1 - v} = \frac{u_1^2}{P_1 V_1} = \gamma M^2 \qquad (7)$$

* All figures are given in section 9, pp 140 - 182.

which is a straight line on the p-v plane, passing through the point corresponding to the initial conditions of the gas. This is called the Rayleigh line, and any point on this line satisfies the mass and momentum relationships. Therefore, the point of intersection of this line with an R-H curve will satisfy all three conservation equations for that value of ϵ. Unfortunately, there are an infinite number of such intersections, so an additional relationship must be found. For this purpose, let us consider the nature of the p-v diagram.

From equation (7) it can be seen that the slope of the Rayleigh line varies as $-u_1^2$. As u_1^2 must always be positive, the slope must always be negative. There are two possible solutions :

$$p > 1; \quad v < 1;$$

and $$p < 1, \quad v > 1.$$

The latter, because of the decrease in pressure over the reaction zone, corresponds to the propagation of a plane combustion wave. Therefore, only the former applies to detonation.

For this case, in the classical treatment, there are two points of intersection of the curve $\epsilon = 1$ by each Rayleigh line. The Chapman-Jouguet hypothesis is that the detonation velocity is the minimum value possible. As this occurs when the slope of the Rayleigh line is a minimum,

it follows that the condition of the burnt gas at the instant of complete chemical reaction is given by the point of tangency of the Rayleigh line to the R-H curve for $\theta = 1$. This is known as the C-J plane.

It is not possible to determine the point of tangency of the Rayleigh line to the R-H curve analytically as all of the parameters vary along the R-H curve. As there is some uncertainty as to which velocity of sound should be used in the calculations (see section 1.2.2), it is necessary to construct the R-H curve for thermodynamic equilibrium ($\theta = 1$) and to find the minimum detonation velocity by trial and error.

A necessary part of this construction is the calculation of the equilibrium composition at the C-J plane. This is both pressure and temperature dependent and therefore must enter into the trial and error calculation. The appropriate values of c and q can then be found from enthalpy and heat of formation data respectively. A sample calculation is given in Appendix A.5.1, page 203.

On testing this theory experimentally, it has been found (Berets, Greene and Kistiakowsky, 1950 a) that, in the majority of cases, the experimental detonation velocities are lower than those calculated, the discrepancy being more pronounced in the fuel-rich and fuel-lean

regions. Several minor improvements have been made to the theory to give better agreement with the experimentally determined velocities.

1.2.2. Modifications to the classical theory:

Kirkwood and Wood (1954) considered the case where some of the reactions involved have slow reaction rates, and which reach equilibrium some distance behind the C-J plane. This occurs, for example, during detonations in cyanogen-oxygen mixtures (Dixon, 1893, 1903) and where condensation of detonation products occurs.

Zeldovich (1940) considered the lower experimental velocities to be due to energy losses at the walls of the containing tube. He proposed that the C-J condition should be modified so that the flow of the burnt gas becomes sonic when the rate of chemical reaction balances the frictional forces and heat losses to the walls. His results were substantiated by the work of Kistiakowsky et al (1952 a, b and c; 1955), Manson and Guenoche (1954), Manson (1955, 1957) and Cook, Pack and Gey (1959). The additional effects of viscosity, diffusion and chemical kinetics have also been considered (Hirschfelder and Curtiss, 1958; Hirschfelder, Curtiss and Barnett, 1959).

Shchelkin (1940, 1945, 1947) inserted a helical wire into a tube and found that this could decrease the

detonation velocity by up to 50%. He therefore suggested that the roughness of the walls can play a significant role in the determination of detonation velocities.

The speed of sound at the C-J plane used by the Zeldovich - von Neumann - Doering model is the equilibrium value, that is the speed of sound in the products once they have reached thermodynamic equilibrium. However, Brinkley and Richardson (1953) and Kirkwood and Wood (1954) suggested that the pressure in the detonation wave is a function of composition as well as hydrodynamic factors and consequently, for velocity calculations, the speed of sound should be calculated for no local change in chemical composition at the C-J plane, that is the "frozen" speed of sound. Further study of the problem (Duff and Knight, 1958; Duff, Knight and Rink, 1958; Duff, 1958; Fay and Opel, 1958; Wood and Parker, 1958; Fay, 1959; Wood and Salsburg, 1960) has failed to ascertain conclusively which value should be used.

Even with the introduction of these additional factors, the hydrodynamic theory only applies to steady state detonation propagation. It cannot account for the failure of detonations outside certain limiting compositions, as has been observed experimentally. Other factors must therefore be introduced to explain this non-steady state phenomenon.

1.2.3. Detonation limits:

Wendlandt (1925) noted that, for a given experimental arrangement, it was impossible to propagate a stable detonation outside a certain composition range. The upper and lower compositions of this range are called the limits of detonability, or the detonation limits. Near the detonation limits the velocity deviates only slightly from the calculated value, but decreases almost instantaneously at the limiting composition (Berets et al, 1950 a; Zeldovich, 1949). Schuller (1954) has found that, if a gaseous mixture outside the limiting compositions is initiated by another detonation, a process similar to detonation can occur, but it is unstable. For short distances after initiation, these "false" detonations can propagate with velocities which coincide with an extrapolation of the "true" detonation velocities. It follows that, in order to determine the detonation limits accurately, a tube of sufficient length must be used.

The reasons for this failure to propagate are still not fully understood, but several proposals have been made. They all regard the limits as resulting directly or indirectly from a decrease in chemical reaction rates or, more specifically, from a lengthening of the induction period before the onset of rapid chemical reaction. These

theories fall into three main groups:

(i) As the extreme fuel-rich and fuel-lean regions are approached, the reaction rates in the detonation wave may become so slow that the reaction zone moves into the rarefaction wave with a consequent decrease in the energy transmitted to the shock front (Brinkley and Richardson, 1953). This would result in a decrease in temperature and pressure in the shock front which, in turn, would result in a further decrease in reaction rates.

Another factor which could decrease the energy transmitted to the shock front is frictional drag at the walls (Manson, 1955, 1957). This could lead to a lengthening of the induction zone as above. The wall area over which energy could be lost would therefore be increased, resulting in a further loss of energy, and so on. The limiting composition is defined as the composition at which the energy losses to the walls are sufficient to cause a decrease in the reaction rates. This argument leads one to expect that a larger tube diameter would allow wider detonation limits, as has been shown to be the case over a rather limited range of diameters by Kogarko and Zeldovich (1948) and Pusch and Wagner (1965).

(ii) It is known that small perturbations can occur in the reaction zone of a steady state detonation, their width being

in the order of the induction zone width (Shchelkin and Troshin, 1965). As the induction zone increases in length the size of the perturbations increases until, when the perturbation width exceeds the tube diameter, the detonation front as a whole becomes unstable and fails (Shchelkin and Troshin, 1965)

A similar treatment has been developed which considers the acoustic properties of the reactant gases (Strehlow and Fernandes, 1965; Barthel and Strehlow, 1966), but which only applies to rectangular tubes. Each mixture composition has characteristic acoustic properties, and the dimensions of the tube determine the number of pressure heads caused by hydrodynamic vibration in the detonation front. As the limits are approached, the number of heads decreases until, at the limit, only one can exist. Beyond the limit resonance cannot occur and the detonation front becomes unstable.

(iii) An accepted condition for detonation to occur is that the rate of formation of chain carriers exceeds their rate of removal (Belles, 1959). During steady state detonation the chain carriers are removed by third body recombination reactions, the rates of which are governed by the efficiencies of the gaseous components as third

bodies. If an increase in dilution results in an increase in third body efficiencies, the rates of removal of chain carriers with respect to their rates of formation increase until, at the limit, the rates are equal (Belles, 1959). However, recent experimental kinetic data (Skinner and Ringrose, 1965) casts doubt on the quantitative treatment used by Belles.

Owing to lack of reliable kinetic data for chemical reactions in detonations, none of the above theories has yet been quantitatively substantiated.

Because of the great number of factors which could influence detonation limits - reaction rates, gas composition, initial temperature and pressure, hydrodynamic properties, tube diameter, etc. - a complete account of the phenomenon should be rather complex. Some light has been thrown on the subject by the study of the detonation front near the limits, especially of the so-called "spinning" and "pulsating" detonations, first observed in 1926.

1.2.4. Detonation instability:

Campbell and Woodhead (1926, 1927) noticed that wave speed photographs of detonations, under certain conditions near the limits, show that the velocity of propagation displays an oscillatory nature. Campbell and

Finch (1928) proposed that, in these circumstances, the luminous head of the detonation progresses along a helical path followed by a luminous tail, which is the path of the heated particles streaming through the head. They referred to this phenomenon as spin. In order to account for the striations in the wake of the detonation, it was necessary to assume that the burnt gas as a whole rotates inside the tube. Bone and Fraser (1932) carried out similar experiments, but with a longitudinal fin projecting from the tube wall. They found that the fin did not alter the results, and concluded that the gas does not rotate. However, they did find (Bone et al, 1936) that the head of the spinning detonation followed the same path on successive detonations with the same gas composition. Campbell and Finch (1928) did not find this, observing both clockwise and anti-clockwise rotation of the spin head. They did not state, however, whether the spin head followed the same path for each direction of rotation.

Becker (1936) and Jost (1946) gave slightly differing interpretations of what is essentially a one-dimensional process. Both visualised the detonation as a cyclic process in which the combustion zone falls behind the shock wave, but which subsequently overtakes the slowed shock, or generates a new combustion zone behind the shock

by means of compression waves. This would account for the oscillatory nature of the velocity, but not for the helical propagation of the detonation front, or the dependence of the spin pitch on the tube diameter found by Campbell and Woodhead (1926, 1927).

Martin and White (1959) and White (1961) studied density variations in the front of a spinning detonation, and found that the shock is not planar, and that density gradients exist normal to the tube axis. Therefore spin must be regarded as a three-dimensional process.

Bone et al (1936) observed that, on a wave speed photograph of a spinning detonation, two systems of luminous paths are evident, in addition to the nearly horizontal striations normally present. One runs forward in the direction of propagation, and appears to be the path of the hot products. The other runs backward, and is considered to be the retonation wave observable during the initiation of detonation. They stated that two pairs of these traces originate with each spin, and the intersection of these form the horizontal striations. However, this interpretation of the spin photograph does not account for the persistence of the striations after the detonation has passed the open end of the tube, or for the type of striation found in a conical tube by Campbell and Finch.

Several mathematical models have been developed to try to describe spin propagation. Manson (1947) and Fay (1952) considered natural vibrations in the column of gas, in particular the transverse vibrations. They stated that the revolving luminous field is due to the revolving pressure peak of the vibrating system. The pitch to tube diameter ratio calculated from this model agrees well with experimental values. This theory was further developed by Barthel and Strehlow (1966).

For cylindrical tubes, Denisov and Troshin (1959, 1960, 1962) and Duff (1961) studied the path of the detonation front past a smoked film attached to the tube wall. They found that the detonation head can etch two distinct types of pattern in the soot layer, one being a single helix and the other two or more counter-rotating helices forming a series of diamonds. The former is due to a single spin head, and occurs during "true" spinning detonation. It is noteworthy that the existence of two or more non-interacting helices has never been observed. The latter corresponds to a multiple head structure, where there is always a periodic motion of the disturbances towards each other. This is not a spinning detonation, and is referred to by Denisov and Troshin (1962) as a "pulsating" detonation.

In order to understand the processes leading to the occurrence of these helices and the structure of the spin head, a knowledge of the development of the spin head would be useful. In fact, during the past eight years there has been a great deal of research in this field.

1.2.4.1. Perturbation theory of spin development:

Photographs (Voitsekhovskii et al, 1958 b) show distinctly that small disturbances can occur in the reaction zone of a steady state detonation resulting, for example, from slight inhomogeneities in the composition of the fuel mixture. The disturbance becomes larger as the limit is approached and as the pressure is reduced. Conditions for which these perturbations enlarge and distort the shock front have been considered (Shchelkin and Troshin, 1965).

The exponential dependence of the reaction time on the temperature leads to the assumption that the reaction proceeds instantaneously to completion some distance behind the shock. Figure 1.2 shows the structure of the initially disturbed detonation front.

In the direction of wave motion the state and velocity of the gas do not change, but remain as they were before the appearance of the perturbations. However, unstable pressure gradients result in a direction perpendicular to the wave motion, therefore allowing the shocked gas to expand in

this direction. This means that the combustion products behind L will be compressed, and forward moving compression waves will result in a decrease in reaction time ahead of L. Conversely, the sideways expansion ahead of K will result in a drop in pressure, and a consequent increase in reaction time. The perturbations will therefore grow larger.

As soon as the expansion of the gases begins, the C-J condition ceases to hold at the points K and L, and compression and expansion waves will move ahead of the reaction zone and cause deformation of the shock front. Thus the instability of the reaction zone leads simultaneously to the instability of the whole detonation front.

For geometric reasons, the compression waves which amplify the forward moving perturbations reach the shock front before the rarefaction wave leaving the trailing edges. They also suffer less from sideways expansion than the rarefaction waves. Therefore, only their effect on the shock front will be considered.

It should be noted, however, that for this instability to occur the initial perturbations must be sufficiently large to allow the sideways gas movement to affect the reaction time before the instabilities leave the reaction zone. This means that their size would have to be in the order of, or greater than, the induction zone width. An approximate mathematical model shows this to be the case for most detonable gas mixtures.

Every perturbation which overtakes the shock front leads to a break in its leading edge. These breaks, having no preferred direction of motion, propagate in random directions over the surface of the shock front igniting gas as they go, especially at their points of collision. The number of such breaks would be reduced by decreasing the tube diameter, or by increasing the induction time - for example, by approaching the detonation limits.

Erpenbeck (1963) pointed out that this instability argument, when assuming non-reactive flow through the induction zone, is not strictly accurate. Also, because of the high sensitivity of the reaction rate to temperature changes, a more complicated mode of propagation is indicated. However, for the purpose of understanding the possible factors leading to instability near the limits, the theory is adequate, and has been used to formulate models for the structure of the detonation front during spin.

1.2.4.2. Structure of detonation during spin:

Although the existence of spin has been known for a long time, early investigators were only concerned with characterising and interpreting the specific nature of the process behind the wave. Now, after identification of single and multiple headed spin, more attention has been paid to the structure of the wave front.

The Shchelkin theory (section 1.2.4.1) describes the propagation of small oblique portions of the wave travelling in different directions relative to the main direction of propagation of the front. The intersection of one of these oblique portions with the wave travelling normal to the direction of propagation is qualitatively similar to the intersection of two shock waves. The latter is precisely an irregular triple (Mach) configuration as arises during supersonic flow about two plane wedges (see Courant and Friedrichs, 1948). In order to fulfil the conservation laws near the point of intersection, another shock wave (reflected shock) and a tangential discontinuity (slipstream) must pass through the point of intersection, as shown in figure 1.3. The wave which corresponds to the oblique portion of the perturbation is called the Mach stem, and that corresponding to the normal detonation front, the incident shock. The point of intersection is called the triple point.

Because of the chemical reaction accompanying the intersection of two detonation waves, the configuration is more complicated than that for the intersection of non-reactive shocks. Even in the special and widely investigated case of single headed spin in circular tubes, there is disagreement about the exact structure. Denisov and Troshin (1962) considered the wave front to consist of two closely coupled Mach interactions, the one Mach stem being common to both. The incident shock of one propagates approximately parallel

to the tube axis whilst the other propagates approximately normal to the axis (figure 1.4) thereby leading to the helical propagation of the spin head.

However, Duff (1961), after studying the head-on collision of a spinning detonation with a weak non-reactive shock, concluded that only one Mach configuration was present. This model was further improved by Schott (1965) who used the same experimental method in conjunction with heat detecting probes. He proposed a model based on that of Voitsekhovskii et al. (1962), and which is shown in figure 1.5.

A and B are Mach triple points with Mach stems AS and BC respectively, and CG is the reflected shock wave which acts as the coupling between the detonation front and the acoustic vibrations which stabilise spin (Strehlow and Fernandes, 1965). The second incident shock, BD, because of its short length, is not fully understood. CF and AE are slipstreams.

Multiple headed spin is regarded by both Duff and Schott as being the superposition of two or more of these configurations rotating in opposite directions. But because of the complex nature of the multiple spin head, this proposal cannot be fully substantiated.

1.2.4.3. Velocity fluctuations:

Another phenomenon which has been observed near the detonation limits is the occurrence of small fluctuations or "bumps" on the velocity-composition curves (Schuller, 1954).

These have been accounted for in several ways.

Schuller attributed the small fluctuations to the propagation of "false" detonations which are unstable, but fade slowly. These could be misinterpreted as being steady state detonations unless the velocity measuring stations were located sufficiently distant from the initiating source for the unstable detonations to degenerate completely.

The fluctuations could also be due to the detonation front alternately accelerating and decelerating as it propagates down the tube (Brinkley and Richardson, 1953). This pulsating mode of propagation could be due to a rarefaction wave entering the reaction zone, thereby decreasing the reaction rate. Part of the enthalpy of reaction would therefore not be transmitted to the shock front, and the detonation velocity would be decreased. If chemical reaction were to continue in the rarefaction wave, a pressure pulse would eventually overtake the front of the rarefaction wave and increase the strength and velocity of the detonation front, and so on.

Another factor could be the rate of equilibration of internal degrees of freedom. In a detonation wave, the gas is heated and compressed by the shock wave, the compression taking place over several mean free paths (Thomas, 1944). It is known that in very rapid changes of state the translational and internal degrees of freedom need different times to reach

equilibrium. The translational degrees are usually equilibrated after a few collisions. There are indications (Miles, Munday and Ubbelohde, 1962) that, in a shock wave in near limiting mixtures, the internal degrees are still unexcited or not fully excited at the reaction zone, resulting in a translational temperature which is higher than the equilibrium temperature of the unreacted gas. The subsequent excitation of the other degrees of freedom lowers this temperature. This higher translational temperature could possibly alter the activation energy of the reaction process, thereby altering the detonation velocity.

Still another factor was proposed by White (1961), who determined the pressure in the reaction zone by interferometric means, and found it to be lower than the C-J value. He proposed that this lower pressure is due to turbulence in the reaction zone. This is in agreement with Gordon's (1949) experimental findings. This could explain why some experimental detonation velocities are higher than the calculated values, for detonations referred to by Kirkwood and Wood (1954) as "pathological" (Kistiakowsky et al., 1952 a).

So far, only steady state detonations and their failure have been discussed. If observed detonation limits can be influenced by the mode of initiation, as is indicated by the work of Schuller (1954)(see page 34), then a knowledge of the mechanism of initiation would be helpful in

understanding more fully the reasons for detonation failure.

1.2.5. Initiation by shock waves:

Although several methods can be used to initiate detonations, such as placing an explosive charge at the end of the tube, passing a spark through the gas, or passing a shock or detonation into the reactive gas, all detonations in these researches were initiated by an established detonation wave. As this is essentially the same as initiation by shock waves, a discussion of the latter would be relevant to the discussion.

The fact that an explosive gas can be ignited by a shock wave has been known for a long time (Vieille, 1899). Chemical reaction results from the heating and compression of the gas by the shock wave. However, several factors should be borne in mind when considering the ignition in a detonation front.

Failure to equilibrate internal degrees of freedom (see page 34), and the directed velocity component of the heated gas in the flame front could possibly alter the activation energy of the reaction processes in detonations. These two effects might render ignition by shock waves different from ignition by adiabatic compression (Jost, 1956).

Much work has been done on ignition by adiabatic compression (reviewed by Mullins, 1955). The main facts

are:

(i) Normally there exists an induction period, the time between the end of compression and the onset of explosion;

(ii) This induction time shortens as the temperature is increased;

(iii) For a given apparatus, pressure and composition, there is a critical lower temperature below which explosion cannot be observed.

Several experiments (Berets et al, 1950 b; Mooradian and Gordon, 1951; Fay, 1953) have shown that ignition temperatures are lower for shocks than for adiabatic compression, but this conclusion could be erroneous due to extraneous effects such as the bursting of the diaphragm separating the initiating and test sections. Whether or not the mechanism is the same for both has yet to be resolved, although Borisov and Kogarko (1963) claim to have shown that the front of the reaction zone in detonation coincides with the front of self-ignition of gas heated by a shock wave of the same strength as that in the detonation front.

No mention has been made, so far, of the possibilities and effects of diffusion of light particles, for example electrons, from the reaction zone, as would be expected from their high thermal velocities. Although the related case of strong ionising shocks has been considered

(Appleton, 1966) no conclusive work has been done in this field for detonations.

The knowledge gained from these previous investigations may now be used as a guide for further research into the mechanism of detonation under marginal conditions.

1.3. Experimental Approach:

There are two possible procedures that may be adopted for the elucidation of the factors controlling the limit phenomenon. One is to measure all relevant parameters of the detonation front under marginal conditions, and the other is to observe the effect on the limits of altering, in turn, each of the parameters influencing the limits. Intensive detonation parameters such as reaction temperature, pressure and density are difficult to measure with certainty, thereby restricting the reliability of the former approach. The velocity of propagation, on the other hand, can be determined both simply and accurately. If a rapid drop in the detonation velocity is used as the limit criterion, the latter approach would consequently lead to more dependable information about the nature of the limits.

In order to ascertain which parameters influence the limits, and the extent of their influence, it is

necessary to observe the effect of altering as many factors as possible. The ideal solution is to vary one parameter at a time, whilst keeping the others constant. In practice, though, this is not always possible, and the desired information must be induced from superimposed effects.

It is first necessary to select which parameters to consider, and then find a way of varying them separately. From the existing knowledge of detonation limits, the relevant parameters appear to be :

(i) the nature of initiation;

(ii) initial conditions - temperature, pressure;

(iii) wall effects - tube shape and dimensions, surface roughness;

(iv) hydrodynamic factors - density, specific heats; and

(v) reaction chemistry - heat release, reaction rates.

It is also possible that mass effects such as diffusion, and electric effects such as ionisation potential play a significant role.

The detonation limits for an underdriven detonation, that is where the initial velocity of propagation is less than the extrapolated steady-state value, will depend on the ability of the detonation front to accelerate to this value. This acceleration will be more difficult for the lower initial velocities resulting

from weaker initiation sources. However, overdriven detonations, where the initial velocity exceeds the extrapolated steady-state value, must eventually decay until this value is reached. Therefore, the limits should not be affected by the strength of initiation and, provided that the detonation is observed beyond the region required for the detonation front to be stabilised, the need for reproducible initiation conditions is averted.

As the purpose of this research is to study the decay of established detonations, and this requirement was only met with in the latter case, the same overdriving initiation method was used in all cases.

Initial conditions and the nature of the tube can readily be varied, but their precise control is difficult. Without this control, it would not be possible to achieve the desired reproducibility of these factors or, consequently, to determine their effects with certainty. Because of this, experiments were conducted in similar tubes of the same dimensions and at the same initial conditions throughout, and the main emphasis of this research was placed on the effects of the hydrodynamic factors, reaction chemistry, and the possible electrical and diffusional effects.

The hydrodynamic factors can be varied by the addition of various unreactive gas diluents to a reactive

"base" mixture, the reaction kinetics of which are well known, and which does not suffer from such complicating factors as solid deposition. Dilution with inert gases, which have practically identical properties except for their molecular masses, viscosities and ionisation potentials, could lead to an estimation of the effect of these properties on the limits. Dilution with polyatomic molecules could, in addition, indicate the effect of the specific heat ratio, γ .

The use of different reactive bases, diluted as above, could yield information on the effect of the reaction chemistry. Fuels with different atomic components would be expected to have different diffusion characteristics, and their use could show the effect of diffusion of the reacting species within, and ahead of, the detonation front.

1.4. Choice of experimental parameters:

The simplest, and most commonly used, method of initiating detonation in a test mixture is by passing a strong and easily initiated detonation into it. As this research required the use of a strong, overdriving detonation, a stoichiometric (2:1) hydrogen-oxygen mixture was used for the primary detonation. In this choice it was assumed that the energy liberation of the primary detonation was the main factor influencing the occurrence of an overdriven detonation, but it is possible that other

factors such as its velocity could have an effect. Care was therefore taken to ensure that the composition of the priming mixture was the same in all velocity determinations, so that reproducible results could be obtained in the event of an underdriven detonation being generated.

All mixture compositions were determined from partial pressures, and detonation velocities from the time taken for the disturbance to pass successive wave front detecting probes on the tube wall. Preliminary experiments showed that the detonation velocity decays very quickly beyond the limiting concentrations. Therefore, as the limits were to be investigated, it was necessary only to determine the mixture composition with high accuracy, and not to attempt the same degree of accuracy in the velocity measurements.

A stoichiometric (2:1) mixture of hydrogen and oxygen was used as the main reactive base. Because of their low cost and availability, the diluents used were helium, argon, hydrogen, oxygen, carbon dioxide and ammonia. It should be noted that the results obtained with the last two might be more difficult to interpret because of the possibility of their participation in the chemical reaction.

As a further variant, the replacement of hydrogen

by deuterium was examined as this had the effect of altering only the molecular mass and electrical properties of the fuel. Therefore, a stoichiometric (2:1) mixture of deuterium and oxygen was used as the second reactive base.

A 1 : 1 cyanogen-oxygen base mixture was also examined as it is free from light atoms, therefore presumably being less sensitive to diffusional effects, has a high heat of reaction, and the resulting detonation velocity is relatively insensitive to water vapour.

Once this procedure was decided upon, the experimental apparatus could be designed.

CHAPTER 2.

APPARATUS AND EXPERIMENTAL METHOD.

The experimental aspect of this research was primarily concerned with the measurement of detonation velocities for various mixture compositions. The equipment used therefore had to be capable of producing a homogeneous gas mixture of the desired composition with high accuracy, and of measuring the detonation velocity with sufficient accuracy for its use as a reliable limit criterion (see section 1.3).

2.1. Desired accuracy :

The accuracy requirement for the determination of the mixture composition depended upon the composition interval between the limiting concentrations for the various systems under consideration, so that differences in the limit values could be reported reliably. As these were not previously known, a probable minimum value had to be inferred from previously published limit data. From the results of Pusch and Wagner (1965) and Miles et al (1962), it appeared that the minimum difference in concentrations at the limits should be in the order of 1% of diluent with respect to the reactive base. An accuracy of $\pm$ 0.1% of diluent was therefore considered sufficient for the purpose of comparison between the different systems.

The detonation velocity, on the other hand, was used primarily as a means of detecting the limiting concentrations. As detonation limits are marked by a very steep decrease in velocity for a small composition change, an approximate value for the detonation velocity should be sufficient. However, in the event of there being irregularities in the velocity- composition relationship which could give further information on the nature of the limits, it would be necessary to determine the velocity with sufficient accuracy for meaningful fluctuations to be detected reliably. From the magnitude of the irregularities found by Schuller (1954), an accuracy of $\pm$ 50 metres/second was considered to be adequate for this purpose.

3.2. Equipment:

The experimental apparatus consisted of three principal sections :

(i) the detonation tube;

(ii) the gas mixing unit; and

(iii) the time measuring unit.

Provision was also made for the addition of further equipment, for example, to study the causes of any velocity fluctuations incurred. Such additional equipment will be discussed in the appropriate section.

2.2.1. Detonation tube:

Detonation in the test mixture was initiated by subjecting it to the impact of a detonation in a stoichiometric hydrogen-oxygen mixture. For this purpose, the detonation tube was in two parts; a priming section to contain the stoichiometric initiation mixture, and a test section to contain the mixture to be investigated, and onto which five detonation front detecting stations were mounted. The two sections were separated by a valve to allow their separate filling and which, when open, offered no resistance to gas flow between the two sections (see figure 2.1).

Both sections were of 1.00" diameter 10 gauge extruded stainless steel tubing. An additional 1.00" diameter 10 gauge brass tube internally coated with phenol-formaldehyde resin ("Araldite" PZ820, applied according to the manufacturer's instructions) was available for use as the test section. Both the priming and test sections could be evacuated or filled with gas through a 1/4" diameter hole via a 1/2" diameter tube fitted with a 1/2" spherical ball valve. Connection was made between adjacent tube sections by vacuum tight unions, one of which is illustrated in figure 2.2, thus facilitating assembly and dismantling. To the far end of the test section a blank end piece was fitted, and which could be replaced by an additional length of tubing.

The priming section was 4½ feet long, and a spark

was used to ignite detonation in the priming mixture. In view of the work of Laffitte (1928) who found that the predetonation distance for stoichiometric hydrogen-oxygen, ignited by a spark, was approximately 60 cm at atmospheric temperature and pressure, this length was considered fully adequate to ensure a fully developed detonation at the moment of impact with the test mixture.

Because of the uncertainty of the distance required, after impact, for the detonation in the test mixture to reach steady state conditions, a minimum test section length could not be specified. However, as the laboratory space limited the length to 12 feet, the last four being required for the velocity determination, only eight feet were available for stabilisation of the detonation. It was therefore necessary to ascertain in all cases whether the measured velocity was the steady state value. The method used for this will be discussed in the fifth precaution mentioned on page 65.

The valve originally used to separate the priming from the test section was the "rotating disc" type described by Munday (1963). This valve, however, proved unreliable and was subsequently replaced by a one inch bore stainless steel spherical ball valve.

The entire tube was securely clamped onto a rigid heavy frame at several positions along its length. The clamps could be adjusted to ensure that the tube was as straigh as possible before use. This clamping was necessary in

view of the momentum transferred to the tube when a detonation was reflected at the far end, resulting in a considerable force being exerted momentarily along the tube axis. Unless the tube was rigidly held in position, this force could have caused a sudden movement of the tube which could possibly have impaired the proper functioning of the time measuring equipment.

The priming mixture was ignited with an automobile sparking plug which was mounted in the end of the priming section, the circuit shown in figure 2.3 being employed.

2.2.2. Gas mixing unit:

Mixtures were prepared by successive admission of each gas into a constant volume vacuum tight vessel. After each gas was admitted the pressure of the system was measured and the composition of the mixture determined from the partial pressures of the constituents.

2.2.2.1. Construction:

The initiating and test mixtures were prepared in ten litre spherical vessels which were connected, via a manifold, to a vacuum pump, the gas supply cylinders, and the detonation tube. The equipment is shown schematically in figure 2.4. The material used throughout was glass to enable easy fabrication and the use of high grade glass vacuum

stopcocks for the control valves.

To enable fine control of the mixture composition, the gases were introduced from the supply cylinders, via the manifold, into the mixing vessels by means of fine adjustment P.T.F.E. diaphragm valves. Provision was also made for the more expensive gases to be introduced directly from the cylinders. The partial pressures of the constituent gases in the mixing vessels were read from 3/8" diameter open ended mercury manometers which had a range of two atmospheres. Boxwood metre rules were used for the manometer scales.

The gas mixing unit, together with both sections of the detonation tube, could be evacuated by a "Speedivac" 1SP 30B positive displacement vacuum pump. The manifold pressure was read on a 1/2" diameter Torricellian mercury manometer, also with a boxwood scale, and with the two arms in contact. It was found that the entire system could be evacuated to approximately 0.1 mm Hg in half an hour. This residual pressure would cause a maximum error of 0.01% in the mixture composition which was considered to be sufficiently small for the purpose of this research.

2.2.2.2. Gas homogenisation :

To achieve full homogeneity of the gas mixture in the two mixing vessels, it was necessary to fulfil the following requirements:

(i) no recesses in the vessels where gases can stagnate;

(ii) large paddles to ensure maximum turbulence;

(iii) high rotatory speeds of the paddles; and

(iv) a paddle design to give the maximum net movement of the gas.

To meet with these requirements, a "push-pull" propeller system was chosen. This consisted of a central shaft, located in two nipples in the mixing vessels, to which two sets of paddles were attached - one in the centre of the vessel, and a smaller set in the neck. To avoid gas leakage, an external magnetic drive was used for the rotation of the shaft (see figure 2.5).

The bearings used for the paddle system were cones made from P.T.F.E., as were the paddles themselves, so as to minimise chemical interaction with the gas mixture and to give maximum ease of rotation without the need for lubricants. Two independent "Gallenkamp" SS420 sparkless electric motors were used for the drive, and their speed regulated with a 5 amp. auto-transformer. Speeds of up to 200 r.p.m. could be comfortably accommodated by this system.

2.2.2.3. Safety features :

As an explosion in the glass mixing unit could prove dangerous to the operator, the entire unit, apart from the supply cylinders and the vacuum pump, was located inside an explosion proof steel cabinet with heavy glass observation windows. Steel shafts were used to operate the valves from

outside the cabinet.

To minimise the chance of an explosion travelling back from the detonation tube into the mixing unit, each tube feed line incorporated a sharp bend which caused a sudden change in the direction of any gas passed down the line. Their positions are shown in figure 2.4. They were made of thin glass so that, in the event of an accelerating flame propagating along the line, the sudden increase in pressure and momentum change would break the glass. This would relieve the pressure behind the flame and therefore reduce the possibility of a detonation forming. In fact no hazardous explosion was experienced throughout this work.

The manifold was made fully floating by using thick-walled rubber vacuum tubing for connection to the gas supply cylinders, vacuum pump and detonation tube, and a small brass bellows to connect it to the mixing vessels. The chance of the equipment being broken by sudden blows or a slight movement of one of the components was therefore reduced.

The manifold itself had to be rigidly clamped into position so as to reduce the possibility of breakage due to the torsional forces produced by the operation of the stopcocks. For this purpose the manifold was fixed onto a 1/2" thick "Tufnol" backing board by a system of clamps, one being located on either side of each stopcock. As the thermal expansion of Tufnol is similar to that of glass, and

there was some degree of axial movement allowed by the clamps, the risk of breakage due to thermal expansion was reduced.

2.2.3. Time measuring unit:

The detonation velocity was determined by measuring the time taken for the detonation front to pass between consecutive detection stations, a known distance apart. Each station produced an electrical signal which was displayed on an oscilloscope trace. The trace started when the detonation front passed a trigger station located upstream of the detection stations. This trace was photographed and the time intervals determined by comparison with a similar photograph of a time mark signal.

It was not known at which region in the detonation front the detectors fired, but it was reasonably assumed that, if successive detectors were identical, they would fire at the same instant after the passage of the shock front, and therefore the correct velocity would be obtained. An estimate of the validity of this assumption can be made from the length of the reaction zones in hydrogen-oxygen detonations found by Wagner ("Les Ondes de Detonations", Centre National de la Recherche Scientifique, Paris, 1962, page 241). From his results it can be shown that the reaction zone width for a mixture of $4H_2 + O_2$ (detonation velocity

3630 m/sec.) is approximately 3.6 mm. Therefore the maximum error in the velocity determination introduced by random firing of the detection stations in the reaction zone is approximately 13 m/sec., which is within the desired accuracy.

The detecting stations were of two types:

(i) ionisation detectors; and

(ii) light detectors.

2.2.3.1. Ionisation detectors:

When an ionised gas passes between two conductive wires with an electrical potential across them, current will flow between the wires provided that the gas is strongly enough ionised and the wires are not too far apart. Therefore the sudden increase in conductivity between two terminals as a detonation front passes them can be used to discharge a capacitor. Such a system can be used to detect the passage of a detonation front with high precision (cf. Gaydon and Hurle, 1963, p. 118). To attain this high precision, the distance between the wires must be large enough to prevent the passage of current through the unreacted gas, but small enough to allow the passage of sufficient current to discharge the capacitor as the detonation front passes.

Two such ionisation detectors were used in this

research, and placed a fixed distance of approximately 1.00 metres apart at the end of the test section. Each consisted of two 0.008" diameter copper wires passing down an insulated block mounted in the side of the detonation tube. The wires were orientated in the direction of the tube axis, and mounted 0.040" apart inside the tube. Care was taken to ensure that this orientation and distance were the same for both probes so that they gave corresponding signals.

The bottom of each probe was carefully shaped to match the curvature of the tube so that no disturbace could be caused to the detonation front in transit, except for the two wires which protruded about 0.002". This protruberance was necessary to reduce the risk of their being covered with any high resistance residue from the detonation, and to facilitate their cleaning. The probes were firmly cemented in place with "Araldite" adhesive so as to render them immovable and vacuum tight.

A d.c. potential of 120 volts was applied across the two wires, and the signal obtained by discharging a 47pF capacitor. Matched lengths of coaxial cable transmitted this signal to the oscilloscope, necessitating the use of a cathode follower in conjunction with the probe circuit in order to

maintain a fast rise time. The circuit is shown in figure 2.6, together with that used for mixing the two signals before transmitting them to the oscilloscope. The characteristics of the output signal were tested by replacing the ionisation probe by a 1MΩ resistor - to simulate the resistance of the detonation front - connected in series with a mercury-wetted relay. This gave repetitive make-break signals which could be readily observed on an oscilloscope. For this system, the circuit was found to have an output of 80 volts, and to give a rise time of less than 1μ second.

All electrical equipment was shielded to eliminate extraneous signals, and mounted on a wooden base attached to the detonation tube.

2.2.3.2. Light detectors:

It is theoretically possible to detect, by means of a monochromatic light filter in conjunction with a photomultiplier, characteristic wavelengths for various reacting species in a chemiluminescent reaction zone of a detonation. This could give an idea of the nature and speed of the reactions involved, but the interpretation of the results so obtained would be difficult, and their value to this research doubtful. It is much simpler to use the emission of light of all wave lengths to detect the passage of the reaction zone.

Three light detection stations were placed a

fixed distance of approximately 1.005 metres apart at the end of the test section. At each station a 1/8" diameter glass window was cemented with Araldite into the wall of the tube so as to be vacuum tight and free from protruberances inside the tube. This was covered with an aluminium ring with a 1/8" diameter hole drilled directly above the window. In this a Texas IN2175 photo-duo-diode was fitted, suitably shielded from external light, and 1/4" away from the tube wall so that it would only detect light directly in front of the window.

The signal was produced and transmitted to the oscilloscope by an arrangement similar to that used for the ionisation detectors, the circuit being shown in figure 2.7. These circuits were also shielded and attached to the detonation tube. The circuit, without the photo-diode, was found, as before, to give a seven volt signal with a rise time of 5μ seconds.

2.2.3.3. Oscilloscope trigger:

The trigger used to start the oscilloscope trace was an ionisation probe and circuit as described in section 2.2.3.1, without the cathode follower. As the trigger signal always had to be greater than the signal picked up from the spark by the oscilloscope, the trigger probe was mounted in the priming section, six inches from the separating valve. In this way, the same strong trigger signal was obtained each

time, and the trigger sensitivity setting on the oscilloscope was constant.

2.2.3.4. Time interval determination equipment :

The signals from the detecting stations were displayed on a "Tektronix" type 551 dual beam oscilloscope. Two type L plug-in units were used, each with a variable sensitivity from 0.005 to 20 volts/cm. The ionisation detector signals were always displayed on the lower beam and the light detector signals on the upper so as to avoid confusion.

The traces were photographed with a camera mounted on the oscilloscope. Ilford HPS film, DIN rating 30, was used except where rapid results were required, when it was replaced by a polaroid camera using 2000 ASA film. A typical record is shown in figure 2.8.1.

For some systems, failure of the oscilloscope trace to stabilise between the first and second ionisation signals made readings impracticable. It was therefore necessary to use one trace for each signal, and to disconnect the light detectors. A typical record is shown in figure 2.8.2.

After development of the film, the distances between the signal peaks were measured with a travelling microscope. A similar photograph was taken of the signal output from a "Tektronix" type 181 time mark generator with

the same time base, giving a trace as shown in figure 2.8.3. The distance between adjacent peaks corresponded to 1 m. second , and this distance was used as a calibration for the time interval determinations.

2.3. Accuracy of results:

Before any experimental records could be used with confidence, it was first necessary to know the magnitude of the errors introduced by the equipment and the method used to find them. The maximum desirable errors were given in section 2.1, and the equipment was tested to see whether its accuracy lay within these limits.

2.3.1. Gas mixing :

Probable errors in the mixture composition could be caused by a variety of factors such as the existence of stagnation zones in the mixing vessels, inhomogeneous mixtures, inaccurate manometer readings due to parallax and resolution errors, the effects of surface tension and changes in atmospheric conditions on the manometer readings; and systematic errors due to neglect of intermolecular forces in the determination of the composition and impurities in the component gases. Instead of analysing each factor separately, preliminary experiments were performed to estimate the overall error. The estimate for the probable error was made by testing the reproducibility of the velocities obtained for mixtures of the same composition made on separate occasions

and for different orders of addition of the constituents into the mixing vessel; and for the systematic error by analysing the prepared gas mixture.

To obtain a meaningful estimate of the probable error, it would have been necessary to perform these experiments in a composition range where a small change in composition resulted in a large change in detonation velocity. As the velocity-composition relationships were not known accurately at this stage, only an approximate estimate of the probable error could be made. A more accurate estimate was later made from the results obtained during the progress of the research. The method assumed that the velocity determinations were accurate, but this assumption was later shown to be justified (see section 2.3.2).

The component gases were obtained from commercial cylinders, the purities being given by the manufacturers as : hydrogen 99.9%; oxygen 99.5%; helium 99.95%; argon 99.95%; ammonia 99.9%; carbon dioxide 99.95%; deuterium 99.5%; cyanogen 99.95%.

The systematic error of the mixture composition was determined by analysing the test mixture, after it had been admitted to the test section of the detonation tube, with a "D.C.L.Servomex" portable gas analyser (see Appendix A.2.1.). These experiments showed that gas mixtures could be prepared to an accuracy of $\pm$ 0.02% of diluent with respect to the

reactive base, which is well within the accuracy requirement.

To test the time taken for full mixing of the gas in the mixing vessels, successive velocity determinations were made 5, 10 and 30 minutes after the final manometer reading. As all three gave the same velocities, within the range of accuracy, complete mixing was assumed to occur within five minutes. The same argument applied to this test as to the above, so 20 minutes were always allowed for the mixing. The validity of this assumption was later justified by further experiments as above.

2.3.2. Velocity determination:

Errors in the velocity determination could be introduced by inaccurate measuring of the distance between probes, non-identical probes and circuits, and low resolution of the distance between the peaks on the trace. Once again, all errors were treated together.

The reproducibility of the time interval determinations was tested by comparing the results of several consecutive determinations with the same gas mixture, and the accuracy by comparing the mean value with published figures for the same composition. Since the stoichiometric hydrogen-oxygen mixture has been the subject of a considerable amount of study in the past, this was chosen as the test mixture.

The average of four published detonation velocities is 2822 $\pm$ 3 m/second (Wagner, 1961) which compares

favourably with the value of 2814 metres/second found in this research. The maximum deviation over three separate measured determinations was 23 metres/second, which is within the desired value.

2.4. Experimental method :

From the experience gained in these preliminary investigations, the following method for the determination of the composition-velocity relationship was developed.

2.4.1. Procedure :

2.4.1.1. Gas mixing :

With reference to figure 2.4:

With valves G,B,B_1 and E closed and A,A_1, A_2 and V open, the vacuum pump was switched on and the mixing vessels evacuated. The pressure inside the system was read from the manometer M_3. The valves A,A_1 and A_2 were then closed, the supply cylinder containing the first gas to be admitted was connected and the valve G opened. The readings on the vessel manometers M_1 and M_2 were then recorded and the desired readings after the addition of the first gas were calculated.

When the manometer M_3 again showed the system to be evacuated, the gas supply cylinder valve was opened and the gas allowed to purge the manifold for several seconds. The valve V was then closed and the pressure in the manifold raised to slightly exceed the desired final pressure in the

mixing vessel by means of the gas cylinder control valve. The gas was then passed into the mixing vessels through the fine adjustment valves A and A_1 or A_2 until the desired pressure was obtained in each. The gas cylinder control valve was then closed. Care was taken to ensure that the gas in the vessels had returned to room temperature before the manometer readings were recorded, this usually requring about five minutes. The stirrer was turned on, the valve V opened, G closed, the next cylinder connected, G opened, and the process repeated for the other constituent gases, the manometer readings M_1 and M_2 being recorded after each further addition.

With the stirrer running, the valve G was closed and B, B_1, D and D_1 opened, so that the detonation tube could be evacuated.

2.4.1.2. Filling detonation tube :

When the tube was fully evacuated (about 20 minutes) valves B_1, D_1 and V were closed and the tube filled to 76.0 cm Hg with the priming gas by means of the valve A, and the separating valve closed. When the rotating disc valve was used, it was left closed during the entire filling operation. However, as the volume inside the spherical ball valve was equivalent to $1\frac{1}{4}$ inches of the tube, the valve was left open during the filling of the priming section, and then closed. In this way it was filled with the priming mixture.

Valve D was then closed, the manifold evacuated,

and valve B closed. Valves B_1 and D_1 were then opened and the test section evacuated and filled in the same way.

2.4.1.3. Detonation :

The time base was determined from preliminary calculations, the oscilloscope set on "single sweep" and, after checking that valves D and D_1 were closed, the sparking plug battery connected. The separating valve was then opened, the camera set, and the sparking plug fired. To reduce the interdiffusion of the gases at the interface, the sparking plug was fired as soon as possible after the separating valve was opened.

2.4.1.4. Determination of detonation velocity :

Once the film was developed and dried, the distance between the peaks on the two traces was measured on the travelling microscope, the corresponding time intervals determined, and the detonation velocities for each set of probes calculated from these time intervals and the distance between the probes.

2.4.1.5. Calibration :

Before each new reaction system was investigated, two calibration photographs were taken on the same time base as used for the time interval determinations. From these, the average distance corresponding to 1 m.second was determined, and the time intervals corresponding to the

distances between adjacent peaks on the test photograph could then be found by direct ratio. A typical velocity calculation and calibration is given in Appendix A.1.

2.4.2. Precautions :

Nine separate precautionary measures were taken whilst determining each velocity:

(i) To reduce the error which would result from stagnation of small pockets of the first gas to be admitted to the mixing vessels, the component with the greatest mole fraction was admitted first. In this way a smaller fraction of this component would be lost from the mixture than if a lesser component were admitted first. The stirrer was then kept running whilst the other gases were admitted.

(ii) Near the limiting concentrations, hydrogen and oxygen (or the components of the other reactive bases) constitute only a small fraction of the total mixture. A small error in the manometer reading during this admission would therefore lead to a large error in the stoichiometric composition. The remainder of the previous priming mixture was therefore used as the reactive base for diluent concentrations greater than 75% for the hydrogen-oxygen system. It should be noted that this necessitated the addition of the lesser component first.

(iii) The stirrer was always stopped after the addition of each gas and about five minutes allowed for the mixture to return to room temperature before the manometer readings were

taken. This reduced the possibility of the gas being heated by the agitation, thereby leading to erroneous manometer readings.

(iv) Before any gas mixture was admitted to the detonation tube, a brass brush was passed down the test section. This served to remove any loose particles that may have been stripped from the tube wall by the previous detonation, and to remove any loose oxide layer that may have formed on the ionisation probe terminals. This process also helped to maintain a consistent surface at the tube wall (see above, p.40).

(v) Because of the similarity between the same type of detonation front detectors, it was assumed that the velocity obtained from both sets would be the same. This was verified by preliminary experiments. The light detectors were therefore used primarily to check whether the detonation had reached steady state conditions before it passed between the ionisation detectors, as the first set of light probes were three feet upstream of the first set of ionisation detectors. Steady state conditions were considered to have been reached when the velocity found between the first and second set of light probes were the same, within experimental error.

(vi) When not in use, the entire equipment was kept under as low a vacuum as possible to minimise water condensation in the tube, and gas adsorption in the gas mixing unit.

Slight traces of water vapour could affect the results, and degassification of the gas mixing unit took several hours.

(vii) To ensure that the gas mixing unit remained vacuum tight, the stopcocks were lubricated with "Apiezon M" grease, which was renewed every two weeks. All cone and socket joints were sealed with "Picien" wax.

In addition, several safety precautions were taken.

(viii) The sparking plug battery was not connected until both priming and test mixtures had been admitted to the tube, and the valves D and D_1 checked to be closed. It was immediately disconnected again after firing. This eliminated the chance of the spark being fired accidentally, which could result in an explosion travelling into the mixing unit with consequent equipment, and possibly personal, damage.

(ix) The toxic gas cyanogen was handled in the same way as the other gases, except that the effluent gas was condensed in a glass vessel which was cooled with liquid nitrogen, and disposed of at the end of each day's experiments.

CHAPTER 3.

EXPERIMENTAL RESULTS AND PRELIMINARY DISCUSSION.

Using the experimental apparatus and procedure described in the previous chapter, the limiting compositions for marginal detonation and the velocity-composition relationships were determined in the stainless steel tube for the stoichiometric mixtures $S_H = 2H_2 + O_2$; $S_D = 2D_2 + O_2$; and $S_C = C_2N_2 + O_2$ diluted to form the following binary and ternary mixtures:

S_H + H_2, O_2, He, A, CO_2, NH_3 ;

S_D + D_2, O_2, He, A; and

S_C + C_2N_2, O_2, He, A.

In addition, the limiting compositions and the velocity-composition relationships were determined in the coated tube for the mixtures:

S_H + H_2, O_2, CO_2, NH_3.

3.1. Limiting concentrations:

The detonation limits were defined as the diluent concentrations at which a further slight increase in dilution resulted in a rapid decrease in the velocity of propagation (see section 1.2.3, p.22). In these researches the detonation limits refer only to the "normal" velocity regime which prevails throughout the entire

composition range. The limiting concentrations are given as a function of percentage diluent added to reactive base in Table 3.1, p. 77 . For the purpose of comparison, the values found by Pusch and Wagner (1965) for S_H diluted with H_2, O_2, He and A (extrapolated to one inch tube diameter) are also given. These values have the same order of magnitude as the values found in these researches.

From the cases reported it can be seen that, for the same reactive base, smaller diluent molecules give rise to wider composition limits. For example, with the reactive base S_H, the effectiveness of the diluents in promoting detonation failure are in the order - polyatomic gases (in the order CO_2, NH_3), diatomic gases (in the order O_2, H_2), monatomic gases (in the order He, A). It can also be seen that, except for S_H based mixtures, dilution with oxygen leads to a more extended composition limit than dilution with fuel. This general order is to be expected in view of the different specific heat ratios of the different gases, and therefore different shock temperatures in the detonation fronts.

This statement can be tested by determining the shock temperatures under limiting conditions (limiting shock temperatures), T_s. These values can be found, with small errors, by means of the relationship

$$T_s = \frac{2T_1 [\gamma M^2 (\gamma - 1) + 2\gamma]}{(\gamma + 1)^2}$$

which is given by Miles, Munday and Ubbelohde (1962). In the present calculations, the values of γM^2 were the approximate experimentally determined values, and were determined by extrapolating the steady state values given in Appendix 2 to the limiting concentrations. The values of γ used were: He and A, 1.667; D_2, H_2 and O_2, 1.4; CO_2, 1.304; NH_3, 1.310; and C_2N_2, 1.256. The last three of these values were taken from "International Critical Tables", volume V, p.86, being the values given for 298°K. The calculated limiting shock temperatures are tabulated in Table 3.2, p.78.

Inspection of these values shows that, with few exceptions, the limiting shock temperatures are similar for each reactive base. As it would be expected that the minimum ignition temperature for a particular reactive base would be approximately the same for all non-reactive diluents, this similarity suggests that a major factor in detonation failure for the systems to which this generalisation applies could be that the shock temperature becomes insufficient for rapid chemical reaction to occur in the detonation front. The small observed differences in the limiting shock temperatures could result from different third body efficiencies of the diluent molecules (Belles, 1959), etc.

Notable exceptions to this generalisation are the calculated limiting shock temperatures for the systems $S_H + NH_3$ and $S_D + D_2$, and the reactive bases S_D and S_C diluted with helium and argon.

The high value calculated for the system $S_H + NH_3$ could be due to ammonia taking part in the chemical reaction. The most likely reaction for this appears to be

$$H + NH_3 \longrightarrow NH_2 + H_2 \qquad \Delta H = 1 \text{ Kcal.}$$

which, in view of the propagation and chain branching reactions

$$OH + H_2 \longrightarrow H_2O + H \qquad \Delta H = 15 \text{ Kcal.}$$

$$H + O_2 \longrightarrow OH + O \qquad \Delta H = -16 \text{ Kcal.}$$

$$O + H_2 \longrightarrow OH + H \qquad \Delta H = -2 \text{ Kcal.}$$

found to occur in the reaction of hydrogen with oxygen (see Lewis and von Elbe, 1961) would remove a large proportion of H radicals from the reaction zone. Therefore, dilution with ammonia would be expected to inhibit the chemical reaction and consequently lead to a higher required ignition temperature.

However, this argument does not apply to the other apparent anomalies, where non-reactive diluents are used. The difference in the limiting shock temperatures in the cases where the reactive bases are diluted with helium and argon, or hydrogen and deuterium is particularly

striking as each of these pairs of diluents has practically identical thermodynamic and hydrodynamic properties.

Some idea as to the factors operative in this behaviour can be gained from inspection of the Mach product - composition curves of the systems concerned. To allow for easy comparison, the curves for similar systems are plotted on the same diagrams in figures 3.1 to 3.3.

From figure 3.1 it can be seen that the values of γM^2 decrease steadily until the limit is reached when $\gamma M^2 \doteqdot 20$. For the system $S_D + D_2$, however, the limit appears to have been reached prematurely at $\gamma M^2 = 23.7$. The reason for this apparent premature failure could have been due to a combination of various factors, such as molecular mass effects or chemical kinetics, leading to the hydrodynamic instability of the detonation front as a whole. This premature failure could also account for the non-existence of a lower velocity regime as described below (section 3.2.2). The same reasoning could also apply to the system S_C + He where the γM^2 - composition curve closely follows that of the S_C + A system, but fails prematurely (see figure 3.3).

The reason for the low limiting shock temperature in the system S_D + He cannot simply be explained in these terms, but appears to have been influenced by the sudden drop in the value of γM^2 near the limiting concentrations

(see figure 3.2), which will be described below.

Possible explanations for these apparently anomalous behaviours will be discussed in much greater detail in Chapter 4.

3.2. Velocity - composition relationships:

The detonation velocities and Mach products (averages of three separate determinations) are recorded as a function of composition in Appendices A2 and A3, and are plotted in figures 3.4 to 3.13. Inspection of these curves shows that, except for near-limiting concentrations, the velocities and Mach products vary smoothly with increase in diluent concentration as has been previously found (see curves given by Wagner, 1961, pp. 331-7). However, near the limiting concentrations, two main classes of abnormal behaviour were found to occur:

(i) Irregularities occurred in the velocities with small changes in composition, these being extremely reproducible; and (ii) A second, lower velocity regime was found with some hydrogen and deuterium based mixtures.

3.2.1. Velocity irregularities:

For the system S_H + A, small regular (sinusoidal) velocity fluctuations of approximately 25 m/second amplitude occurred in the velocity-composition curve in the composition range 88.8% to 90.7% diluent (see figure 3.4,

section B). For dilutions greater than 90.7%, the velocity was found to rise again. This second type of irregularity was not of the same form as the regular fluctuations mentioned above. Similar fluctuations occurred in the S_D + A system, but at slightly lower dilutions (see figure 3.5). These fluctuations could be faithfully reproduced on successive determinations, or upon repeating the determinations over the entire composition range at a later date (see run numbers prefixed by 8 and 9, Appendix A.2.1, p188 , which were conducted at different times).

Of the systems studied, only these two displayed this sinusoidal type of fluctuation. However, some other systems ($S_H + H_2$, S_H + He, $S_H + CO_2$, $S_H + NH_3$, $S_D + D_2$ and $S_C + O_2$) displayed regular fluctuations with the amplitudes varying with composition (see figures 3.6 to 3.9). These fluctuations were also extremely reproducible.

Another form of velocity irregularity was observed in the velocity-composition curve for the carbon-depositing system $S_C + C_2N_2$. The Mach product decreased as the dilution was increased to 35% diluent, but then started to rise again (see figure 3.10). This was similar to the rise in Mach product observed in acetylene-oxygen detonations by Kistiakowsky and Zinmann (1955).

In some systems ($S_H + H_2$, $S_D + O_2$) there is a narrow composition range within the stable region in which the detonation velocity becomes erratic (figures 3.6, 3.11). In this range, the measured velocity can be of the order of 30% lower than the interpolated steady state value. This phenomenon was also noted to occur for detonations of $S_H + O_2$ in the coated tube (see figure 3.12). The magnitude of these erratic velocities was not reproducible, but the composition range in which they occurred was.

3.2.2. Lower velocity regime:

For diluent concentrations greater than 77% in the $S_H + H_2$ system, two stable propagation velocities were found; one lying on an extrapolation of the steady state values which were found throughout the entire composition range, and the other having approximately half that value (see figure 3.13). The former was referred to in these researches as being in the "normal" velocity regime, and the latter in the "lower" velocity regime. The occurrence of normal and lower regime velocities appeared to be unpredictable but, generally speaking, the frequency of occurrence of the lower regime velocities increased as the limits were approached. Similar lower velocity regimes were also found to occur in the systems $S_H + O_2$, $S_H + CO_2$ and $S_D + O_2$ (see figures 3.13, 3.7 and 3.11).

The replacement of the stainless steel tube by the brass tube internally coated with Araldite (see p. 46) always altered the composition range in which the normal and lower velocity regimes occurred, and sometimes resulted in an increase in the magnitude of the lower regime velocities. For example, in the system $S_H + H_2$, no normal velocity regime was found to co-exist with the lower velocity regime in the coated tube, and the lower regime velocities were approximately 300 m/second higher than in the stainless steel tube (see figure 3.13). For the system $S_H + O_2$, the range over which the lower velocity regime occurred was reduced by nearly 2% of diluent (see figure 3.12).

It should be noted that the lower velocity regime was never found to extend beyond the erratic velocity range mentioned at the end of the previous section.

As was mentioned previously (p. 67), the concentrations given in Table 3.1 refer to the failure of normal velocity regime detonations, as these are the only values hitherto quoted in the literature. However, in all cases where a lower velocity regime was observed, the composition limits occurred at greater dilutions in the lower velocity regime. For some systems the difference between these two limits was greater than for others (12.6% diluent for $S_H + CO_2$, 0.24% diluent for $S_H + O_2$).

As the above mentioned anomalies occur only near the limiting concentrations, it is very likely that the factors influencing their occurrence also influence the detonation failure to some extent. Elucidation of these factors should give valuable information about the nature of detonation failure. Further experiments for the investigation of, and possible explanations for the anomalies will be discussed in some detail in Chapter 5.

TABLE 3.1. Detonation limits for the mixtures under consideration.

System	% diluent at limit	Pusch and Wagner extrapolated to 1" diameter.
$S_H + H_2$	78.73	79
$S_H + O_2$	76.74	79
$S_H + He$	89.1	82
$S_H + A$	91.91	88.5
$S_H + CO_2$	40.0	
$S_H + NH_3$	41.1	
$S_D + D_2$	72.1	
$S_D + O_2$	74.48	
$S_D + He$	88.76	
$S_D + A$	91.50	
$S_C + C_2N_2$	51.8	
$S_C + O_2$	72.0	
$S_C + He$	88.20	
$S_C + A$	90.4	

The values are listed above with the number of significant places depending upon the accuracy of determination. This accuracy was restricted in some cases by the limited quantity of gas available.

TABLE 3.2. Calculated shock temperatures at limiting concentrations for the systems under consideration.

System	γM^2 at limiting concentration	calculated T_s ($^\circ$K)
$S_H + H_2$	20.0	1120
$S_H + O_2$	20.5	1140
S_H + He	16.3	1170
S_H + A	14.4	1070
$S_H + CO_2$	19.6	1050
$S_H + NH_3$	40.1	1850
$S_D + D_2$	23.7	1270
$S_D + O_2$	20.5	1140
S_D + He	12.3	950
S_D + A	15.0	1100
$S_C + C_2N_2$	65.5	2460
$S_C + O_2$	52.5	2400
S_C + He	51.0	3000
S_C + A	31.5	2000

CHAPTER 4.

DETONATION LIMITS.

4.1. Introduction:

As was shown previously (section 1.2.1), steady state detonation velocities can be accurately predicted in terms of thermodynamic and hydrodynamic parameters. However, outside limiting concentrations detonations fail to be self-propagating, and rapidly degenerate into plane combustion waves or shocks (see section 1.2.3).

The reasons for this failure to propagate are still not fully understood, but several proposals have been made. They all regard the limits as resulting directly or indirectly from a decrease in chemical reaction rates or, more specifically, from a lengthening of the induction period before the onset of rapid chemical reaction. The lengthening of the induction period has hitherto been attributed solely to thermodynamic and hydrodynamic factors (see section 1.2.2, p.20). It is therefore quite surprising that mixtures with practically identical thermodynamic and

hydrodynamic properties can display different concentration limits, as was shown in these researches (see section 3.1).

This finding indicates that several important factors have been omitted from the above treatments. These include molecular mass effects such as diffusion of the reacting species; and electrical effects such as ionisation, with the possibility of an electrical dipole within the detonation front.

The comparison in the present researches was primarily between hydrogen and deuterium as fuels, and helium and argon as diluents.

4.2. Results:

For the purposes of comparison, the Mach products of similar mixtures are plotted on the same diagrams as a function of percentage diluent added near the limit. Figure 3.1 shows plots for the binary mixtures of hydrogen and deuterium with oxygen. The results for the ternary mixtures with helium and argon as diluents are plotted in figure 3.2. Figure 3.3 shows similar plots for the non-proton forming mixtures of cyanogen and oxygen diluted as above.

Additional information concerning the electron structure of the detonation wave could be induced from the

oscilloscope traces of the ionisation probe signals. For near-limiting mixtures of S_H diluted with argon, the passage of the detonation front past each ionisation probe produced a negative signal, closely followed by a positive signal (see figure 4.1). Reversing the probe circuit polarity and removing the probe circuit battery altered the relative magnitudes of the signals, but did not alter their sign. This suggested the presence of an electrical dipole in the detonation front.

4.3. Discussion:

As can be seen from figures 3.1, 3.2 and 3.3, the limiting concentrations varied widely between the different systems. The differences between hydrogen and deuterium as fuels and helium and argon as diluents are quite marked. This behaviour is quite unexpected in view of the nearly identical thermodynamic and hydrodynamic properties of each pair, and can only partly be explained by the existing theories for the existence of detonation limits (see section 1.2.3 above).

4.3.1. Application of existing theories:

The induction zone width for deuterium based mixtures should be greater than for hydrogen (Gray & Smith, 1967) The existing theories (section 1.2.3) can therefore qualitatively explain the wider limits observed for hydrogen based mixtures.

The differences between the limits for helium and argon admixtures cannot, however, be explained in this way except in terms of the relative efficiencies of helium and argon as third bodies. Their third body efficiencies w.r.t. hydrogen are given as 0.36 and 0.20 respectively (Lewis and von Elbe, 1961, p29), although these data are obtained from boiling point data and their applicability is uncertain. If these figures are in the right sense, dilution with helium should result in a greater rate of removal of chain carriers, and therefore lead to narrower composition limits than dilution with argon.

However, the larger molecules formed in the reaction zone (e.g. H_2O) would have much greater third body efficiencies than the diluents (H_2O = 14.3 w.r.t. hydrogen). This effect should therefore be small and should not give rise to differences as large as those observed.

It therefore appears that other factors should be introduced to explain this phenomenon, or the existing theories modified in some way.

4.3.2. Wall effects:

It has been observed that a decrease in detonation tube diameter results in a narrowing of detonation limits (Pusch and Wagner, 1965). However, even with the results obtained in these researches, experimental results do not extend to tube diameters larger than one inch.

It is quite possible that an infinite detonation wave may have no composition limits. For such a wave, dimensional analysis indicates that very little energy is required to sustain a "weak" detonation (Ubbelohde, 1953). Also, marginal conditions are associated with a spinning wave front. If the constant pitch to diameter ratio indicated by the acoustic theory can be generalised, an infinite wave would have an infinite spin pitch or, in other words, zero spin.

But, whereas the burnt products are free to move in any direction behind an infinite wave, they would be hindered in this free movement by the introduction of a tube wall. Deflection at the walls and the resultant transverse perturbations would tend to orientate the detonation front normal to the tube axis. This deflection could impose a restraint on the detonation, reducing its stability at fuel-rich and fuel-lean regions, thus imposing limits only when the detonation is confined by walls.

If these considerations are relevant to existing limit data, then tube diameter effects (section 1.2.3(ii) and above) may be of importance for relatively large tube diameters, but with an increasing contribution from energy losses as the tube diameter is decreased. In both cases the boundary layer is an important factor.

4.3.2.1. Microturbulence losses at the walls:

When a shock wave travels down a cylindrical tube, more or less intense microturbulence may be set up at the walls (Greene and Toennies, 1964, p132). For a detonation wave, differences in density and viscosity, due to the replacement of hydrogen by deuterium or helium by argon, would alter the degree of turbulence at the walls in the reaction zone.

Following the usual Reynolds principles, transition from laminar to turbulent flow could be expected to occur at a critical Reynolds number. When this happens, the amount of heat lost to the walls would increase considerably. If this can be applied to the Manson theory (section 1.2.3) then the limit could be related to the onset of turbulent flow.

For a steady state detonation a Reynolds number, Re, can be defined for a point in the boundary layer a distance z behind the shock front as

$$Re = \frac{\rho_z w_z z}{\mu}$$

where ρ_z = density at that point,

w_z = local particle velocity relative to the containing wall, and

μ = viscosity at that point.

Between the shock front and the front of the rarefaction wave, steady state conditions exist so the mass flow rate, $G = \rho_z w_z$, is constant.

$$\therefore \quad Re = \frac{Gz}{\mu} \tag{1}$$

Now z = induction zone length

$$= \int_0^T w_z dt$$

where T is the induction time. Assuming w_z is constant in the induction zone and the reaction zone length is small,

$$z = w_z T$$

$$= \frac{GT}{\rho_z} \tag{2}$$

Substituting (2) into (1),

$$Re = \frac{G^2 T}{\rho_z \mu}$$

If the reaction mechanism is the same for two systems, then we can assume that ρ_1/ρ_z is the same for each in the reaction zone. Therefore for a pair of systems I and II under comparison, in the reaction zone

$$\frac{Re_I}{Re_{II}} = \frac{G_I^2 (\rho_1)_I}{G_{II}^2 (\rho_1)_{II}} \cdot \frac{\mu_{II}}{\mu_I} \cdot \frac{T_I}{T_{II}} \tag{3}$$

Now the Mach product,

$$\gamma M^2 = u_1^2 \rho_1 / P_1 \qquad \text{eqn. (7), section 1.2.1.}$$

Defining G as $\rho_1 u_1$,

$$\gamma M^2 = \underline{G}^2 / \rho_1 P_1$$

It was observed experimentally that the Mach products for each pair at a given composition near the limits were nearly the same (see Table 3.2, p. 78).

ie. $$\frac{(\gamma M^2)_I}{(\gamma M^2)_{II}} = \frac{\underline{G}_I^2 (\rho_1)_{II}(P_1)_{II}}{\underline{G}_{II}^2(\rho_1)_I (P_1)_I} \doteq 1 \qquad (4)$$

Substituting (4) into (3), together with the fact that $(P_1)_I = (P_1)_{II}$, and assuming that, because of the hydrodynamic similarity between the systems I and II, $G/\underline{G}$ is constant,

$$\frac{Re_I}{Re_{II}} = \frac{\mu_{II}}{\mu_I} \cdot \frac{T_I}{T_{II}} \qquad (5)$$

On this basis, a decrease in viscosity or an increase in induction time would accelerate the onset of turbulence and lead to narrower limits. If it is assumed that the induction time for a certain degree of dilution of any particular reactive base is constant, then $T_{helium}=T_{argon}$, and

$$\frac{Re_{argon}}{Re_{helium}} = \frac{\mu_{helium}}{\mu_{argon}} \doteq 0.8$$

Since the induction time for deuterium mixtures should be about twice that for hydrogen mixtures (Gray and Smith, 1967), then

$$\frac{Re_{hydrogen}}{Re_{deuterium}} \doteq \frac{\mu_{deuterium}}{\mu_{hydrogen}} \times 0.5 \doteq 0.7$$

These diluents appear in the limit mixtures in concentrations greater than 80%, so the mixtures would be expected to behave similarly to the pure gases.

Thus the onset of turbulence, and therefore the limits, should occur at lesser dilutions of helium than argon, and at lesser dilutions of deuterium than hydrogen. This is what was observed in practice. Although the mathematical treatment given above is very approximate, it does show that the transition from laminar to turbulent flow could contribute significantly to the failure of detonation.

Some other factors which have not been mentioned so far could also play an important role in detonation failure.

4.3.3. Transfer between translational and internal energy:

It has been suggested (Miles, Munday and Ubbelohde, 1962) that the distribution between translational and internal degrees of freedom may fail to equilibrate near the detonation limits, although contradictory evidence has been found (White and Moore, 1965). The question has yet to be fully resolved. If this failure to equilibrate is important, then the efficiency of the diluent molecules in promoting internal energy transfer might be related to detonation failure. From previous findings (references in Cottrell and McCoubrey, 1961) the sequence of efficiencies would be expected to be $H_2 > D_2 \doteqdot He > A$.

On this basis, the use of argon as a diluent would lead to higher translational temperatures and lower vibrational temperatures than in corresponding mixtures diluted with helium. A higher translational temperature could result in a greater rate of chain carrier formation on the plausible assumption that molecules react rapidly before equilibriating their internal energy. In this case the induction zone would be longer for helium admixtures than argon admixtures, and narrower limits would be expected.

Conversely, a lower vibrational temperature could lead to a slower rate of dissociation in the induction zone, with the opposite effect to that mentioned above.

The conflicting nature of the results for helium vs. argon and hydrogen vs. deuterium gives no indication as to which of the above processes is operative. In view of the lack of knowledge about rates of equilibration in detonation fronts, no specific conclusions can yet be drawn.

4.3.4. Molecular diffusion:

Thermal diffusion could lead to marked "Soret" concentration gradients of atoms and molecules normal to the shock front. In view of the large mass differences between hydrogen and the other molecules, the effect could be quite pronounced.

On this basis, concentration gradients of hydrogen should be more marked with argon than with helium, the

similar gradients of deuterium being less marked. Although the narrower limits for $S_D + D_2$ than for $S_H + H_2$ might be explained in this way, the limits for helium and argon admixtures are in the wrong sense.

A possible reason for this anomaly could lie in the difference in the relative masses of helium and argon w.r.t. the fuel and oxygen. For hydrogen and deuterium based mixtures, helium would tend to separate the reacting species whilst argon would not. However, for cyanogen based mixtures, the opposite effect should be observed. As it was not, it appears that the above arguments cannot alone explain the difference in the limiting concentrations.

Until more evidence is available, these proposals cannot be properly tested.

4.3.5. Diffusion of electrically charged particles:

Because of their high thermal velocities, electrons would be expected to move ahead of the detonation front. This phenomenon has been observed in shock waves (Weymann, 1960). This would leave a net positive charge within the detonation front. There was evidence that such a charge separation occurred near limiting concentrations in the present research (see section 4.2).

Such a "detonation dipole" may be of more importance in controlling the onset of chemical reaction than the Soret concentration gradients mentioned above.

This suggestion is strengthened by the difference in limiting concentrations between S_C + He and S_C + A (8.2%) being greater than between S_H + He and S_H + A (2.8%) where greater concentration gradients should exist. If a detonation dipole is important, then the above results seem to indicate that a larger dipole would result in a shorter induction time, and therefore wider limits.

Argon has a lower ionisation potential (15.76 ev) than helium (24.58 ev) and therefore, if ionisation is important, its addition to an explosive mixture should lead to wider limits than the same degree of dilution with helium. This was found to be the case. Similarly, hydrogen (15.44 ev) led to wider limits than deuterium (15.5 ev).

It seems that the greater limiting concentration difference between helium and argon dilutions for the cyanogen based mixtures than for the other reactive bases (see above) cannot be simply explained in terms of any Soret effects. However, as different reaction chemistry and kinetics are concerned, and other factors contribute to detonation failure as well, this is not necessarily a criticism against mass effects operating in the other systems.

All of the above mentioned factors would contribute to the failure of detonation, but insufficient knowledge was gained to allow an estimation of the relative contribution of each.

4.4. Conclusions:

Detonation limits for gaseous mixtures can only be partly explained by the existing theories. There are now indications that the following factors may contribute to detonation failure:

(i) A critical Reynolds number at the wall in the reaction zone above which turbulent flow occurs, ultimately resulting in a rapid increase in the heat losses to the containing walls;

(ii) Failure to equilibrate internal degrees of freedom, therefore altering the induction zone length and consequently the limits;

(iii) A Soret concentration gradient of reactant atoms and molecules across the detonation front which alters the rates of chemical reaction; and

(iv) An electrical "detonation dipole" across the detonation front which could have a controlling influence on the rate of energy liberation in the detonation front.

Insufficient results were obtained to allow a quantitative evaluation of the contribution of each of these factors, but a guide is given for further research in the field. This knowledge, once obtained, could result in a much better understanding of the mechanism of detonation and of detonation failure.

CHAPTER 5.

DETONATION VELOCITY IRREGULARITIES.

5.1. Introduction:

It is well known that experimental detonation velocities can be accurately predicted by the hydrodynamic theory (see section 1.2.1, p.13) except at or near marginal conditions, and have been found to vary regularly with change in composition (see curves given by Wagner, 1961). Near the limiting concentrations, small fluctuations in the velocity-composition relationships have been observed and attempts have been made to explain their existence (see section 1.2.2, p.20).

Despite these fluctuations, only one stable velocity of propagation has been hitherto observed for any particular non-solid-depositing explosive gas mixture. This is to be expected as the enthalpy change of the chemical reactions is fully determined and itself determines the hydrodynamic rate of advancement. The separate case for solid-depositing explosive gas mixtures is discussed below (see section 5.4.1.4, p.113).

In the present researches, various types of velocity irregularities were found to occur with small changes in composition. These were extremely reproducible (see section 3.2.1, p.72). In addition, a second reproducible velocity regime was observed in the non-solid-depositing mixtures

of hydrogen and deuterium with oxygen.(section 3.2.2, p. 74). In an attempt to elucidate the factors controlling these anonalous phenomena, some earlier results were re-examined, and some further experiments were conducted.

5.2. Additional apparatus:

Three additional sets of experiments were designed to investigate the following properties:

(i) The peripheral profile of the ionisation front;

(ii) The composition of the burnt gases immediately behind the C-J plane; and

(iii) The residual pressure of the product gases in the detonation tube after detonation.

5.2.1. Ionisation profile at the walls:

Errors in detonation velocity measurements could result from a non-planar ionisation front, that is the region in the detonation wave which triggers the ionisation probes (see results section below). To investigate the peripheral profile of the ionisation front, an additional short length of tube was fitted to the end of the test section. Into this, four identical ionisation probes were mounted, equally spaced around a circumference (see figure 5.1). The same probe circuits were used as previously described (section 2.2.3.1) with the cathode followers omitted, and each circuit connected to the oscilloscope via a Harwell 2000 series Type 2151 amplifier. The probe signals were displayed on two

dual-beam oscilloscopes (Tektronix, Types 551 and 555), one signal on each trace. So that the time bases for the two oscilloscopes were the same, the time base for one was externally connected to the horizontal amplifier of the other.

An ionisation probe mounted six inches upstream of the measuring probes was originally used to trigger the oscilloscopes. However, as this proved to be unsatisfactory, the trigger probe in the priming section was used in conjunction with the time delay unit which was built into the Type 555 oscilloscope, the delay time having been previously found by trial and error. To reduce interference to the oscilloscope trigger by the sparking plug, the sparking plug circuit was replaced by a Brandenburg Type S.0530/10 high voltage generator in conjunction with a 1 μF photoflash capacitor.

A 50 μ second time mark signal was z-modulated onto each beam so as to calibrate each oscilloscope for each run, and to give a datum point for the time interval determinations. The time intervals between one particular time mark signal (reference time) and the passage of the ionisation front past the individual probes was then determined in the usual way (see section 2.4.1.4).

Using the acoustic theory of spin (Fay, 1952), the pitch to diameter ratio for a spinning detonation head is

given approximately as

$$\frac{P}{d} = \frac{\pi (\gamma_1 + 1)}{\gamma_1 k_n}$$

where k_n = 1.841 for single headed spin, and 5.35 for four-headed spin; and γ_1 is the specific heat ratio of the unreacted gas. The angle of incidence at the wall of the detonation front to the line of centres of the probes, θ, can then be calculated.

After passing an ionisation probe, any particular point on the ionisation front periphery travels at this angle θ to the line of centres of the probes with a velocity $u_1/\sin \theta$, where u_1 is the average detonation velocity along the axis of the tube. The value of u_1 can be found from the velocity-composition relationship, and $u_1/\sin \theta$ determined from the value of θ calculated as above.

The distances travelled after the reference time by those points on the ionisation front periphery which pass each probe can then be calculated from the time intervals determined as above and the velocity $u_1/\sin \theta$. When the probe locations are marked on a development of the tube wall, the ionisation front profile can be found by plotting these distances in the direction θ to the line of centres of the probes. Unfortunately, the direction of rotation of the spin head is uncertain, but was later shown to be the same in all cases.

As a further test for the structure of the spin head, and therefore the ionisation front, an "end plate soot pattern" was determined by the method used by Duff (1961) for detonations in mixtures of the same composition as were used in the above experiments. These patterns were obtained by coating a glass disc with soot from a wooden match, and rigidly attaching it to the end of the test section. After the detonation, the disc was carefully removed and coated with varnish so as to keep a permanert record.

5.2.2. Composition of detonation products:

5.2.2.1. Collection:

In special experiments to enable the product gases to be collected before any additional reaction could occur, a cooled "dump chamber" was fitted to the end of the test section. This consisted of an expansion section leading into a six inch diameter glass tube. A pointed one inch diameter glass tube was centrally mounted inside the larger tube, with provision for filling it with a freezing mixture of acetone and solid carbon dioxide. The composite vessel was evacuated before each detonation by a positive displacement vacuum pump (figure 5.2).

The dump chamber was separated from the expansion section by a "melinex" diaphragm which burst on impact from the detonation front, allowing the product gases to condense and subsequently freeze on the cooled central tube in transit.

Preliminary experiments with the test mixture under investigation showed that no reflected shock could be discerned on the oscilloscope traces of the ionisation probe signals, therefore suggesting that the collected products were not subjected to a second shock wave.

During each detonation, the detonation velocity was determined in the usual way to ascertain whether the velocity was in the upper or lower regime. To avoid interference with the analysis by the introduction of atmospheric oxygen, the tube and dump chamber were filled with 99.5% argon immediately after each detonation.

5.2.2.2. Analysis :

The products were analysed qualitatively for the presence of hydrogen peroxide. The method used was that described by Egerton, Smith and Ubbelohde (1935), which consists of adding 20% potassium iodide solution to the test solution together with a few drops of saturated ammonium molybdate solution. A positive test is indicated by the solution turning yellow after about 30 seconds.

After collection of the products in the dump chamber, the freezing mixture was removed, the vessel allowed to return to room temperature and removed from the detonation tube. The central freezing tube was washed with 20 ml. of 20% potassium iodide solution and the wash then transferred

to a flask. A few drops of saturated ammonium molybdate solution were added and the colour change noted. Preliminary tests with a known concentration of hydrogen peroxide showed the sensitivity of the test to be about 5×10^{-4} g./20 ml. of solution. An increase in the concentration resulted in very little colour change above 5×10^{-2} g./20 ml. of solution. In view of the gradual change of the sample colour with time, quantitative estimation was impracticable.

5.2.3. Residual pressure:

A manometer was attached, via a length of rubber vacuum hose and a valve, to the end plate of the test section. After detonation, the valve was opened and the pressure recorded. The residual pressure was then determined by the method given in Appendix A.4.2.

5.3. Supplementary results:

5.3.1. Sinusoidal fluctuations:

The regular nature of these suggested that they might be due to the rotation of a non-planar ionisation front past the ionisation probes. In order to determine the circumferential profile of the ionisation front, a ring of probes, as described in section 5.2.1, was mounted at the end of the test section. Preliminary investigations showed that the spin head detected in this way always followed the same path down the tube for any one mixture composition, even if

another composition were used in between the determinations (see figure 5.3). Possible reasons for this phenomenon are discussed below in section 5.4.1.2.

This fact was used to determine a twelve point profile by rotating the ring of probes through 30° after each of three determinations, and superpositioning the three sets of results.

Twelve point profiles were determined for detonations in the S_H + A system, one determination in section A (ref. figure 3.4), two in section B, and one in section C. These profiles are shown in figures 5.4.1 to 5.4.4.

In section A (88.00% A) there appeared to be four spin heads with a line of weaker ionisation extending back into the burnt gas from each of the four trailing edges (see figure 5.4.1). However, definite interpretation was difficult.

In section B (89.17 and 89.86% A), only one spin head was found. Unlike section A, two trailing lines of ionisation were found to occur; one from the trailing edge, and one from the leading edge (figures 5.4.2 and 5.4.3). The former could have been due to the reflected shock described by Schott (line CG, figure 1.5), but the reason for the occurrence of the other was not apparent. The maximum

axial distance across the ionisation front (1.9 cm) was considerably greater than in section A (0.3 cm) in both cases.

In section C (91.21% A) only one spin head occurred, but the circumferential location of the trailing edge varied on successive determinations (figure 5.4.4). However, the profiles had the same general nature as those found in section B, but with slightly less axial distance across the front.

The end plate soot patterns obtained for the same mixture compositions as above are shown in figures 5.5.1 and 5.5.2. In section A (88.00% A) the large number of lines etched in the soot could not be definitely interpreted, but appeared to be due to a multiheaded spin front, therefore partially substantiating the ionisation front profile found for section A. In section B (89.17% A) the soot pattern was similar to that found by Duff (1961) for single headed spin.

Duff found that a single spin head etched three lines on the end plate, these being arranged as a distorted "Y". He proposed that they were the impressions of the line of intersection between the incident shock and the Mach stem, the boundary of the incident shock, and the boundary of the Mach stem. In the present experiment, a similar "Y" was also etched on the end plate, with the lines described by Duff corresponding to the lines OM, OA and OB in figure 5.5.2 respectively. The other, fainter lines found on the end

plate cannot be simply accounted for, but could be due to shock interaction after reflection from the end plate.

The effect on the velocity-composition curve of altering the distance from the impact surface to the first probe was determined by filling the ball in the separating valve with test mixture instead of priming mixture as before. The resulting horizontal shift of the fluctuations is shown in figure 3.5.

5.3.2. Second velocity regimes:

The values of the velocities in the lower regimes suggested (see discussion, section 5.4.2.1 below) that the lower regime detonations derived their energy of propagation from the formation of hydrogen peroxide (34 Kcal/mole) instead of water (58 Kcal/mole) or deuterium peroxide instead of heavy water. This proposal was tested in three ways:

(i) By analysing the product gases for hydrogen peroxide;

(ii) By measuring the residual pressure of the product gases; and

(iii) By comparing the measured upper and lower regime detonation velocities with those calculated from the hydrodynamic theory for both water and hydrogen peroxide formation.

As decomposition of hydrogen peroxide behind the

detonation front could produce enough energy for the existence of a second detonation wave to follow the first, the photographs of the oscilloscope traces were inspected for peaks which could be due to such a wave.

5.3.2.1. Detection of hydrogen peroxide:

Using the cooled dump chamber described in section 5.2.1 the product gases for the mixture S_H + 39.5% CO_2 were analysed for hydrogen peroxide, the detonation velocity being determined in each case. The results (Table 5.1) show a positive test for all lower velocity regime detonations, and a negative test for all normal regime detonations. In all cases, a negative test means a concentration of hydrogen peroxide of less than 5×10^{-4} g./20 ml. and a positive test of greater than 5×10^{-2} g./20 ml. of solution. It should be noted that this latter concentration is equivalent to complete reaction to hydrogen peroxide in six inches of tube.

TABLE 5.1. Test for the presence of hydrogen peroxide in the end products of detonations in S_H + 39.5% CO_2:

% diluent	detonation velocity (m/sec.)	regime	test
39.61	996	lower	positive
39.61	1580	normal	negative
39.61	965	lower	positive
39.48	1350	normal	negative
39.48	1313	normal	negative
39.48	1023	lower	positive

5.3.2.2. Residual pressure measurements:

Residual pressures were determined for detonations in the systems S_H + H_2 and S_H + O_2 at compositions where either regime could occur. The results are tabulated in Appendix A.4.2, together with the calculated values. As only two results were obtained for fuel-rich mixtures for the lower velocity regime, the test only serves as an indication. Analysis of the residual gases for oxygen (formed by decomposition of the hydrogen peroxide) would have rendered the test more meaningful, but this was not practicable.

5.3.2.3. Steady state detonation velocity calculations:

Detonation velocities for the system S_H + 92.5% H_2 were calculated (see Appendix A.5). These are compared with the experimental values in Table 5.2.

TABLE 5.2. Comparison of calculated detonation velocities with experimental normal and lower regime velocities for near-limiting concentrations:

	forming water	forming hydrogen peroxide	ratio
calculated	3800	2245	1.69
experimental	3530	1900	1.86

5.3.2.4. Second detonation front:

On re-examining the oscilloscope traces for the lower velocity regime in the system S_H + CO_2, a second set of signals was observed to lie slightly behind the first (see figure 5.6). These could not be accounted for in terms of a wave reflected from the end of the tube.

In all cases the velocity calculated on the assumption of this being a second detonation front was higher than that of the first front (see broken line, figure 3.7), and the distance of the second wave from the first increased as the limits were approached. The results are tabulated in Table 5.3.

The possible origin of the second detonation front are discussed below, page 119.

TABLE 5.3. Measured velocities of the second detonation front in the lower regime of the system $S_H + CO_2$ and its distance behind the first:

% diluent	velocity of first front (m/sec.)	velocity of second front (m/sec.)	distance between the two (cm.)
39.53	976	993	6
39.80	996	1013	4
39.98	1031	-	-
40.18	1059	-	-
42.00	868	1047	18
45.18	752	1055	39
47.41	745	1077	40
49.97	711	1156	51
50.83	724	1135	51
51.47	716	1095	49
52.17	657	1062	48
52.63	-	690	-

5.4. Discussion:

5.4.1. Velocity irregularities:

The irregularities in the velocity-composition relationships could have either been real, or due to the

experimental method. In the latter case, the measured time intervals could differ slightly from the true values due to a slight increase in dilution, thereby resulting in "apparent" velocity irregularities. This possibility will be discussed in greater detail below. Some idea as to which of these possibilities is operative might be gained from examination of the ionisation front peripheral profiles for the S_H + A systen.

5.4.1.1. Sinusoidal fluctuations:

Inspection of figures 5.4.1 to 5.4.4 shows that sections A, B and C of the velocity curve for the system S_H + A are associated with three different types of profile. That shown in figure 5.4.1 appears to be a four-headed spin front. The maximum axial distance across the front is small, and any fluctuations would be comparable to the experimental error, and therefore would not be observed. On the other hand, the profiles for section B (figures 5.4.2 and 5.4.3) show definitely the existence of a single headed spin front of the type described by Schott (1965) (see section 1.2.4.2, p. 31).

Since only two detecting probes were used in most of the velocity determinations, it would be possible for either a leading or a trailing edge of the ionisation front to pass the probe, resulting in a different time interval measurement in each case. A slight regular increase in dilution could lead to an axial displacement of the spin path, and therefore to fluctuations in the measured time interval as observed. The time difference between the leading edge of the ionisation front passing the tube circumference on which the probe is situated, and the ionisation front passing the probe will subsequently be referred to as the "time displacement". Calculation of the pitch to diameter ratio shows that the pitch changes from 2.749 inches to 2.746 inches across the composition range where the sinusoidal fluctuations occur. It therefore appears probable that the fluctuations occur as a result of the axial displacement of the spin path as the composition is changed.

If the ionisation front is regarded as having a sinusoidal profile on the development of the tube wall at any instant, a regular axial displacement of the spin path with change in composition would result in a sinusoidal time displacement at each probe with change in composition.

The addition of the time displacements at the two probes would result in an overall sinusoidal time displacement, the amplitude being between zero and twice the individual values depending upon the phase difference between them.

The maximum distance between the leading and trailing edges of the ionisation front, measured in the direction of motion of the spin head, for S_H + 89.86% A is 2.6 cm. The maximum fluctuation in the apparent velocity due to this effect would therefore be 2 × 2.6 = 5.2%. The experimental value is 30 m/sec., or 2.7%, which agrees in order of magnitude.

In section C, the spin head had the same nature as in section B, but the head did not always follow the same path down the tube. Consequently, fluctuations that did occur were not reproducible, and the average of several velocity determinations gave a more accurate value for the true axial velocity of the front.

This was partially substantiated by examining the magnitude of the variations over the three separate velocity determinations at each composition (see Appendix A.2.4, values given in parentheses). In section B the average variation is 15 m/sec., whilst in section C it is 25 m/sec. which is approximately the magnitude of the reproducible

fluctuations (30 m/sec.) in section B. However, the reliability of this conclusion must be questioned owing to the small number of results obtained in section C.

5.4.1.2. Spin path reproducibility:

These arguments introduce the perplexing problem of why a spinning detonation front in an axially symmetric tube should always follow the same path down the tube wall for detonations in mixtures of the same composition. If this reproducibility were caused by a previous spin head etching a fine helical groove in the tube wall (as suggested by Bone and Fraser, 1932), and this groove were to stabilise subsequent spin heads, then a slight change in composition should not change the path. Furthermore, one would not expect to reproduce the path of the spin head after several other mixture compositions had been detonated. In fact, the spin path was found to change with composition (note positions of the triple points in figures 5.4.2 and 5.4.3) and to be fully reproducible for any one mixture composition.

These properties of the spin head suggested that the reproducibility could be due to a combination of the two factors: an extremely reproducible pre-spin distance (that is the distance travelled by the detonation between initiation and the formation of a fully developed spin head) in the

test mixture which increased as the limit was approached; and some longitudinal irregularity in the tube wall - such as a scratch or slight bend - which initiated the formation of the spin head. In this way, a slight increase in dilution would result in a slight axial movement of the spin path towards the end of the tube.

To test this hypothesis, the distance from the impact surface to the first probe was increased (see section 5.3.1.1), and the velocity-composition relationship redetermined. The resulting horizontal shift of the fluctuations (figure 3.5) of approximately half a cycle substantiated this model as the increase in distance ($1\frac{1}{4}$ inches) was approximately half the spin pitch ($2\frac{3}{4}$ inches).

The effect of replacing hydrogen by deuterium was to alter the reaction rates involved in initiation, and therefore probably the pre-spin distance, whilst keeping most other factors constant. As expected, this resulted in a horizontal shift of the fluctuations as above (figure 3.5).

These arguments do not, however, account for the sudden increases in velocity at the transitions from sections A to B and B to C in the S_H + A system, or for the fluctuations in the other systems.

5.4.1.3. Irregular fluctuations:

For most of the systems investigated, the

oscillatory nature of the irregular fluctuations suggested that they could result from a non-planar ionisation front as described above. If the ionisation front profile were not truly sinusoidal, the addition of the displacements could give rise to a non-sinusoidal fluctuation for certain phase differences between the individual errors (see figure 5.7). The fluctuations so obtained are similar to those obtained for the systems $S_H + H_2$, $S_H + He$, $S_D + D_2$ and $S_O + O_2$ (figures 3.6 and 3.9). The percentage fluctuations (1.4, 0.7, 0.6 and 3.0 respectively) are in the order of those expected from this type of behaviour (see section 5.4.1.1).

However, to explain the quite large fluctuations in the systems $S_H + CO_2$ and $S_H + NH_3$ (12.9% and 6.5% respectively) in this way, the maximum axial distance across the ionising front would have to be in the order of 6.5 and 3.3 cm respectively. For geometric reasons these values, especially for $S_H + CO_2$, seem excessive.

Inspection of figure 3.8 shows that replacement of the stainless steel tube by the coated brass tube altered the magnitude of the fluctuations in the $S_H + NH_3$ system. Assuming that the ionisation front profile and the pitch to diameter ratio are not affected by the nature of the tube surface, the magnitude of and the phase difference between the individual errors, and therefore the magnitude of the fluctuations, should be the same for the two tubes. This was

not the case. Although the above assumption is not necessarily true, and there is no guarantee that reproducible spin paths were produced in the coated tube, it appears that the irregular fluctuations in the $S_H + NH_3$ cannot be explained in terms of a non-planar ionisation front. Indeed, there is evidence that a reproducible spin path cannot exist for systems with a lower velocity regime (see section 5.4.2.2).

Insufficient information was obtained from the experiments conducted to establish a more plausible explanation, but some indication of the true reason could be obtained from a study of the large irregular fluctuations in the system $S_H + A$. These cannot be ascribed to variations introduced by the structure of the ionisation front, but several possible mechanisms could have some effect on the phenomena.

Inspection of figures 3.4, 5.4.1 to 5.4.4 show that the sudden increases in velocity are associated with a change in the number of spin heads (section A to B) and a loss of restraint on the path of the single spin head (section B to C).

If a certain amount of energy is required to sustain each spin head, as is suggested by the acoustic theory, then a decrease in the number of spin heads would result in an increase in the energy available for linear propagation. But, as no information about the energy required to sustain a spin head is available, this proposal cannot be tested as yet.

It is difficult to explain the rise in velocity in section C in terms of an increase in available energy due to a loss of restraint on the spin path. This is especially true if the reason for the reproducible spin path given above is valid. The only obvious reasons for the spin path becoming random in section C are: a loss in reproducibility of the pre-spin distance; or that the tube irregularity lay wholly within the pre-spin distance, and therefore did not influence the spin initiation. Whatever the reason, for the loss of reproducibility of the spin path to result in a rise in velocity, the mechanisms for the two would have to be related. No such relationship was found in this research.

A more probable explanation is that the increase in velocity and the loss of reproducibility occurring at the same composition was co-incidental, and that the rise in velocity was due to some other factor, for example, failure to equilibriate all the degrees of freedom (Jost, 1935, 1937).

5.4.1.4. Increase in Mach product:

For detonations in the system $S_C + C_2N_2$, it can be seen from figure 3.10 that the values of γM^2 start to increase again at about 35% dilution. This does not appear to bear any resemblance to the increases due to the fluctuations mentioned earlier, but rather to the steady increase observed in fuel-rich acetylene-oxygen mixtures

(Kistiakowsky et al., 1955, 1956).

As the fuel-rich cyanogen-oxygen mixtures also formed a solid carbon residue on detonation, it is quite probable that the reason for the increase is the same in both cases. This phenomenon can be explained (Kistiakowsky and Mangelsdorf, 1956) in terms of the extension of the hydrodynamic theory proposed by Kirkwood and Wood (1954). They proposed that the C-J plane is associated with the condition that

$$\sum_{1}^{n} \sigma_j r_j = 0$$

where j is one of the n possible reactions, σ_j is the effect of this reaction on the pressure of the system due to enthalpy and molecular weight changes, and r_j is the rate of this reaction. The classical C-J condition occurs when all of the rates in the summation vanish separately. However, considering finite reaction times, it is possible that the summation may vanish when positive values of σ are balanced by negative values. This situation is referred to by Kirkwood and Wood as "pathological", and in such cases the actual detonation velocity is higher than that calculated by assuming instantaneous attainment of thermodynamic equilibrium.

As an extension of this argument, two or more zeros could be obtained in the summation, therefore leading to several possible C-J planes. The existence of two separate

C-J planes has indeed been found, for example, during detonations in fuel-rich acetylene-oxygen mixtures (Kistiakowsky and Mangelsdorf, 1956). In this case the second zero corresponds to the C-J plane of a second detonation wave within the rarefaction wave of the first. This second wave derives its energy of propagation from the condensation of the gaseous reaction products of the first. The two detonation waves eventually coalesce, thereby stabilising the process.

Two stable velocities can therefore be measured in different parts of the tube; one in the region before the merging of the two waves, and thereafter a higher velocity which is the velocity of the composite detonation front. The distance travelled by the two waves before merging depends upon the nature of the tube, and the mode of initiation.

5.4.1.5. The unstable region:

In the systems $S_H + H_2$, $S_H + O_2$ and $S_D + O_2$ there occurs a narrow composition range near the limits at which the detonation velocity becomes erratic. This occurs at the same composition as the onset of the lower velocity regime, and the nature of this region and its possible causes will be described below in section 5.4.2.3.

5.4.2. The lower velocity regime:

The tests described in section 5.3.2 showed fairly conclusively that the second velocity regime was due to a

stable detonation wave deriving its energy of propagation from the formation of hydrogen (deuterium) peroxide. But some reservations about the validity of some of the tests must be made.

5.4.2.1. Tests for the formation of hydrogen peroxide:

Before accepting the evidence that hydrogen peroxide is formed, the criticism that the chemical analyses could have been in error due to the interaction of atmospheric oxygen with the reagent must be examined. However, the filling of the dump chamber with argon immediately after detonation, and the negative tests obtained for the normal velocity regime seem to exclude this possibility.

It is also possible that the hydrogen peroxide which was detected was not formed within the detonation front, but in the process of expanding into the dump chamber. This possibility was also excluded in view of a preliminary experiment in which the dump chamber was made exclusively of glass. The detonation front, after entering the vessel, punched a hole of approximately one inch diameter in the opposite wall of the vessel, 30 inches from where it entered. This indicated that the slug of gas did not expand appreciably in the evacuated vessel.

As a positive test was obtained in the above experiment (not listed in Table 5.1), confirmation was obtained that the product gases condensed on the cooling tube

on their first passage past it. It therefore appeared that the chemical analyses were valid.

The measured residual pressures for fuel-rich hydrogen-oxygen mixtures showed good agreement with the calculated values for the normal regime (water formation). They were slightly lower than the values calculated for the lower regime on the assumption that hydrogen peroxide decomposed to water and oxygen (see Appendix A.4.2). This could be explained if the second detonation wave (section 5.3.2.4) had merged with the first before reaching the end of the tube.

All these experiments, although verifying the formation of hydrogen peroxide in the lower velocity regime, do not show the reason for its formation.

5.4.2.2. Formation of hydrogen peroxide:

For the isothermal reaction of hydrogen and oxygen, it has been observed (see Lewis and von Elbe, 1961, p. 24) that an S-shaped line on the pressure-temperature plane marks the transition from steady state reaction to explosion (figure 5.8). Between the second and third limits the reactions

$$H + O_2 + M \longrightarrow HO_2 + M \qquad (I)$$

and

$$HO_2 + H_2 \longrightarrow H_2O_2 + H \qquad (II)$$

are of considerable importance. This has been verified (Pease, 1930; Holt and Oldenberg, 1947) by measuring the concentration of hydrogen peroxide in the reaction zone.

These reactions would not appear to have any bearing on the reactions involved in detonations as the pressures and temperatures existing in a detonation front do not coincide with the values between the second and third explosion limits.

However, it has been found (Voevodsky and Soloukhin, 1965) that a similar sharp line of demarcation exists between two distinct modes of ignition in shock heated gases. This is shown as a dotted line in figure 5.8. Below the line, ignition at a single point is sufficient to lead rapidly to detonation. Above the line, ignition occurs at many points and the combustion surfaces merge to form a "feeble" ignition. As this line of demarcation is essentially an extrapolation of the second limit line, it is possible that the processes leading to the occurrence of the second explosion limit also lead to the occurrence of this limit for ignition in shock heated gases. It would then follow that reaction (II) above could be of importance in the feeble ignition regime.

If the ignition processes in the shock heated gas are similar to those in the gas immediately behind a detonation shock front then, for shock temperatures and pressures corresponding to conditions above the limit line, feeble ignition may occur leading to the formation of hydrogen peroxide in the detonation front. The lower enthalpy release of the reaction could therefore lead to the lower velocity regime.

A second detonation front resulting from the decomposition of the hydrogen peroxide could eventually overtake the first, the system thereby reverting to the upper regime. This mechanism could also occur for the deuterium-oxygen system. This was found to occur (section 5.2.3.4). If the two detonation waves always merged before reaching the detecting stations, then no lower regime would be observed. This could explain the behaviour of the $S_H + A$, $S_H + He$, $S_H + NH_3$ and $S_D + D_2$ systems.

It should be noted that the width of the composition range where both upper and lower velocity regimes could occur indicates that the distance travelled by the two detonation waves before merging is not consistent. If this were so, then the arguments proposed in section 5.4.1.3 for the cause of the irregular fluctuations in terms of a reproducible spin path would be invalid. This question remains unresolved.

As the tube diameter and the distance from the impact surface to the first probe was the same for the stainless steel and the coated tube, the change in the nature of the transition from the upper to the lower velocity regime due to the use of the coated tube (figures 3.13, 3.12 and 3.7.) could only be due to the changing of the tube surface. This effect could, for example, alter the rate of destruction of HO_2 at the walls.

However, as the surface of the coated tube remained constant throughout, this explanation does not account in any simple way for the coated tube inhibiting the lower regime in some mixtures ($S_H + O_2$) and the upper regime in others ($S_H + H_2$). The only explanation of this behaviour is that the distance that the two separate detonation waves must travel before merging depends upon the properties of the diluent as well as the nature of the tube wall. Insufficient information was obtained from the experiments performed to permit a definite choice of the factors involved.

5.4.2.3. Velocity irregularities in the transition region:

As mentioned in section 5.4.1.5, the onset of the lower velocity regime is accompanied by an unstable region in the upper velocity regime (figures 3.6, 3.11 and 3.12). Such a region was probably present in the $S_H + O_2$ system in the stainless steel tube as well, but was not detected. This region could be due to the detonation front being unstable at the moment of merging of the two individual waves, thereby resulting in a variable velocity at the detecting stations.

The one exception to this proposal was the system $S_H + O_2$ in the coated tube, where the unstable region occurred even though it was not accompanied by a lower velocity regime. This finding, together with the

observation that the unstable region did not extend throughout the entire transition region, suggested that the unstable region is a property of the detonating systems, and is therefore not affected by changing the nature of the tube walls or the distance from the impact surface to the measuring stations. This proposal also remains unverified.

5.5. Conclusions:

Most of the systems investigated displayed some form of anomalous behaviour in the velocity-composition relationships near the limits. Some of these anomalies, such as sinusoidal fluctuations on the velocity-composition curves and a second velocity regime, could be attributed to the method of determining the detonation velocities, there being indications that the former would not have been observed if a different method of measuring detonation velocities had been used, or the latter observed if a longer detonation tube had been employed.

There was firm evidence that the sinusoidal fluctuations were due to a non-planar spin head which led to erroneous velocity measurements. The leading edge of the spin head was found to always follow the same path down the detonation tube wall for any one composition, suggesting that the distance travelled by the detonation front before forming a fully developed spin head was remarkably consistent. As the limits were approached, this

consistency was lost. A satisfactory explanation for the spin path reproducibility was not found.

The second velocity regime in detonations in mixtures containing hydrogen and deuterium appeared to be a quasi-steady state initiation phenomenon. Immediately after initiation of detonations in mixtures with nearly limiting concentrations of diluent, a slower detonation front, due to the formation of hydrogen (deuterium) peroxide, was formed. This metastable initiating process could have been due to the ignition processes in the detonation front being similar to those incurred between the second and third explosion limits for the isothermal reaction. Under these conditions, the formation of hydrogen peroxide rather than water would be favoured.

The decomposition of the hydrogen peroxide behind the detonation front resulted in the formation of a second detonation front which propagated faster than the first, eventually overtaking it. When this occurred, the detonation wave changed to the normal velocity regime.

The other anomalies in the velocity-composition relationships, namely irregular fluctuations, a gradual rise in Mach product with increase in dilution beyond a certain value, and a narrow composition range where the detonation velocity became erratic, appeared to be a

fundamental property of the detonating systems. They would not, therefore, be affected by changing the length of the detonation tube or the method of measuring velocities as above. However, this conclusion was not so fully verified in the present researches to be accepted as a definite property of the detonation wave.

These findings can serve as a guide to further researches into the occurrence of detonation limits. When the factors controlling these phenomena are fully understood they should throw much additional light on the mechanism of detonation.

SECTION 6.

SUMMARY AND RECOMMENDATIONS FOR FURTHER RESEARCH.

The limiting concentrations for various gaseous explosive mixtures were determined and tabulated on p 77. It was found that, in the majority of cases, the shock temperature within the detonation front was approximately the same for any particular reactive base. This strongly suggested that detonation fails when the shock temperature is insufficient for rapid, highly exothermic chemical reaction to occur within the detonation front. In some cases, however, other factors appeared to lead to detonation failure before this condition was reached. These factors can be generally classified as:

(i) molecular mass effects; and

(ii) the possible existence of an electrical dipole in the detonation front.

It was also found that several other factors could have considerable relevance in the problem of elucidating the mechanism of detonation at and near the composition limits, these being:

(i) reproducible fluctuations in the velocity-composition relationships; and

(ii) for hydrogen and deuterium based mixtures, a second, lower velocity co-existing with the normal regime.

6.1. Molecular mass effects:

Differences in limiting concentrations between different mixtures with nearly identical properties other than their molecular masses could not be adequately explained in terms of the existing theories for detonation failure. Several additional factors were proposed as having an effect on the composition limits. These included a critical Reynolds number at which flow in the boundary layer in the reaction zone changes fr m laminar to turbulent, molecular diffusion of the reacting species, and failure to equilibrate internal degrees of freedom.

Determination of the Reynolds number parameters by Schlieren or interferometric techniques would ascertain the validity of the first proposal. Molecular gradients of atoms and molecules are extremely difficult to determine, and a test for the molecular diffusion in the front will remain impracticable until a method of determination is found. Information on equilibration times is at present being accumulated by other workers, but as yet is insufficient to allow for quantitative application to limiting phenomena.

6.2. Electrical dipole:

If an electrical dipole is present in detonation fronts, it could control the rates of chemical reaction, and thereby influence the limiting concentrations. No definite

evidence was found for the existence of such a dipole, but confirmation might be obtained by passing the detonation through a coil, and examining the flow of current in the coil as the detonation passed. Such a coil is at present being constructed in this laboratory.

6.3. Reproducible fluctuations:

Some types of irregularity appeared to be a fundamental property of the reacting systems. A more detailed knowledge of detonation processes, for example relaxation rates and spin structure, than is at present available would be required to explain them. However, reproducible and regular velocity fluctuations with change of composition appeared to be a result of a single spin head always following the same path down the tube wall for any particular mixture composition. This indicated that the distance travelled by the detonation from initiation to the onset of spin was extremely constant. Further investigation of the initiation and stablisation of the detonation by photographic or soot etching techniques could determine the validity of this proposal. If it is found to be correct, then initiation of one detonation by another would be a much less random process than hitherto believed. The elucidation of the processes involved, possibly from the above mentioned experiments, might then contribute to the production of a standing detonation.

If the structure of the spin head is important in limiting behaviour, then the technique for determining the structure of the ionisation front, and the soot etching technique, as described in these researches, could possibly be used for the examination of limiting phenomena.

6.4. Lower velocity regime:

There was strong evidence that the lower velocity regime detonations derived their energy of propagation from the formation of hydrogen (deuterium) peroxide instead of water. The reason for this behaviour cannot be properly explained until the nature of the chemical processes in the detonation front is more fully understood.

Some idea as to the reactions involved could be obtained from the investigation of hydrogen-oxygen detonations in tubes with different wall surfaces. A resin coated tube used in these researches altered the nature of the transition from upper to lower regime, but insufficient results were obtained to draw any specific conclusions. Further research of this nature, for example with a tube internally coated with finely divided platinum, could give some indication of the processes involved.

Further information could be obtained from a more detailed study of the second detonation front found to follow the first, possibly photographically, to ascertain

whether it is due to the decomposition of hydrogen peroxide. A spectroscopic study of the detonation front could determine the free radical compositions at different parts of the detonation front, and therefore clarify the chemical reactions which occur.

Once the above factors have been quantitatively determined, limits could be predicted and progress would have been made in fully understanding the mechanism of detonation.

SECTION 7.

NOMENCLATURE.

Roman symbols:

c	Reduced specific heat = $2\bar{C}_p M_1/R$.
$\bar{C}_p$	Average specific heat at constant pressure between T_1 and T_2 (cals/gm ^oK).
d	Tube diameter (inches).
H_1	Enthalpy of the unreacted gas (cals/gm).
H_2	Enthalpy of the burnt gas at the C-J plane (cals/gm).
$\triangle H$	$H_2 - H_1$ (cals/gm).
$\triangle H_f^o$	Free heat of formation at 298^oK. (cals/mole).
M_1	Molecular weight of the unreacted gas.
M_2	Molecular weight of the burnt gas at the C-J plane.
m	Reduced molecular weight = M_2/M_1.
n	Number of moles of product gas at the C-J plane per mole of unreacted gas = 1/m.
P	Spin pitch (inches).
P_1	Pressure of the unreacted gas (dynes/cm^2).
P_2	Pressure of the burnt gas at the C-J plane (dynes/cm^2).
p	Reduced pressure = P_2/P_1.
p'	Residual pressure in the test section after detonation (cm Hg).
Q	Heat of reaction (cals/mole).
q	Reduced heat of reaction = $2M_1Q/RT_1$.
R	Universal gas constant for unit mole of gas (8.314×10^7 ergs/mole ^oK).

R	Overall pressure in detonation tube after detonation (cm Hg).
r_j	Rate of the chemical reaction j.
S_C	Stoichiometric mixture $C_2N_2 + O_2$.
S_D	Stoichiometric mixture $2D_2 + O_2$.
S_H	Stoichiometric mixture $2H_2 + O_2$.
T	Induction time in the detonation front (seconds).
T_1	Temperature of the unreacted gas (^oK).
T_2	Temperature of the burnt gas at the C-J plane (^oK).
ΔT	$T_2 - T_1$ (^oK).
u_1	Velocity of the unburnt gas w.r.t. the detonation front (cm/sec.).
u_2	Velocity of the burnt gas w.r.t. the detonation front (cm/sec.).
V_1	Specific volume of the unreacted gas (cm^3/gm).
V_2	Specific volume of the burnt gas (cm^3/gm).
v	Reduced specific volume = V_2/V_1.
vp	Vapour pressure of water (cm Hg).
w_z	Local particle velocity in the boundary layer a distance z from the shock front (cm/sec.).
z	Distance measured from the shock front to a point in the boundary layer (cm).

Greek symbols:

γ_1 Specific heat ratio for the unreacted gas.

ϵ Degree of completion of chemical reaction in the detonation front.

θ Reduced temperature = T_2/T_1.

μ Gas viscosity in the boundary layer a distance z behind the shock front (poise).

ρ_z Gas density in the boundary layer a distance z behind the shock front (gm/cm^3).

σ_j Effect of the chemical reaction j on the pressure of a reacting system.

ϕ Pressure correction for equilibrium calculations = p/ρ.

Mixed symbols:

γM^2 Mach product = u_1^2/P_1V_1.

SECTION 8. BIBLIOGRAPHY.

Appleton, J.P. (1966) Physics of Fluids, 9, 336.

Barthel, H.O., & Strehlow, R.A. (1966) ibid 9, 1896.

Becker, R. (1922) Z.Phys., 8, 321.

(1936) Z.Elektrochem., 42, 457.

Belles, F.E. (1959) Seventh Symposium (Int.) on Combustion, p745. Butt rworths: London.

- & Lauver, M.R. (1965) Tenth Symposium (Int.) on Combustion, p285. Comb.Inst.: Pittsburgh.

Berets, D.J., Greene, E.F., & Kistiakowsky, G.B. (1950a) J.Am.Chem.Soc., 72, 1080.

(1950b) ibid 72, 1086.

Berthelot, M., & Vieille, P. (1881) C.R.Acad.Sci., Paris, 93, 18.

Bone, W.A. & Fraser, R.P. (1929) Phil.Trans.Roy.Soc., A228, 197.

(1932) ibid A230, 363.

- , Fraser, R.P., & Wheeler, W.H. (1936) ibid A235, 29.

Borisov, A.A. & Kogarko, S.M. (1963) Dokl. Akad. Nauk, S.S.S.R., 149, 623.

Brinkley, S. (Jnr.), & Richardson, J. (1953) Fourth Symposium (Int.) on Combustion, p450. Williams & Wilkins: Baltimore.

Bulewicz, E.M., & Padley, P.J. (1963) Ninth Symposium (Int.) on Combustion, p647. Academic Press.

Campbell, C., & Finch, A.C.	(1928)	J.Chem.Soc., 131, 2094.
- & Woodhead, D.W.	(1926)	ibid 128, 3010.
	(1927)	ibid 130, 1572.
Chapman, D.L.	(1899)	Phil. Mag., (5) 47, 90.
Cook, M.A., Pack, D.H., & Gey, W.A.	(1959)	Seventh Symposium (Int.) on Combustion, p820. Butterworths: London.
Cottrell, T.L., & McCoubrey, J.C.	(1961)	"Molecular Energy Transfer in Gases", Butterworths: London.
Courant, R., & Friedrichs, K.O.	(1948)	"Supersonic Flow and Shock Waves", Interscience: New York.
Denisov, Y.N., & Troshin, Y.K.	(1959)	Dokl.Akad.Nauk, S.S.S.R., 125, 110.
	(1960)	Sov.Phys.-Tech.Phys., 5, 419.
	(1962)	Eighth Symposium (Int.) on Combustion, p600. Williams & Wilkins: Baltimore.
Dixon, H.B.	(1893)	Phil.Trans.Roy.Soc., A184, 97.
	(1896)	Trans.Chem.Soc., 759.
	(1903)	Phil.Trans.Roy.Soc., A200, 315.
Doering, W.	(1943)	Ann.Physik, 43, 421.
- & Schön, G.	(1950)	Z.Elektrochem., 54, 231.
Duff, R.E.	(1958)	J.Chem.Phys., 28, 1193.
	(1961)	Physics of Fluids, 4, 1427.
- & Knight, H.T.	(1958)	J.Chem.Phys., 29, 956.

Duff, R.E., Knight, H.T., & Rink, J.P. (1958) Physics of Fluids, 1, 393.

Egerton, A., Smith, F.L., & Ubbelohde, A.R. (1935) Phil.Trans.Roy.Soc., A234, 433.

Erpenbeck, J.J. (1963) Ninth Symposium (Int.) on Combustion, p442. Williams & Wilkins: Baltimore.

Fay, J.A. (1952) J.Chem.Phys., 20, 942.

(1953) Fourth Symposium (Int.) on Combustion, p501. Williams & Wilkins: Baltimore.

(1959) Physics of Fluids, 2, 283.

(1962) Eighth Symposium (Int.) on Combustion, p30. Williams & Wilkins: Baltimore.

- & Opel, G.L. (1958) J.Chem.Phys., 29, 955.

Fujimoto, S. (1963) Bull.Chem.Soc., Japan, 36, 1233.

Gaydon, A.G., & Hurle, I.R. (1963) "The Shock Tube in High Temperature Chemical Physics", Chapman & Hall: London.

Gordon, W.E. (1949) Third Symposium on Combustion, Flames and Explosion Phenomena, p579. Williams & Wilkins: Baltimore.

Gray, P., & Smith, D.B. (1967) Chem.Communications, p146.

Greene, E.F., & Toennies, J.P. (1964) "Chemical Reactions in Shock Waves", Arnold.

Hinshelwood, C.N., Williamson, A.T., & Wolfenden, J.H. (1934) Proc.Roy.Soc., A147, 48.

Hirschfelder, J.O., & Curtiss, C.F. (1958) J.Chem.Phys., 28, 1130.

-, Curtiss, C.F., & Barnett, M.P. (1959) ibid 30, 470.

Holt, R.B., & Oldenberg, O. (1947) Phys.Rev., 71, 479.

Hugoniot, H. (1887) J.Ecole Polytechn., 57, 3.

(1889) ibid 58, 1.

Jost, W. (1946) "Explosion and Combustion Processes in Gases", McGraw-Hill.

(1956) Z.Phys.Chem., 196, 102.

Jouguet, E. (1899) Phil. Mag., (5) 47, 90.

(1905) J.Math., 347.

(1906) ibid 6.

(1917) "Mecanique des Explosifs", O.Doin: Paris.

Kirkwood, J.G., & Wood, W.W. (1954) J.Chem.Phys., 22, 1915.

Kistiakowsky, G.B., Knight, H.T., & Malin, M.E. (1952a) J.Chem.Phys., 20, 876.

(1952b) ibid 20, 884.

(1952c) ibid 20, 994.

- & Mangelsdorf, P.C. (1956) J.Chem.Phys., 25, 526.

- & Zinmann, W.G. (1955) ibid 23, 1889.

Kogarko, S.M., & Zeldovich, Y.B. (1948) Dokl. Akad. Nauk, S.S.S.R., 63, 553.

Laffitte, P. (1923) C.R.Acad.Sci., Paris, 177, 178

Laffitte, P.	(1925)	Ann.Phys., Paris, 4, 623.
	(1928)	C.R.Acad.Sci., Paris, 186, 951
- & Dumanois, P.	(1926)	ibid 183, 284.
Le Chatelier, H.L.	(1900)	Ann.Chem., 20, 15.
Lewis, B., & Friauf, J.	(1930)	J.Am.Chem.Soc., 52, 3905.
- & von Elbe, G.	(1961)	"Combustion, Flames and Explosions of Gases", 2nd Ed., Academic Press: New York.
Mallard, E., & Le Chatelier, H.L.	(1881)	C.R.Acad.Sci., Paris, 93, 145.
Manson, N.	(1947)	"Propagation des Detonations et des Deflagrations dans les Melanges Gaseux", L'Office Nat. d'Etudes et des Rech. Aeronaut: Paris.
	(1955)	C.R.Acad.Sci., Paris, 240, 1318.
	(1957)	Z.Elektrochem., 61, 586.
- & Guenoche, H.	(1954)	Revue de l'Inst. Francais du Petrole et Ann. des Combustibles Liquides, 9, 214.
Martin, F.J., & White, D.R.	(1959)	Seventh Symposium (Int.) on Combustion, p856. Butterworths: London.
Michelson, V.A.	(1893)	Uch.Zap.Imp.Moskovsk. Univ., Otdel Fiziko-Math., no.10, pp 1-92.
Miles, J.E.P., Munday, G., & Ubbelohde, A.R.	(1962)	Proc.Roy.Soc., A269, 165.
Mooradian, A.J., & Gordon, W.E.	(1951)	J.Chem.Phys., 19, 1166.

Mullins, B.P.	(1955)	"Spontaneous Ignition" Butterworths: London.
Munday, G.	(1963)	J.Sci.Instr., 40, 603.
Paterson, S.	(1958)	T.V.F., 29, 109.
Payman, W., & Titman, H.	(1935)	Proc.Roy.Soc., A152, 418.
Pease, R.N.	(1930)	J.Am.Chem.Soc., 52, 5106.
Peek, H.M., & Thrap, R.G.	(1957)	J.Chem.Phys., 26, 740.
Pusch, W., & Wagner, H.Gg.	(1965)	Z.Elektrochem., 69, 503.
Rankine, W.J.M.	(1870)	Phil.Trans.Roy.Soc., A160, 277.
Schmidt, E.H.W., Steinicke, H., & Neubert, U.	(1953)	Fourth Symposium (Int.) on Combustion, p658. Williams & Wilkins: Baltimore.
Schott, G.L.	(1965)	Physics of Fluids, 8, 850.
- & Kinsey, J.L.	(1958)	J.Chem.Phys., 29, 1177.
Schuller, W.	(1954)	Dissertation, Darmstadt.
Scorah, R.L.	(1935)	J.Chem.Phys., 3, 425.
Shchelkin, K.I.	(1940)	J.E.T.P.(U.S.S.R.), 10, 823.
	(1945)	Dokl. Akad. Nauk, S.S.S.R., 47, 501.
	(1947)	Z.Techn.Phys.(U.S.S.R.), 17, 613.
	(1955)	J.E.T.P.(U.S.S.R.), 29, 221.
- & Troshin, Y.K.	(1965)	"Gasdynamics of Combustion" Mono Book Corp: Baltimore.
Shtsholkin, K.I.	(1945)	C.R.(Dokl.) Acad.Sci., (U.S.S.R.), 47, 482.

Skinner, G.B. & Ringrose, G.H.	(1965)	J. Chem.Phys., 42, 2190.
Soloukhin, R.I.	(1958)	Dokl. Akad. Nauk, S.S.S.R., 122, 1039.
Strehlow, R.A.	(1964)	Physics of Fluids, 7, 908.
- & Fernandes, F.D.	(1965)	Combustion and Flame, 9, 109.
Thomas, L.H.	(1944)	J.Chem.Phys., 12, 449.
Ubbelohde, A.R.	(1953)	Fourth Symposium (Int.) on Combustion, p464. Williams & Wilkins: Baltimore.
Vieille, P.	(1899)	C.R.Acad.Sci., Paris, 129, 1228.
Voevodsky, V.V., & Soloukhin, R.I.	(1965)	Tenth Symposium (Int.) on Combustion, p279. Comb. Inst: Pittsburgh.
Voitsekhovskii, B.V. & Kotov, B.E.	(1958a)	Isv. Sibirsk. Otdel Akad. Nauk, S.S.S.R., no.4, 74.
- , Kotov, B.E., Mitrofanov, V.V., & Topchiyan, M.E.	(1958b)	ibid no. 9, 44.
- , Mitrofanov, V.V., & Topchiyan, M.E.	(1962)	Z.Prikl. Mekh. Tekn. Fiz., (3) 27.
von Neumann, J.	(1942)	O.S.R.D. report no. 549.
Wagner, H.Gg.	(1961)	"Fundamental Data Obtained from Shock Tube Experiments". AGARDograph no.41, pp.320-385, Pergamon.
Wendlandt, R.	(1925)	Z.Phys.Chem., 116, 227.
Weymann, H.D.	(1960)	Physics of Fluids, 3, 545.
White, D.R.	(1961)	ibid 4, 465.
	(1963)	ibid 6, 1011.

White, D.R., & Moore, G.E. (1965) Tenth Symposium (Int.) on Combustion, p.785. The Combustion Inst.: Pittsburgh.

Wood, W.W., & Kirkwood, J.G. (1956) J.Chem.Phys., 25, 1276.

(1958) ibid 29, 957.

- & Parker, F.R. (1958) Physics of Fluids, 1, 230.

- & Salsburg, Z.W. (1960) ibid 3, 549.

Zeldovich, Y.B. (1940) J.E.T.P. (U.S.S.R.), 10, 542.

(1949) "Theory of Combustion and Detonation in Gases", Wright Patterson Air Force Base.

SECTION 9.

DIAGRAMS.

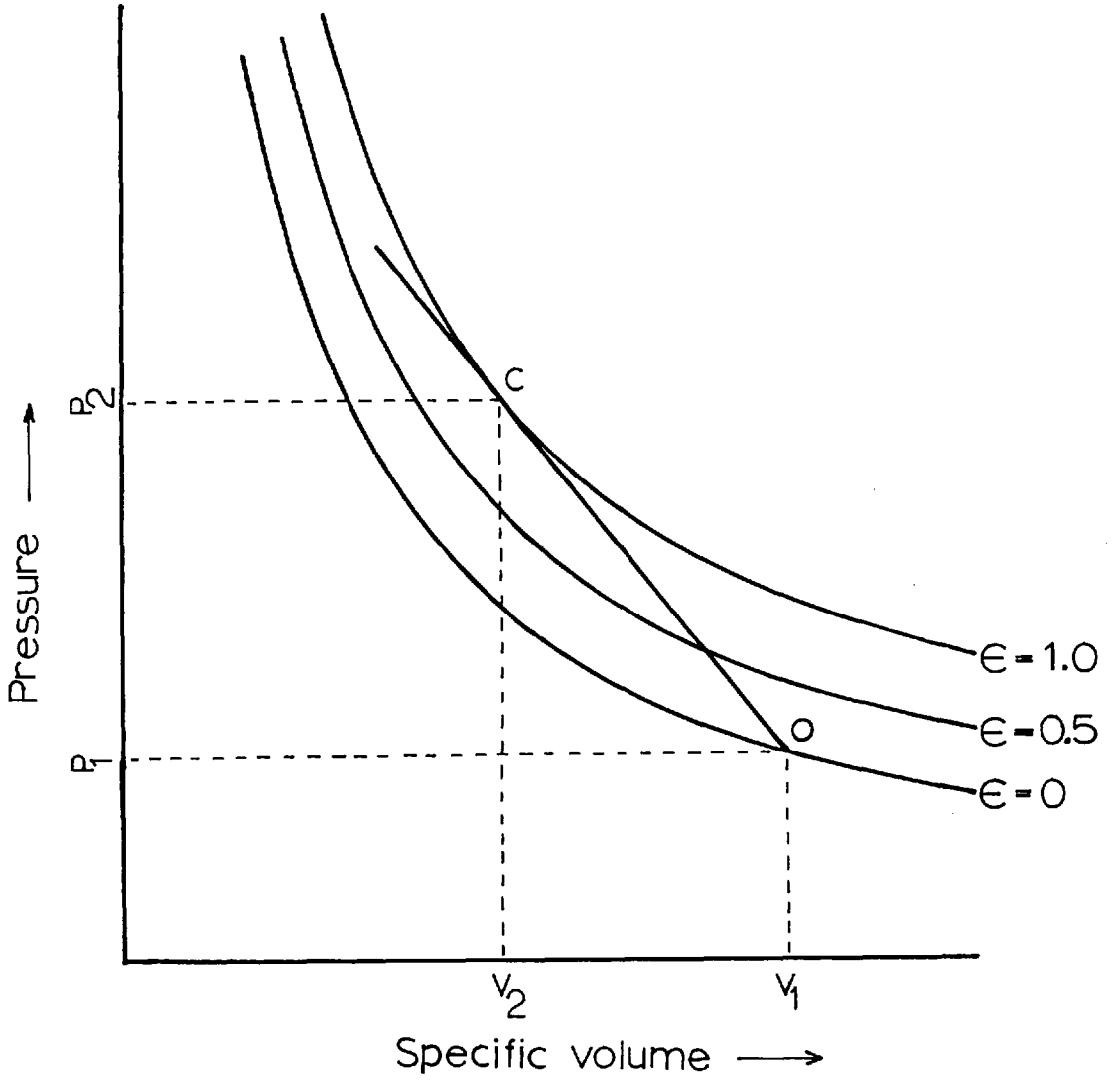

Figure 1.1. Family of R-H curves for detonation. CO is the Rayleigh line.

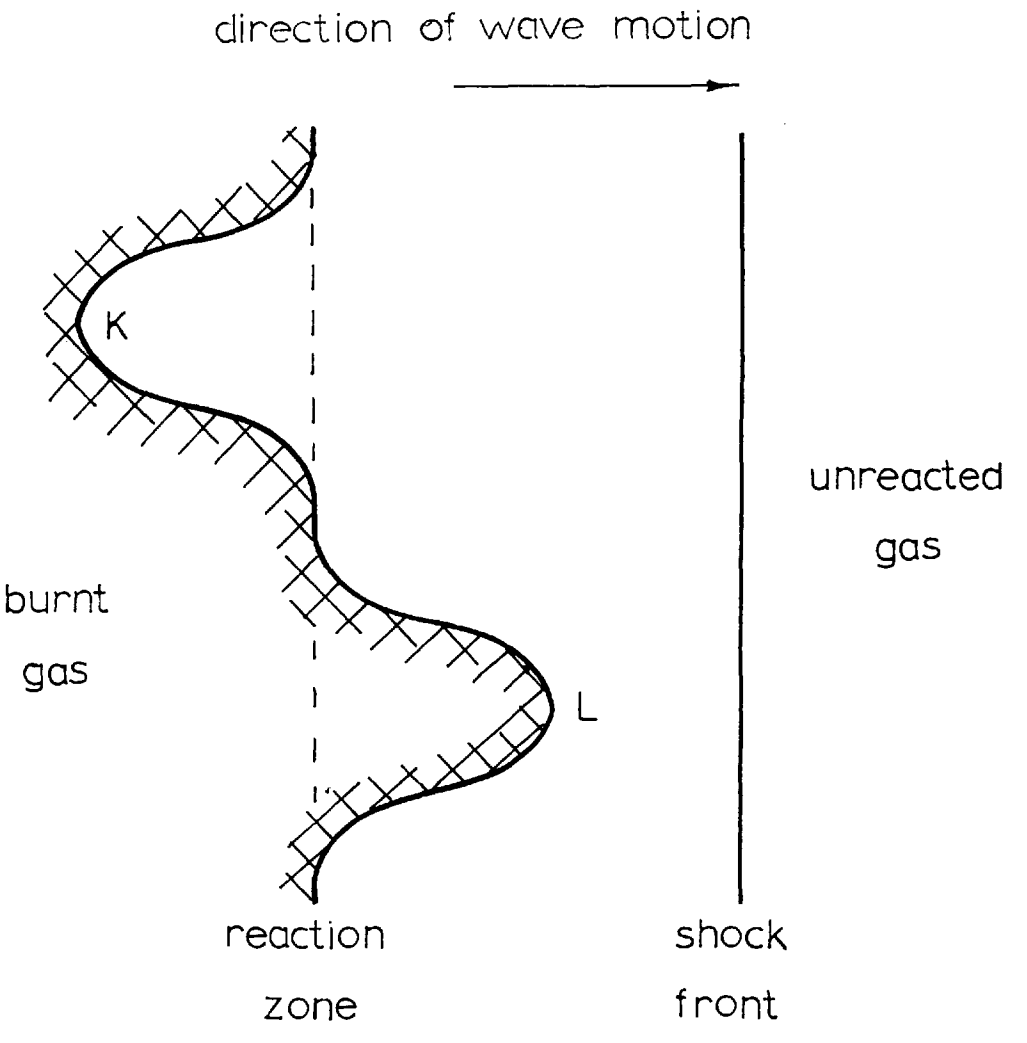

Figure 1.2. Initially disturbed detonation front (After Shchelkin and Troshin).

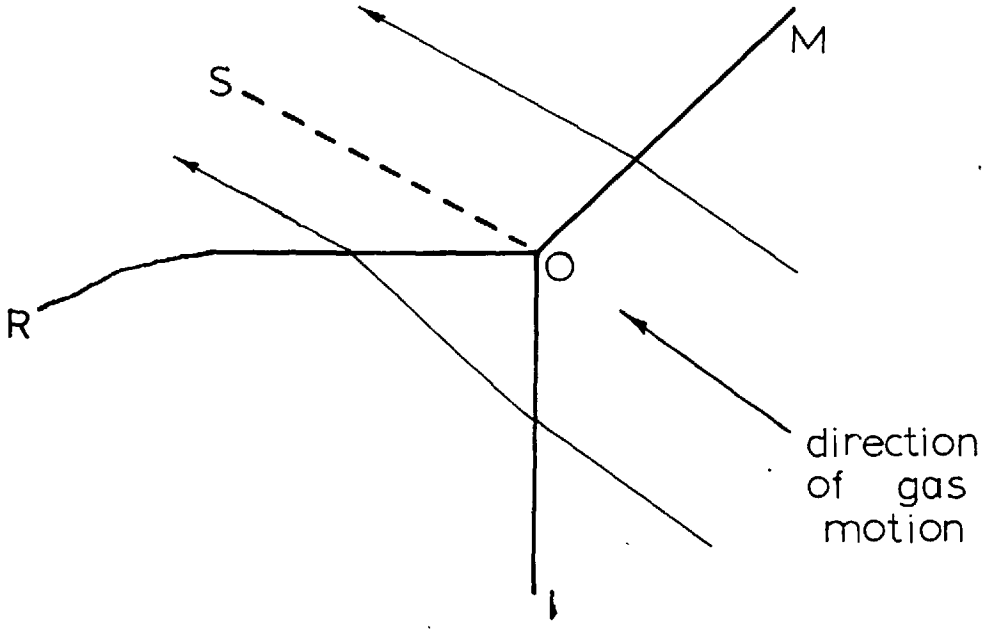

Figure 1.3. Mach configuration for intersection of two shock waves.
OI - incident shock, OM - Mach stem,
OR - reflected shock, OS - slipstream.

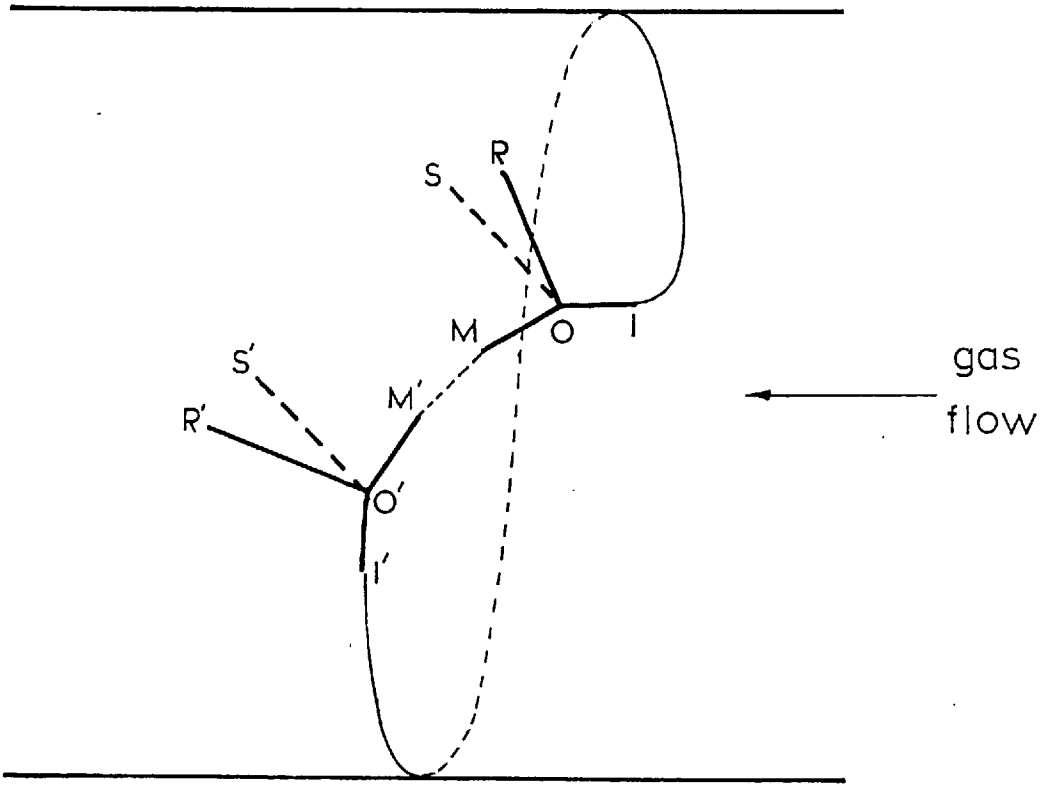

Figure 1.4. Spin head structure in a cylindrical tube (after Denisov and Troshin).

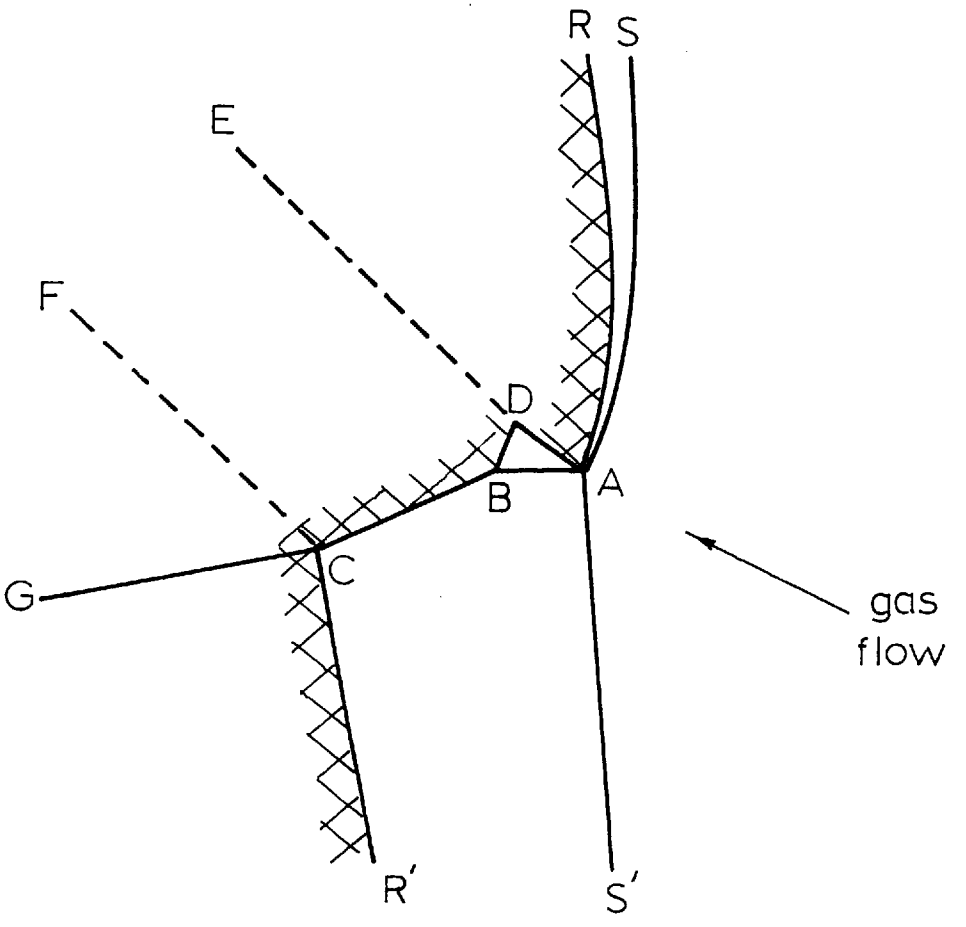

Figure 1.5. Spin head structure in a cylindrical tube (after Schott). Lettering explained in text.

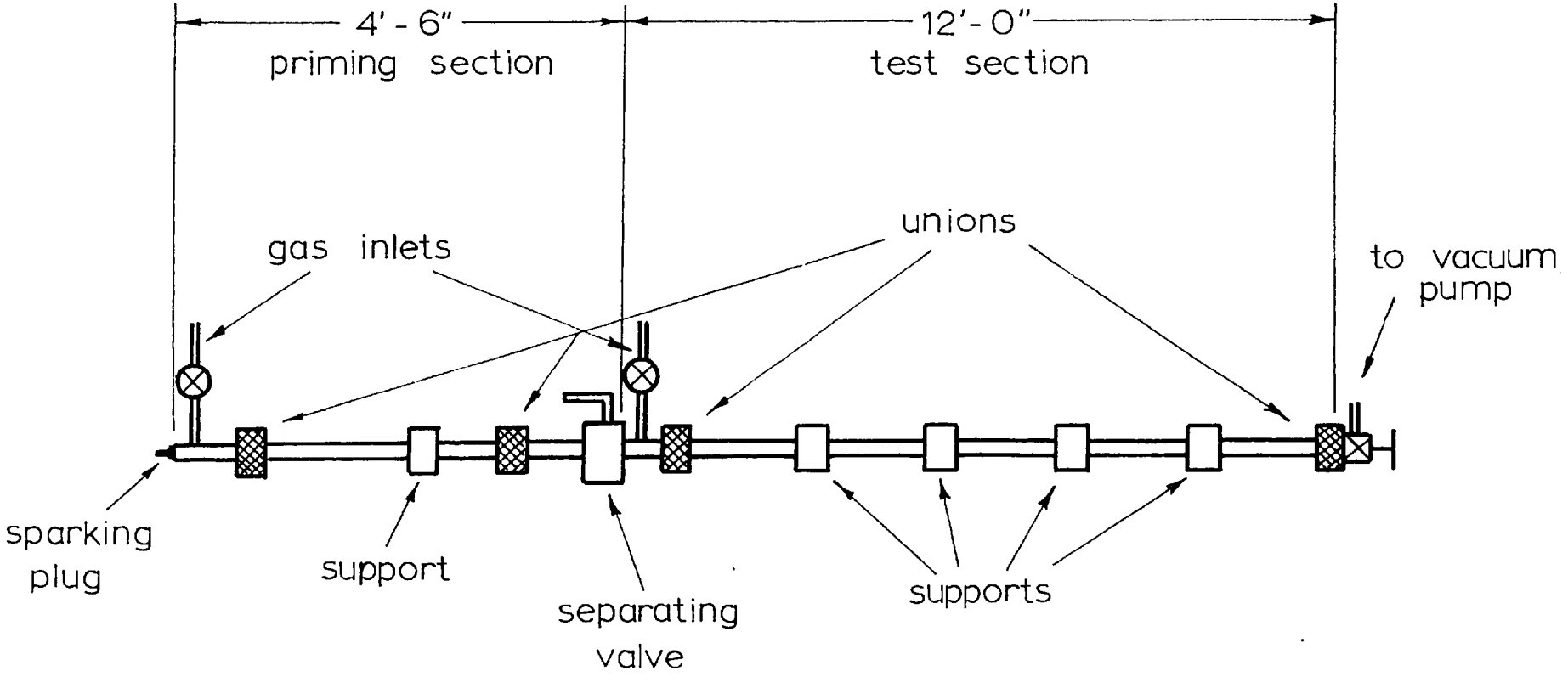

Figure 2.1. Detonation tube assembly.

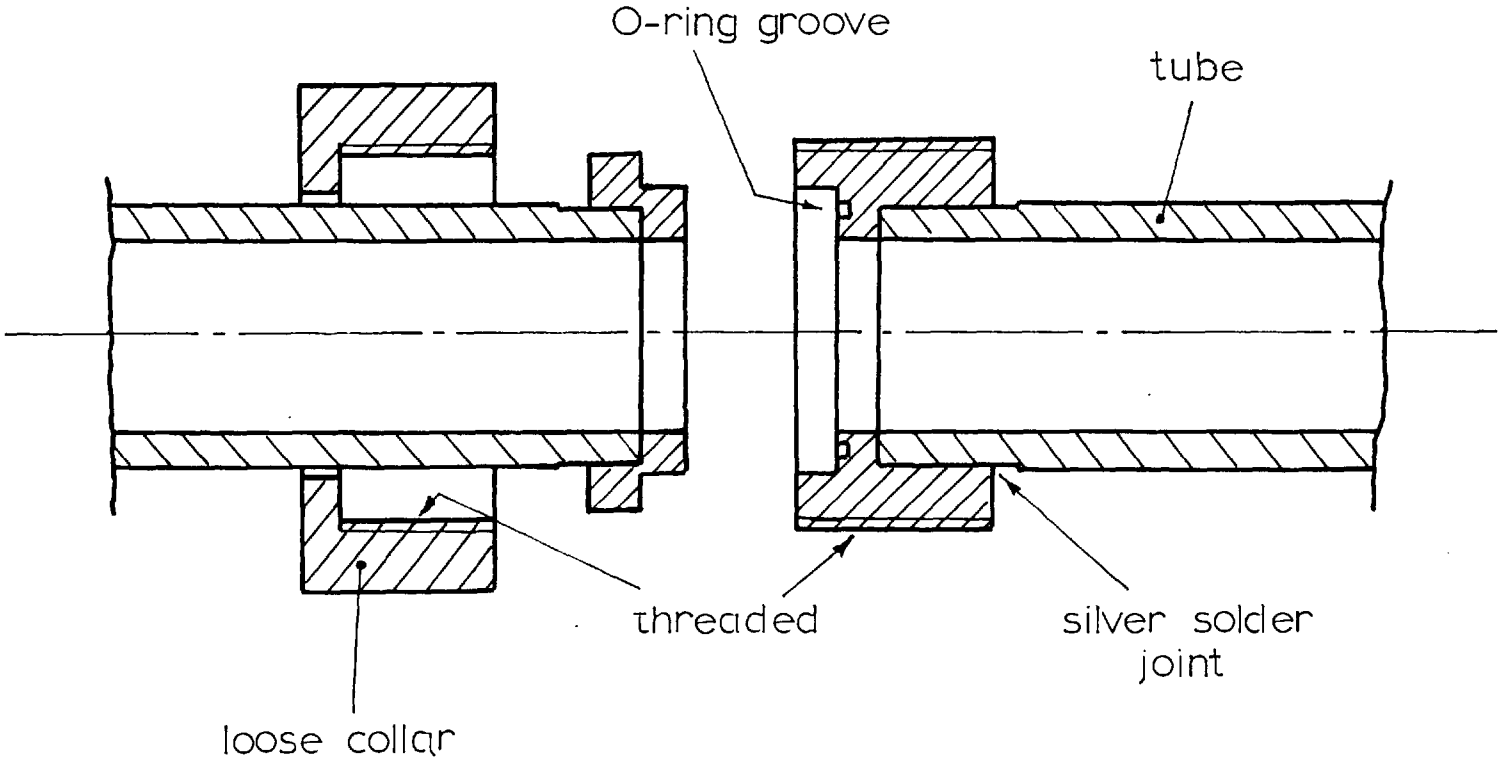

Figure 2.2. Vacuum tight tube connections. Drawn actual size.

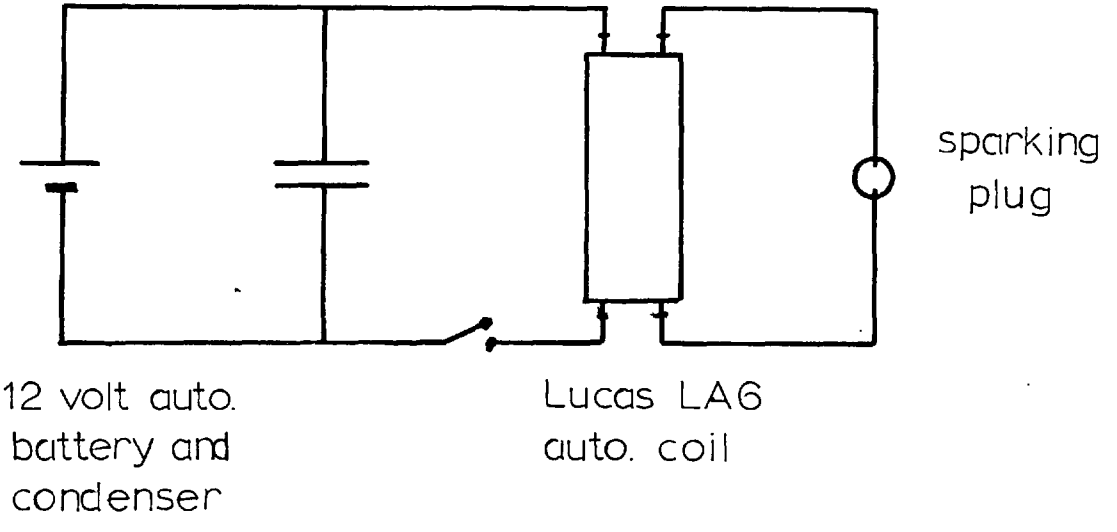

Figure 2.3. Sparking plug circuit.

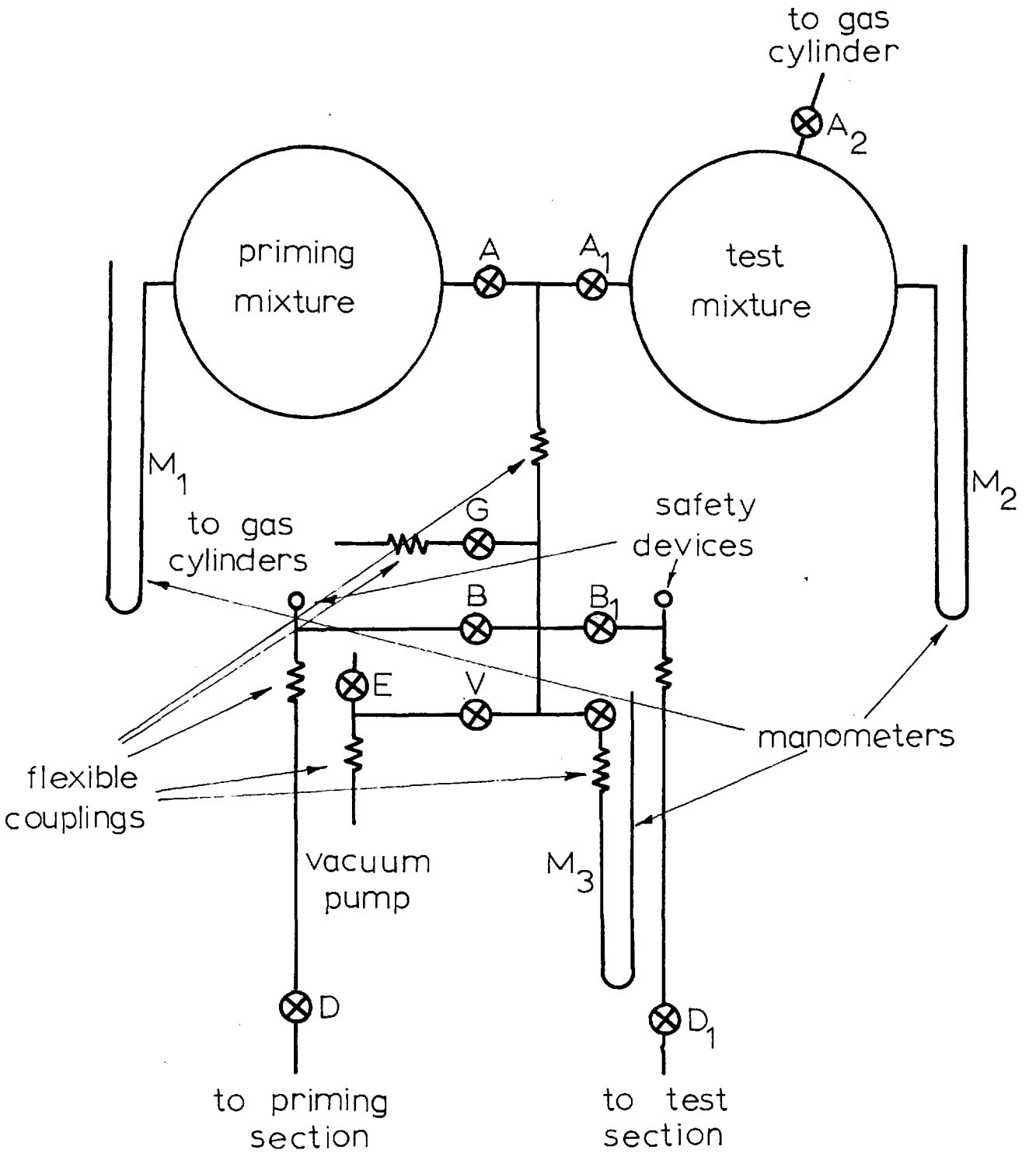

Figure 2.4. Schematic diagram of the gas mixing unit.

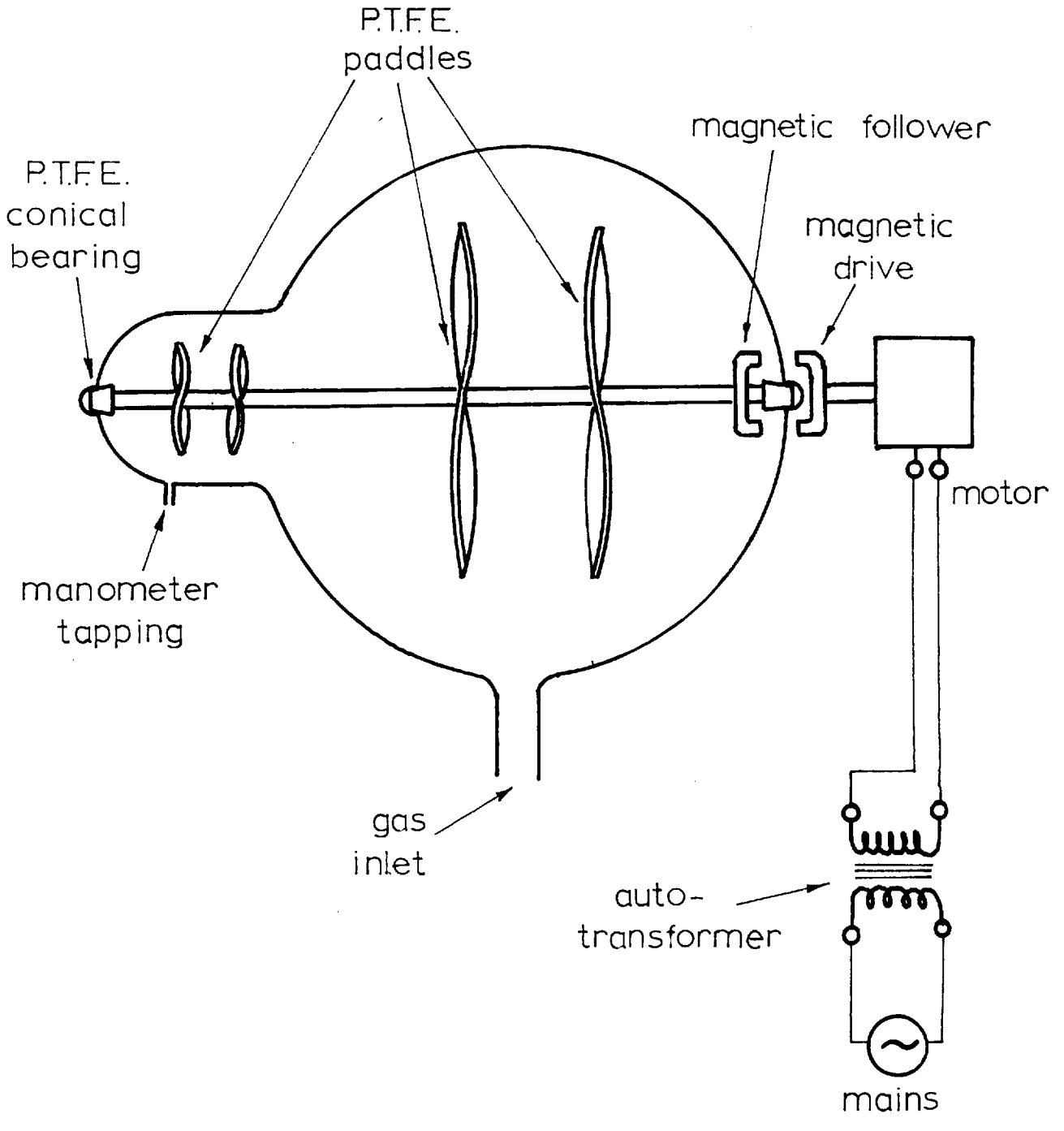

Figure 2.5. Mixing vessel assembly

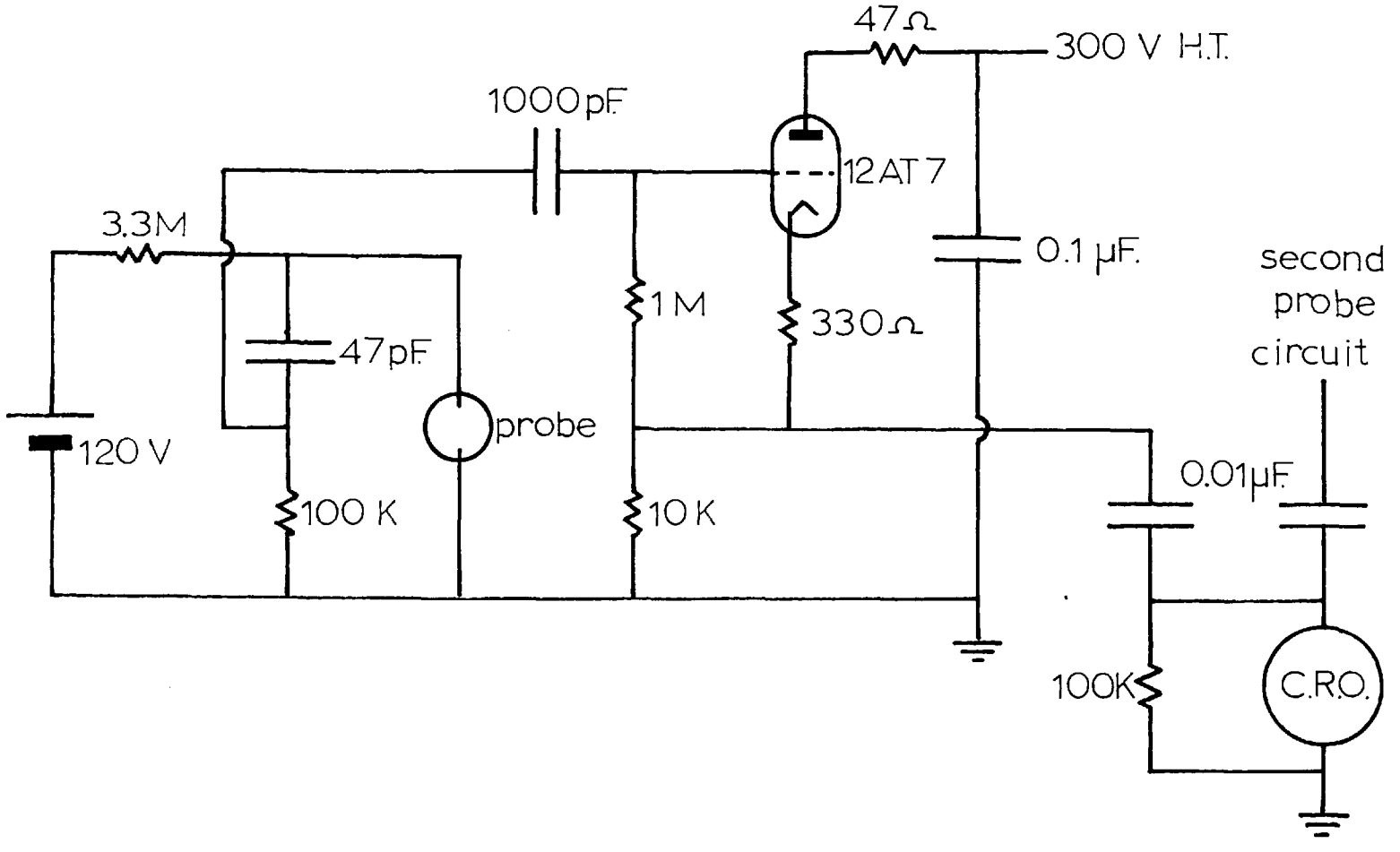

Figure 2.6. Ionisation probe circuit

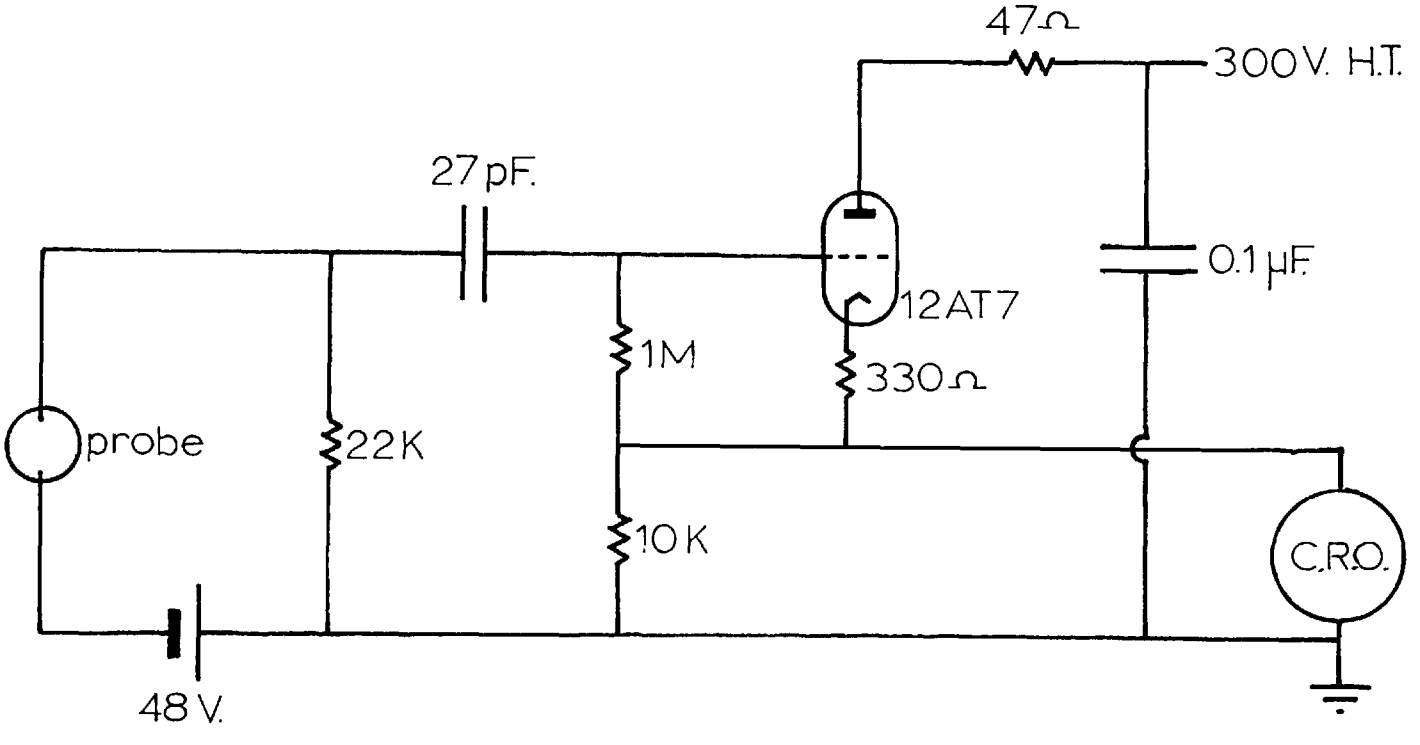

Figure 2.7 Light probe circuit.

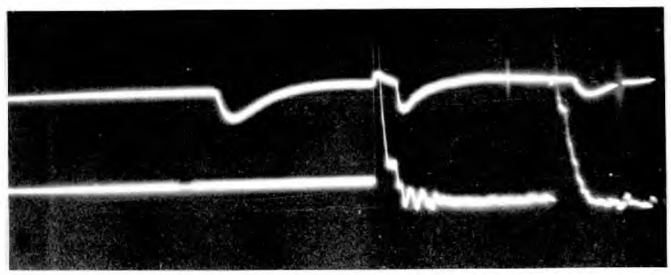

Figure 2.3.1. Ionisation and light probe signals. Upper trace, light detectors, lower trace, ionisation detectors.

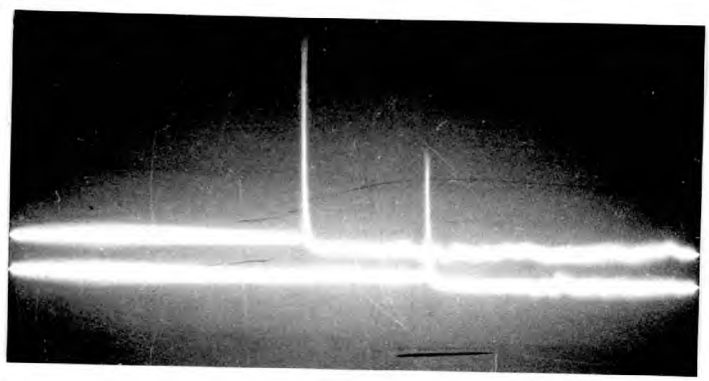

Figure 2.3.2. Ionisation probe signals.

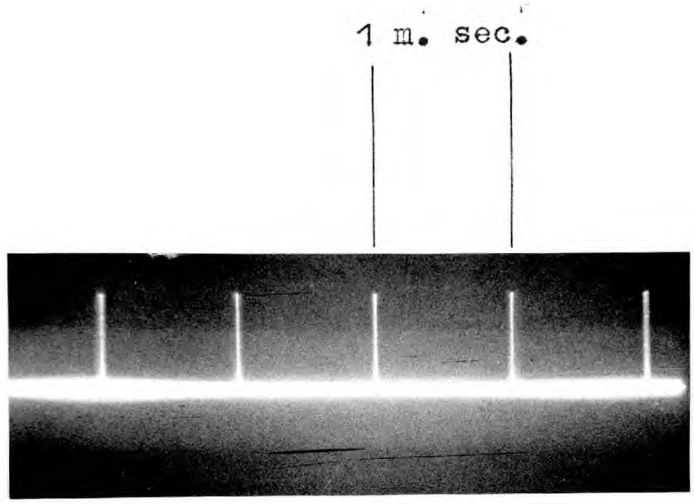

Figure 2.8.3. Calibration trace (time base, 0.5 m. sec.).

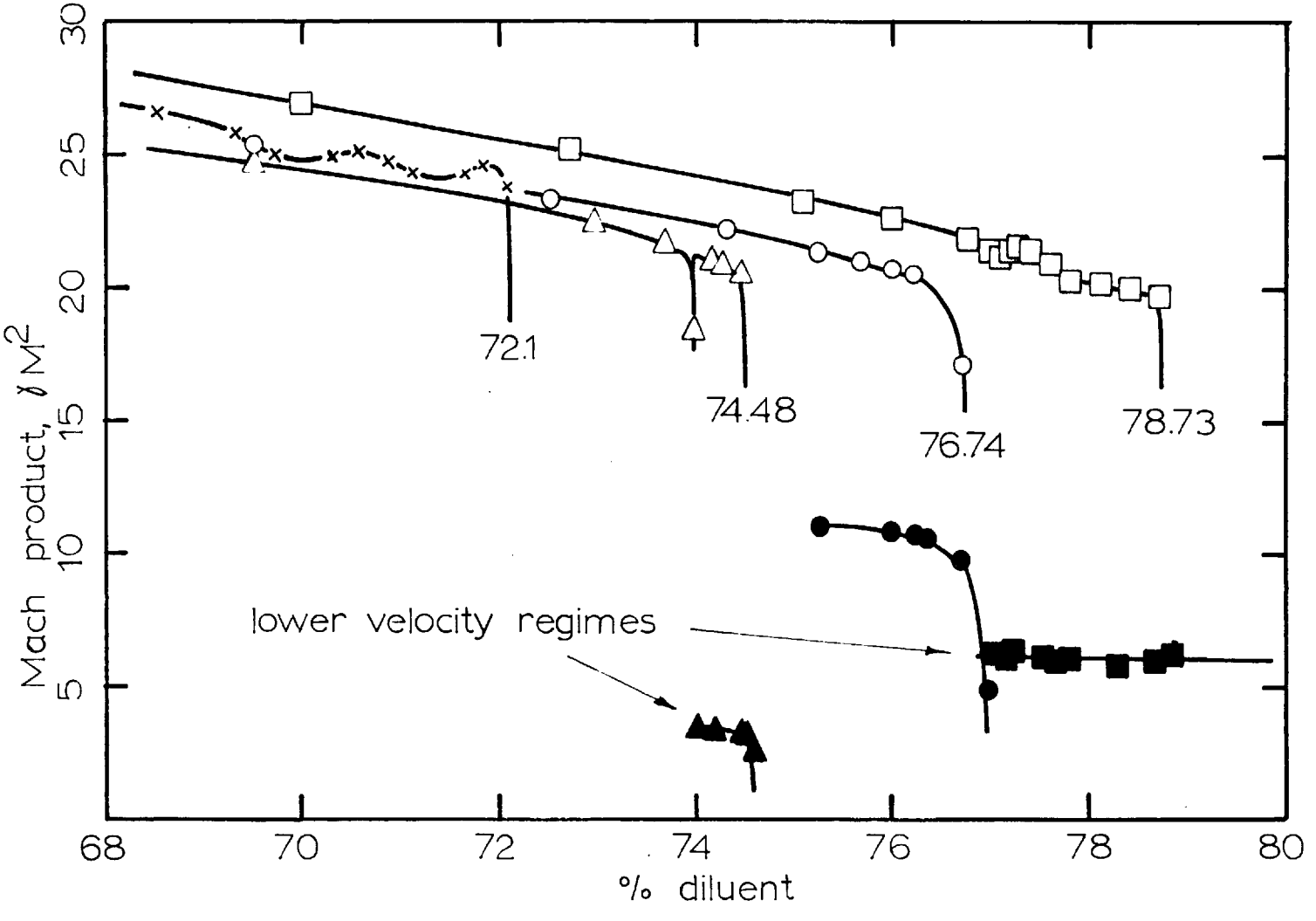

Figure 3.1. Detonation limits for similar binary mixtures with different molecular masses. × $S_D + D_2$; Δ, $S_D + O_2$; ○, $S_H + O_2$; □, $S_H + H_2$.

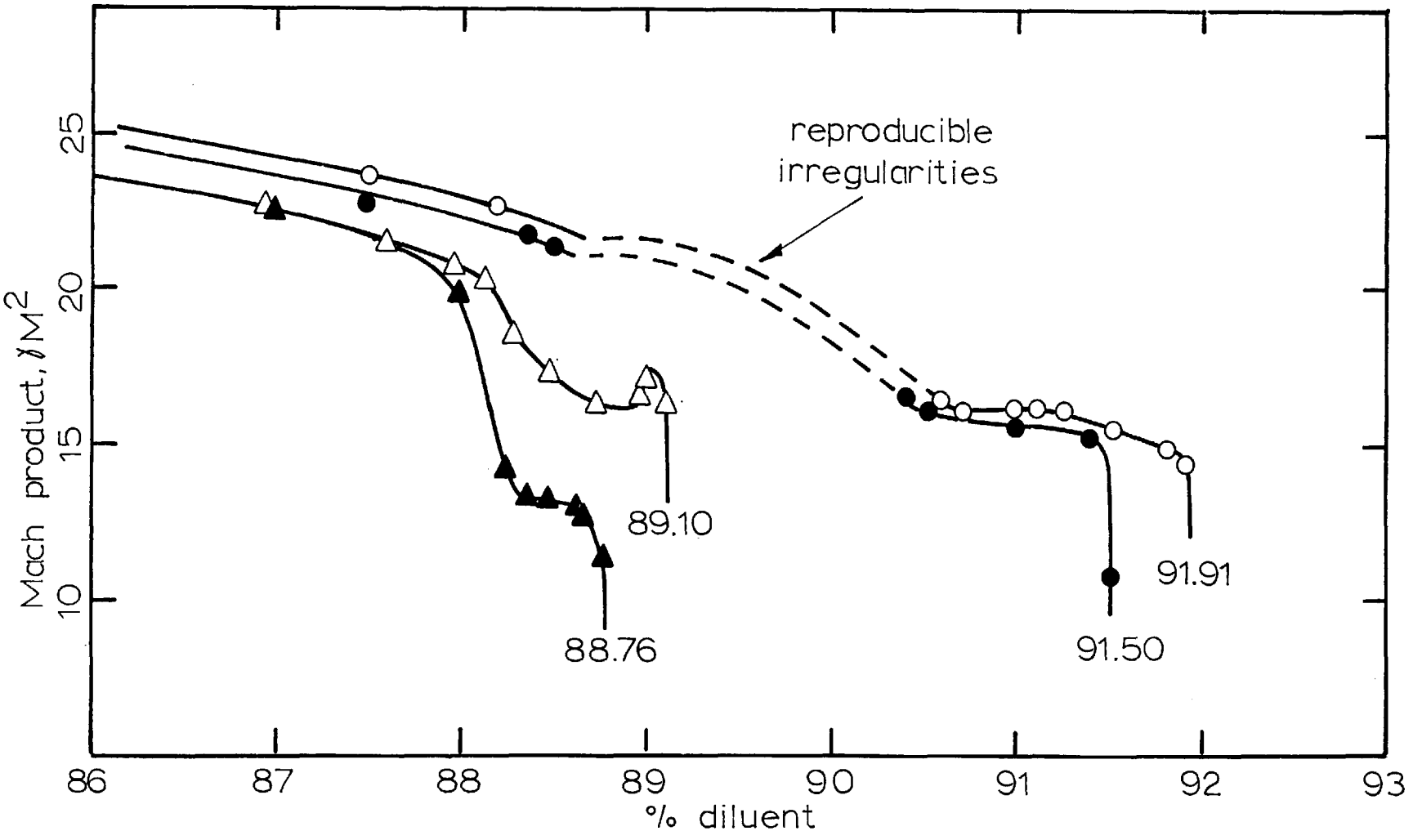

Figure 3.2. Detonation limits for ternary systems with different molecular masses. circles, argon diluent; triangles, helium diluent; open symbols, S_H reactive base; solid symbols, S_D reactive base.

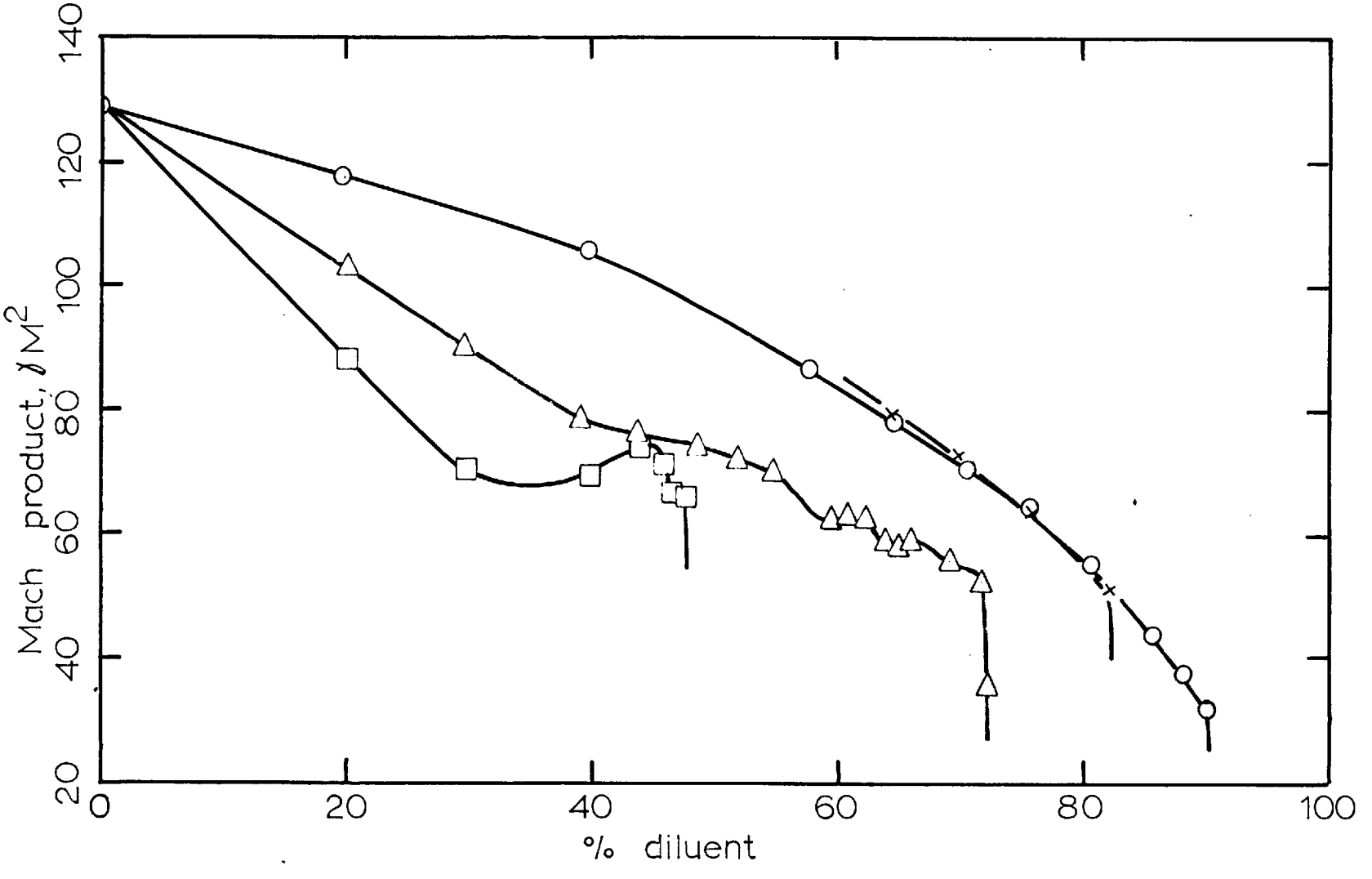

Figure 3.3. Detonation limits for systems containing cyanogen. □ , $S_c + C_2N_2$; Δ , $S_c + O_2$; × , S_c + He; o , S_c + A.

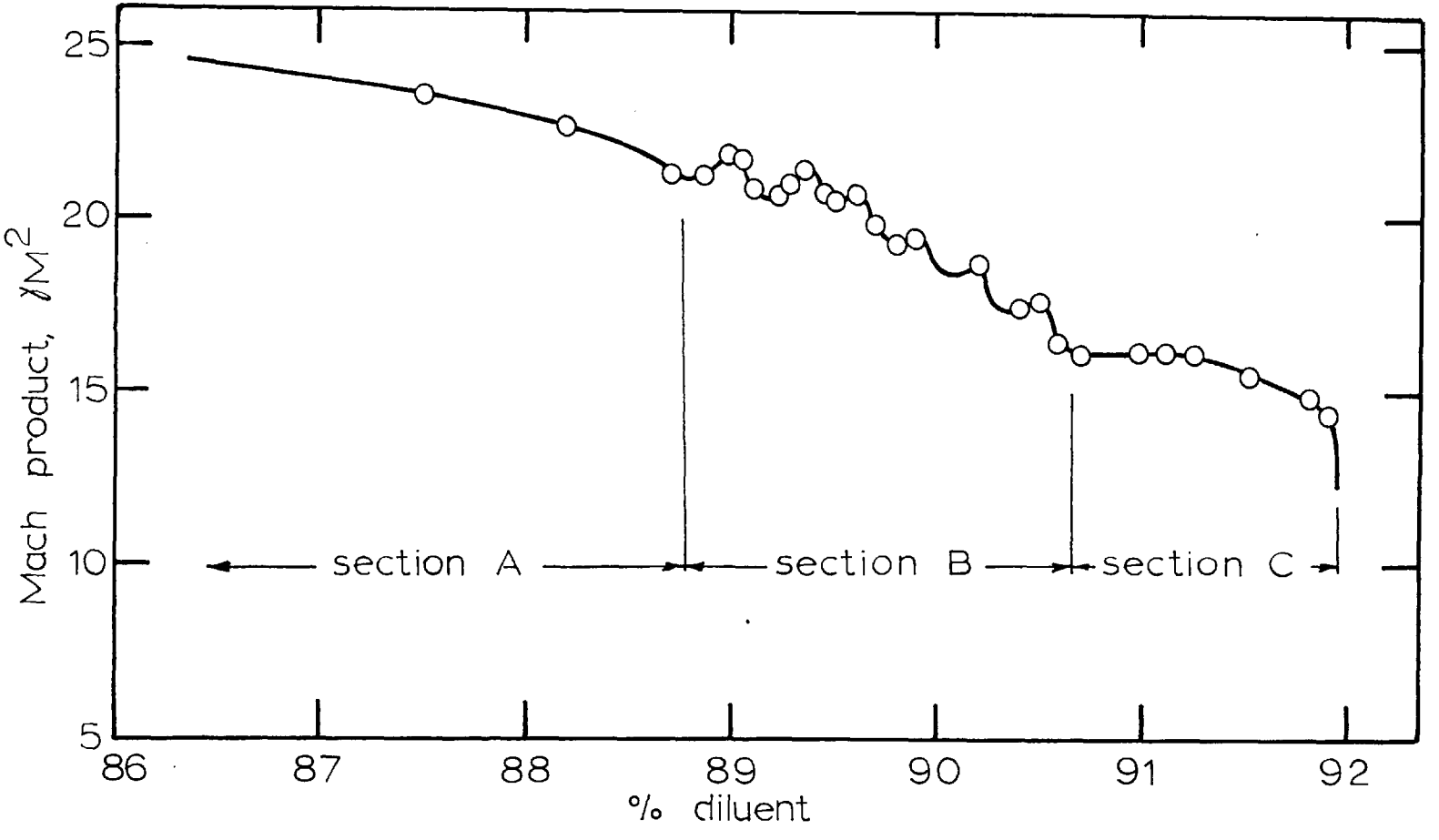

Figure 3.4. Detonation limit for the system S_H + A

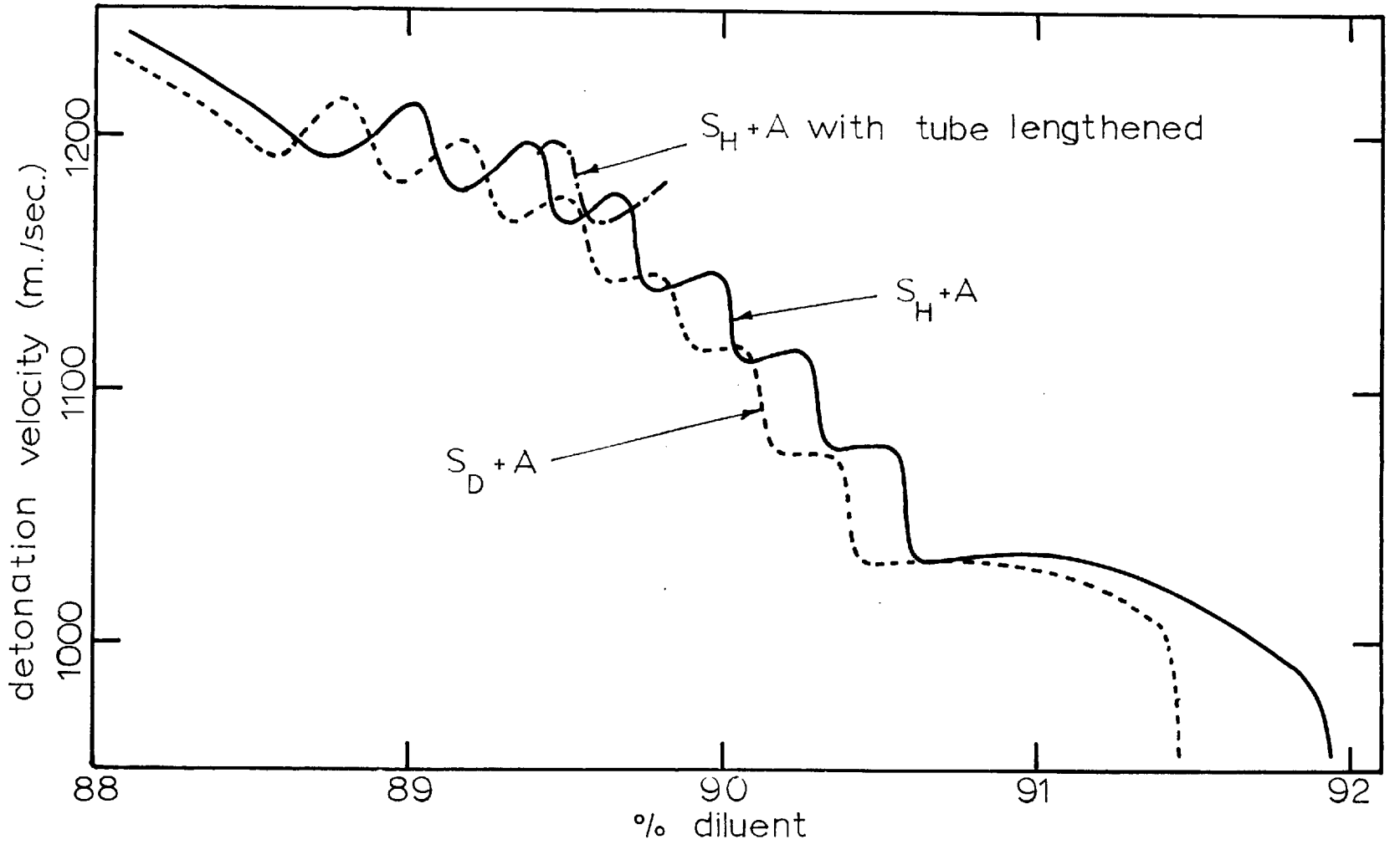

Figure 3.5. Horizontal shift of fluctuations due to replacement of hydrogen by deuterium, and the lengthening of the test section. Individual points have been omitted for clarity.

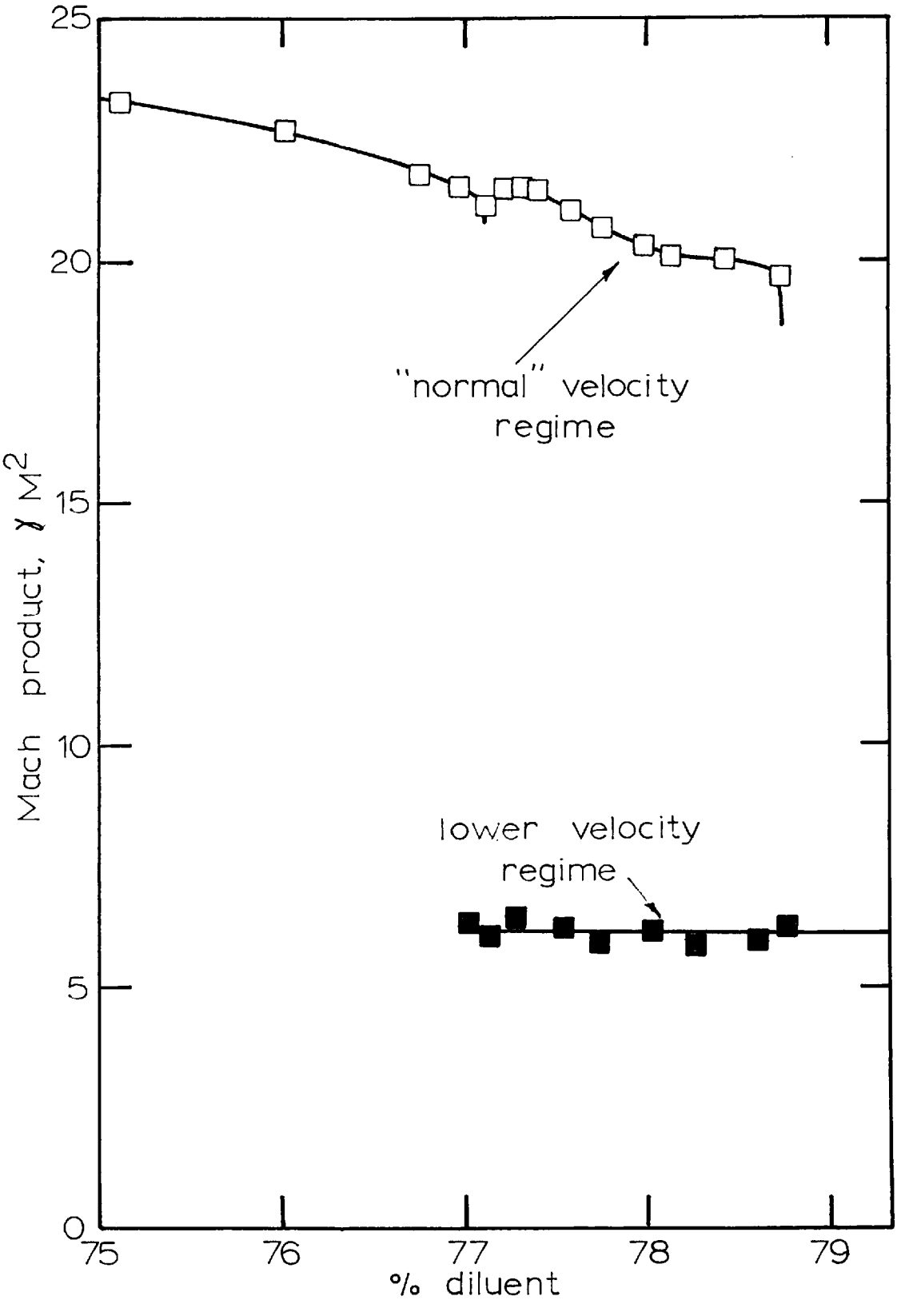

Figure 3.6. Detonation limit for the system $S_H + H_2$.

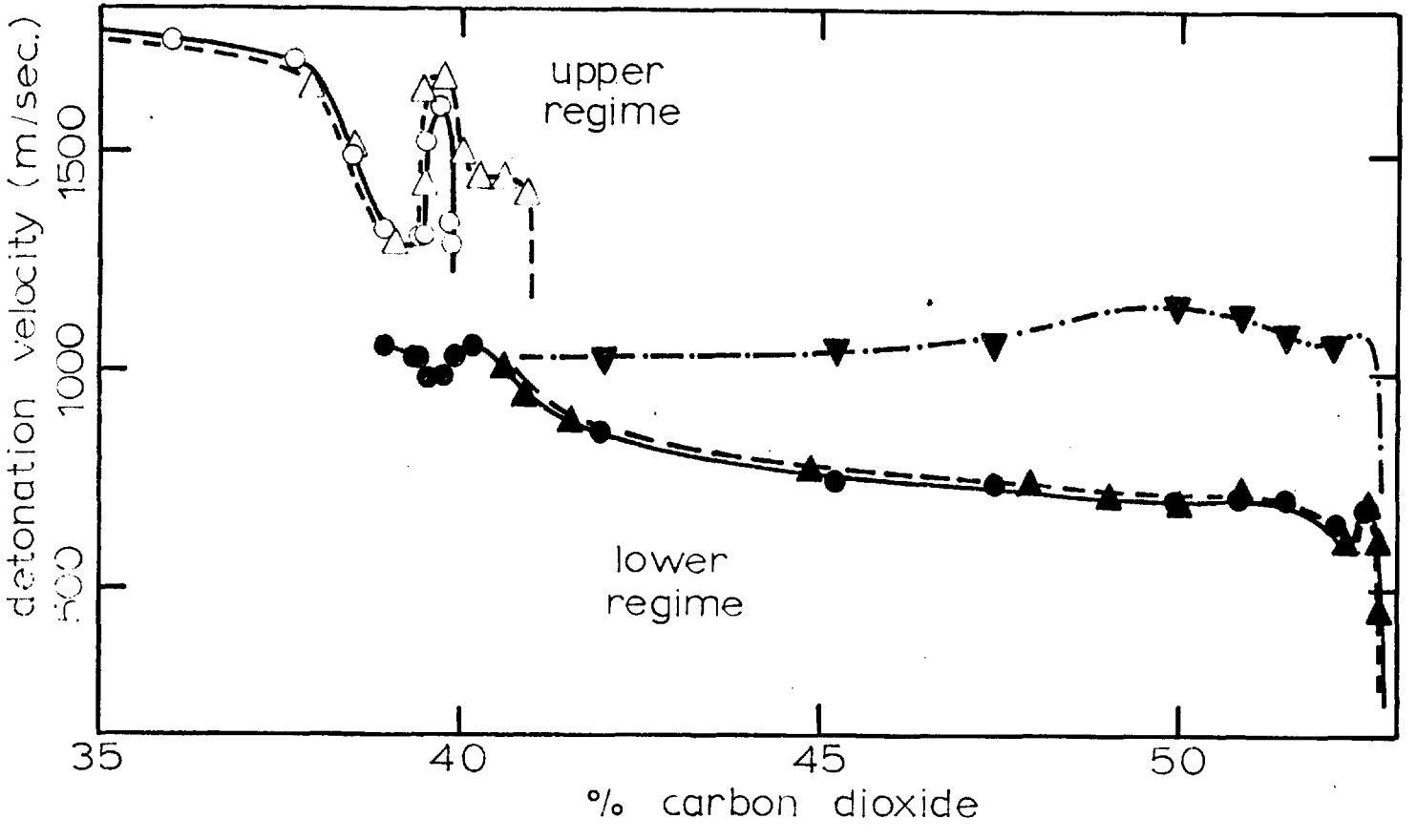

Figure 3.7. Detonation limit for the system $S_H + CO_2$ in the stainless steel and coated tubes. —o—, stainless steel tube; --Δ--, coated tube; —▼—, second detonation wave.

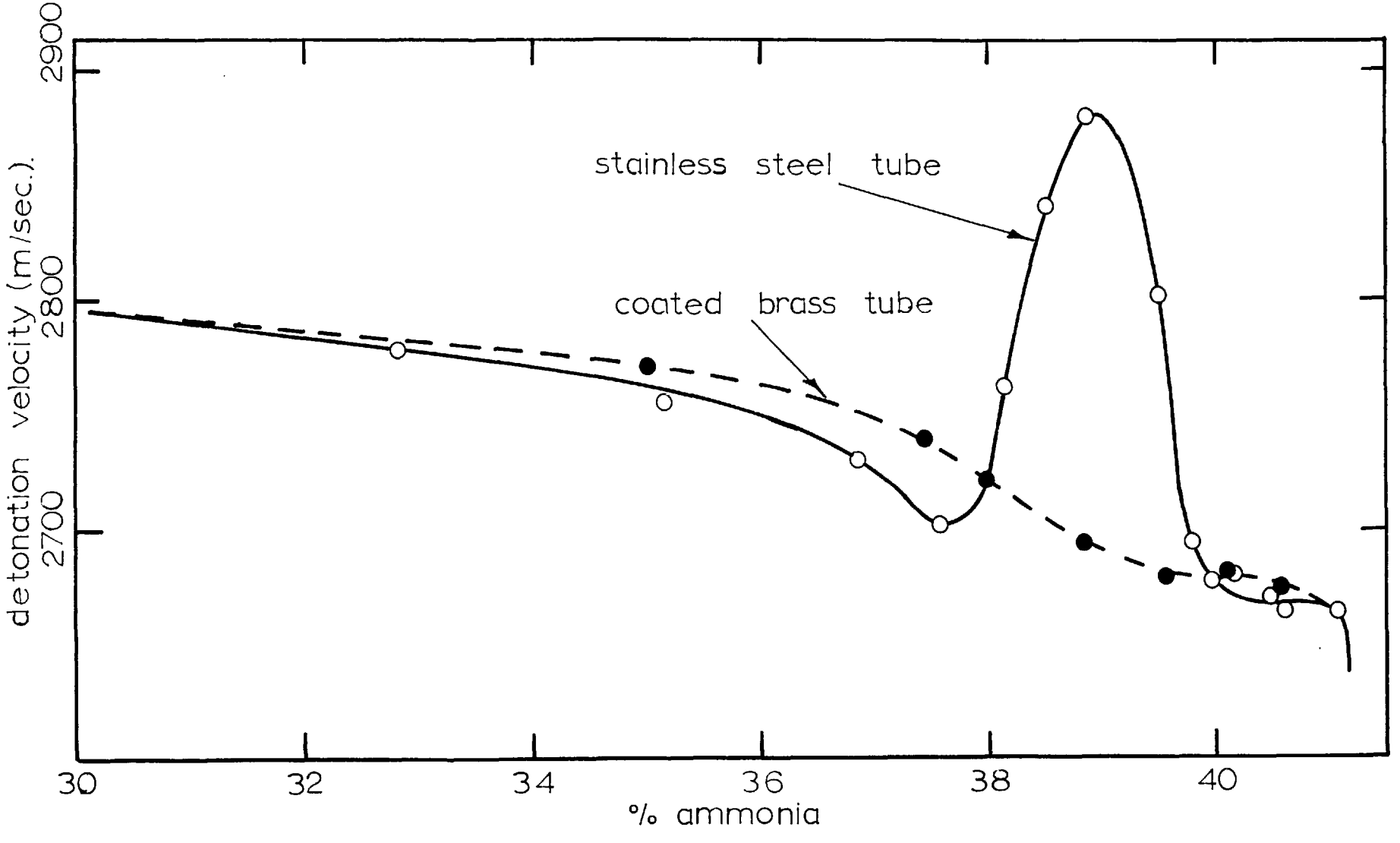

Figure 3.8. Detonation limit for the system $S_H + NH_3$ in the stainless steel and coated tubes.

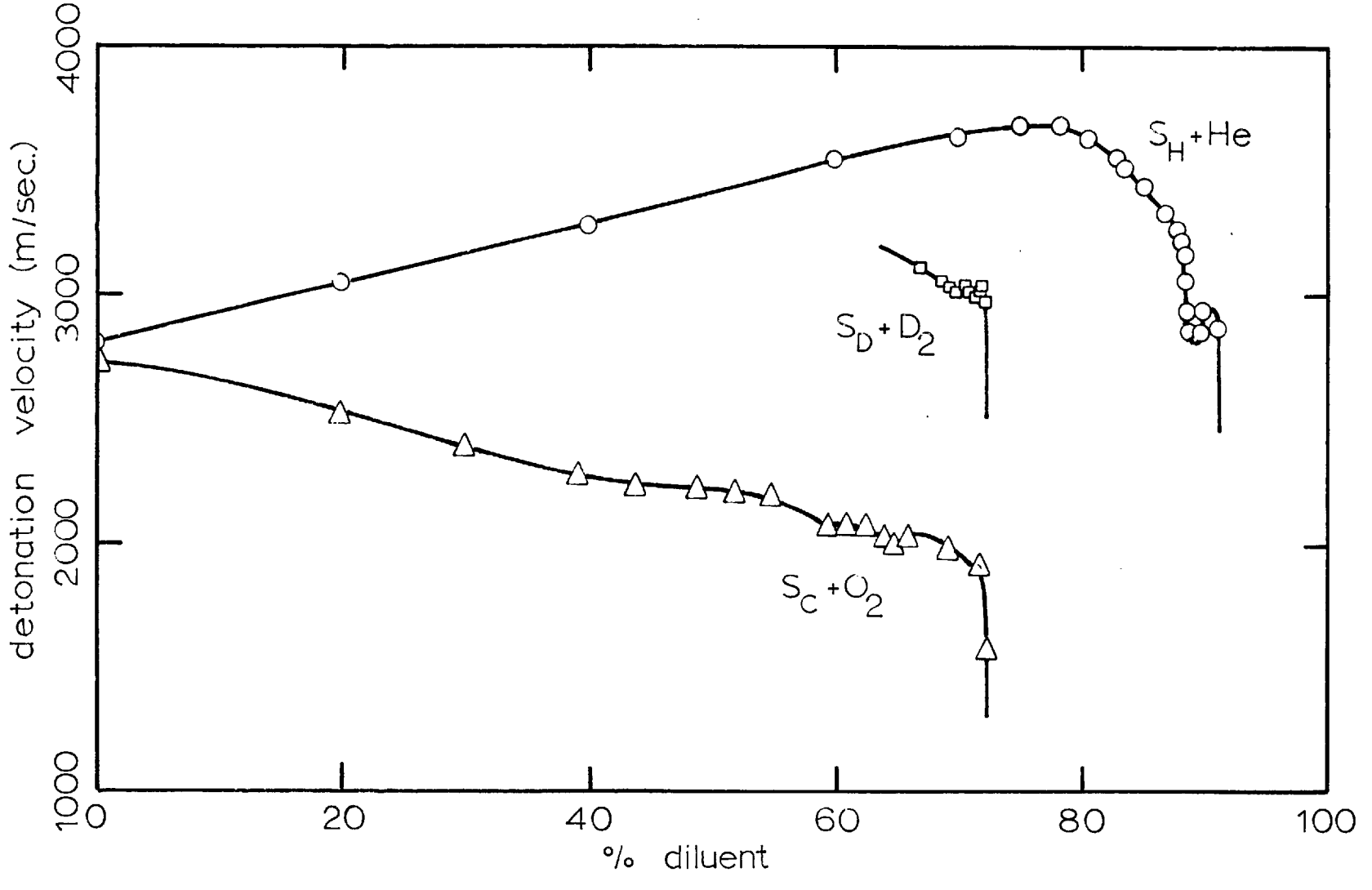

Figure 3.9. Velocity-composition relationships for the systems S_H+He, S_D+D_2, and S_C+O_2.

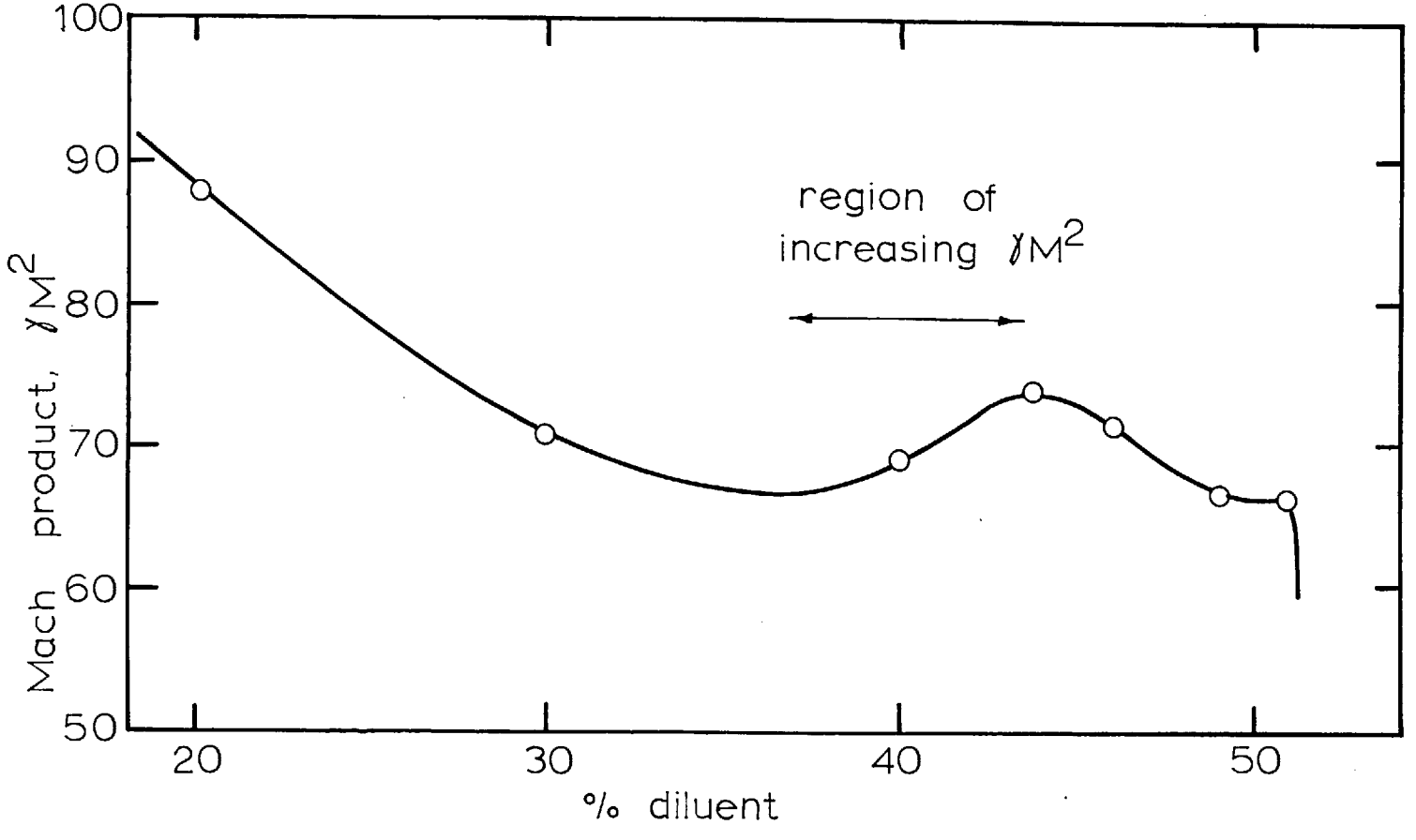

Figure 3.10 Detonation limit for the system $S_C + C_2N_2$.

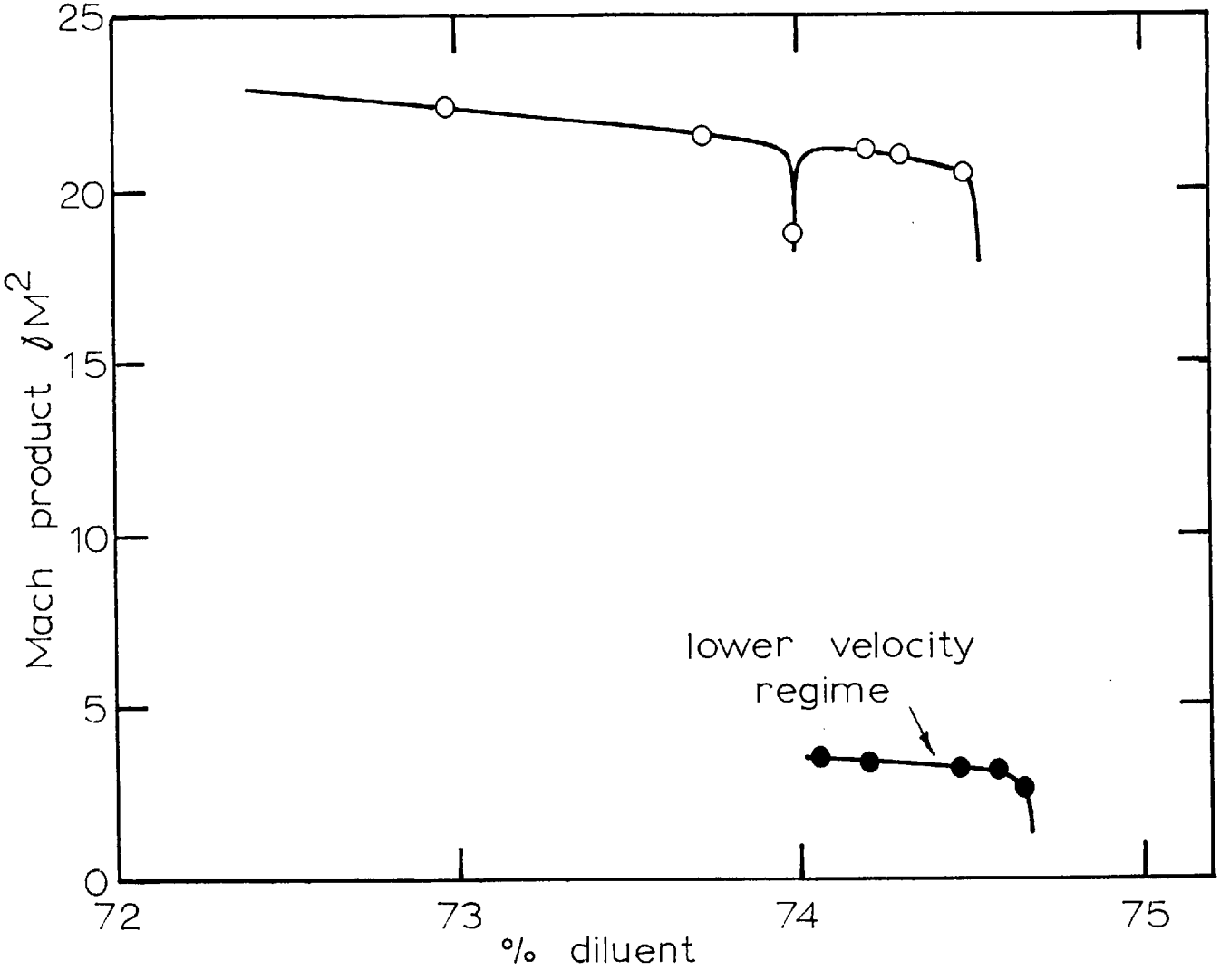

Figure 3.11. Detonation limit for the system $S_D + O_2$

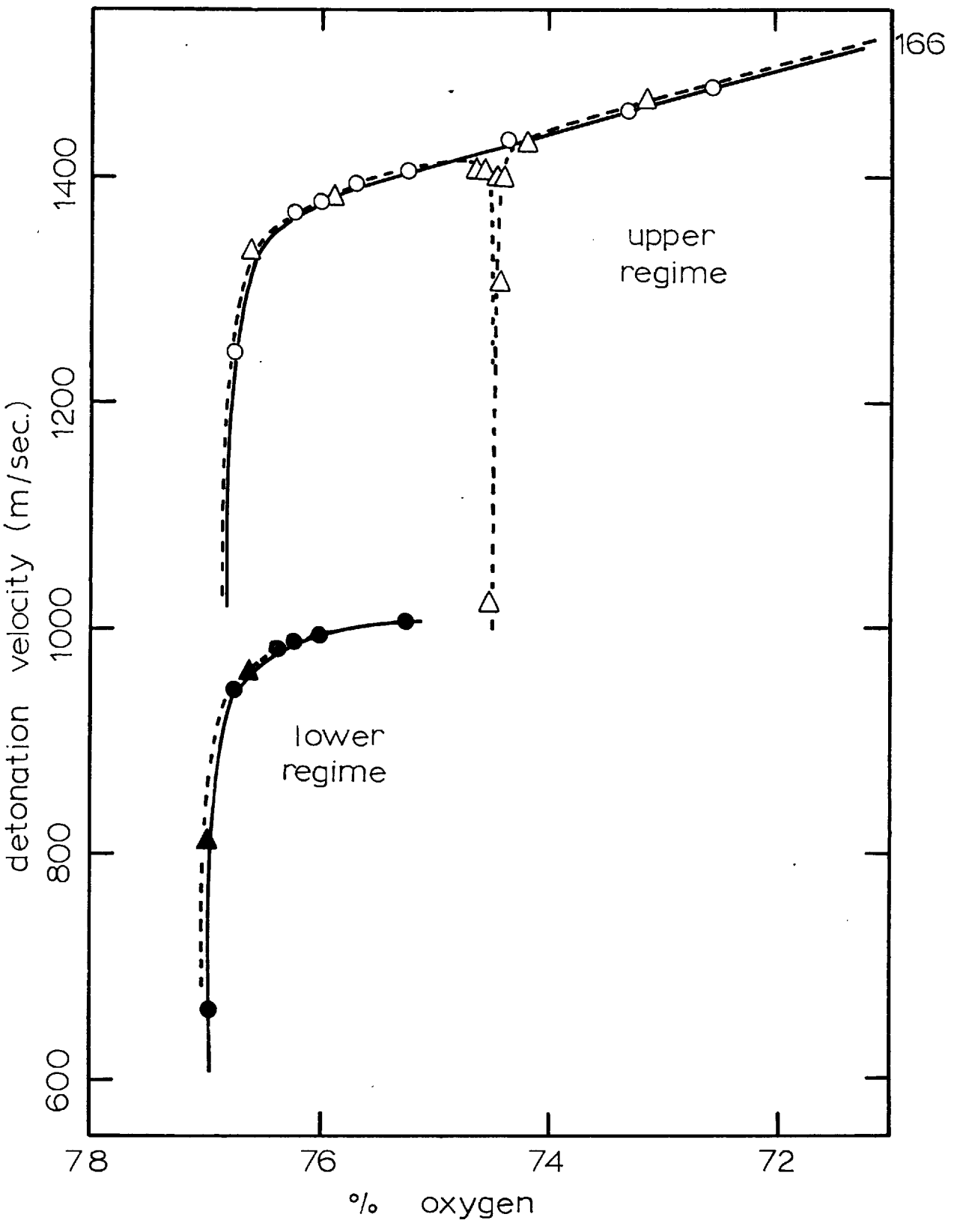

Figure 3.12. Detonation limit for the system S_H+O_2 in the stainless steel and coated tubes. —o—, stainless steel tube; - - -△- - -, coated tube.

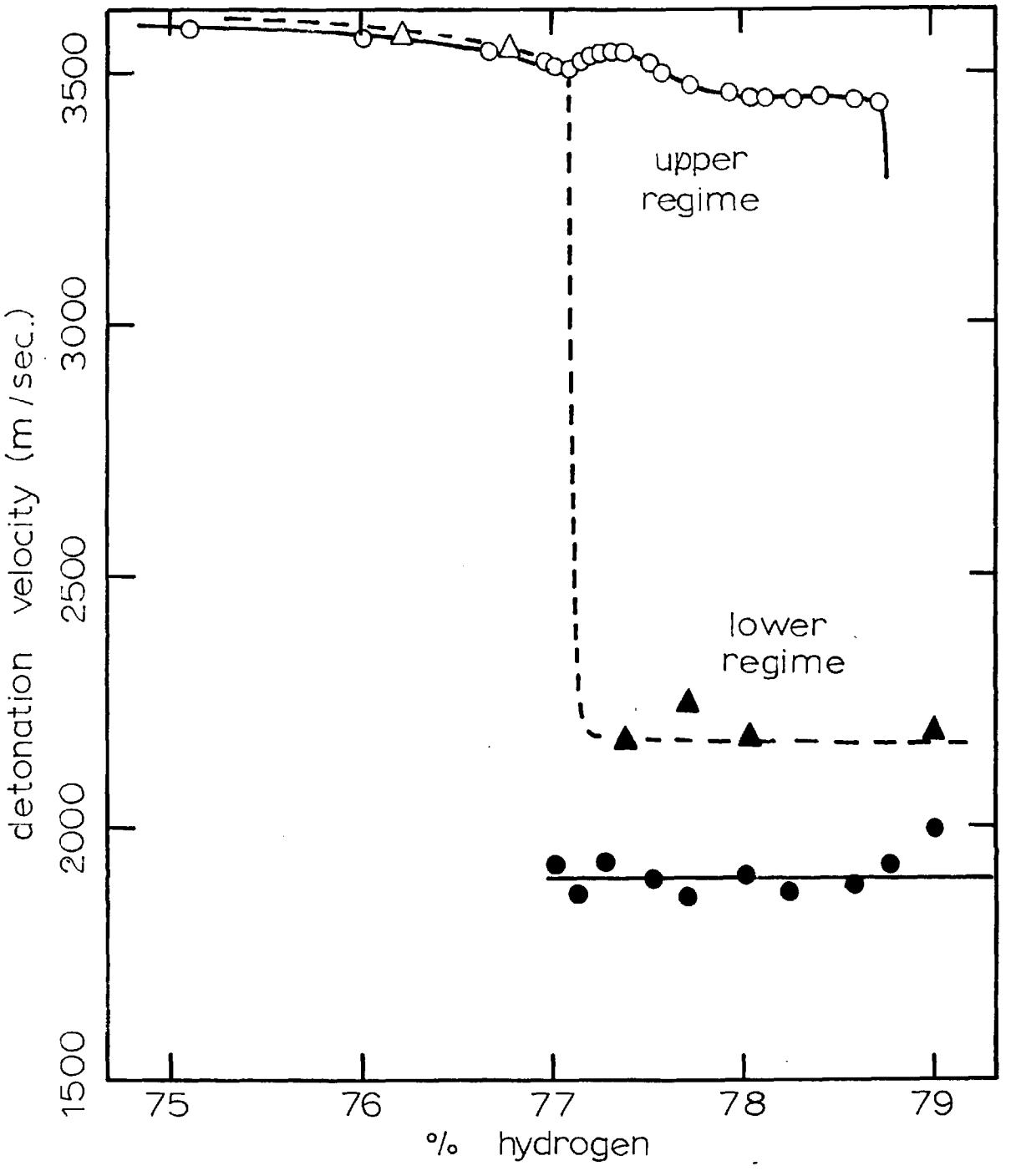

Figure 3.13. Detonation limit for the system $S_H + H_2$ in the stainless steel and coated tubes. —○— , stainless steel tube; --△--, coated tube.

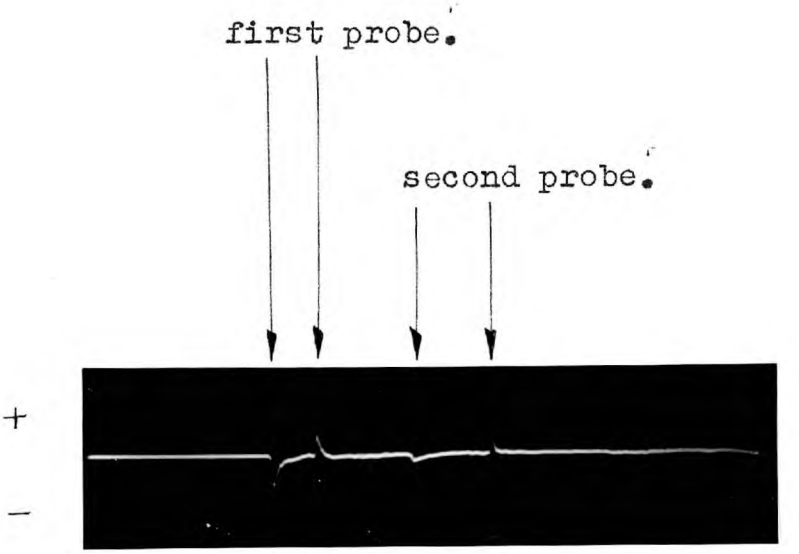

Figure 4.1. Oscilloscope trace indicating the existence of an electrical dipole.

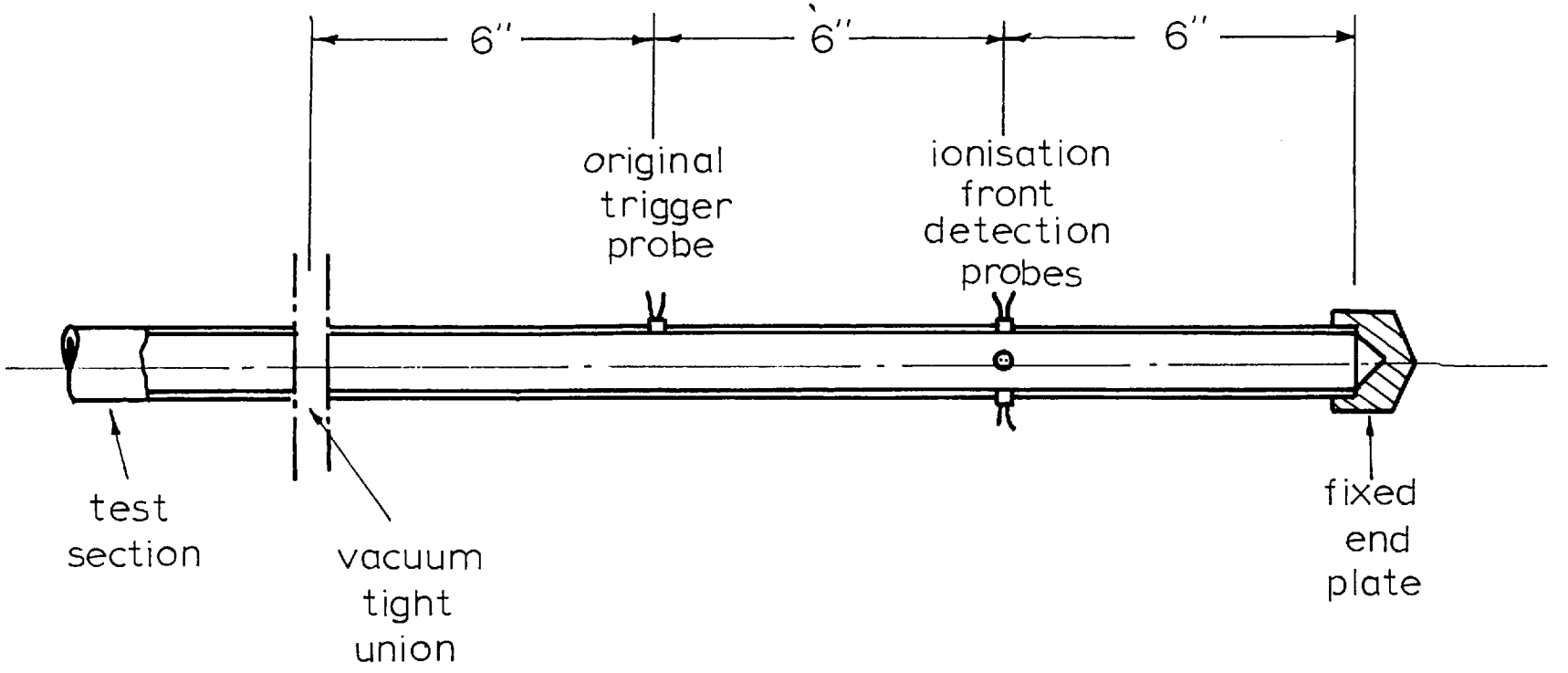

Figure 5.1. Probe ring for investigating the peripheral profile of the ionisation front in a detonation wave.

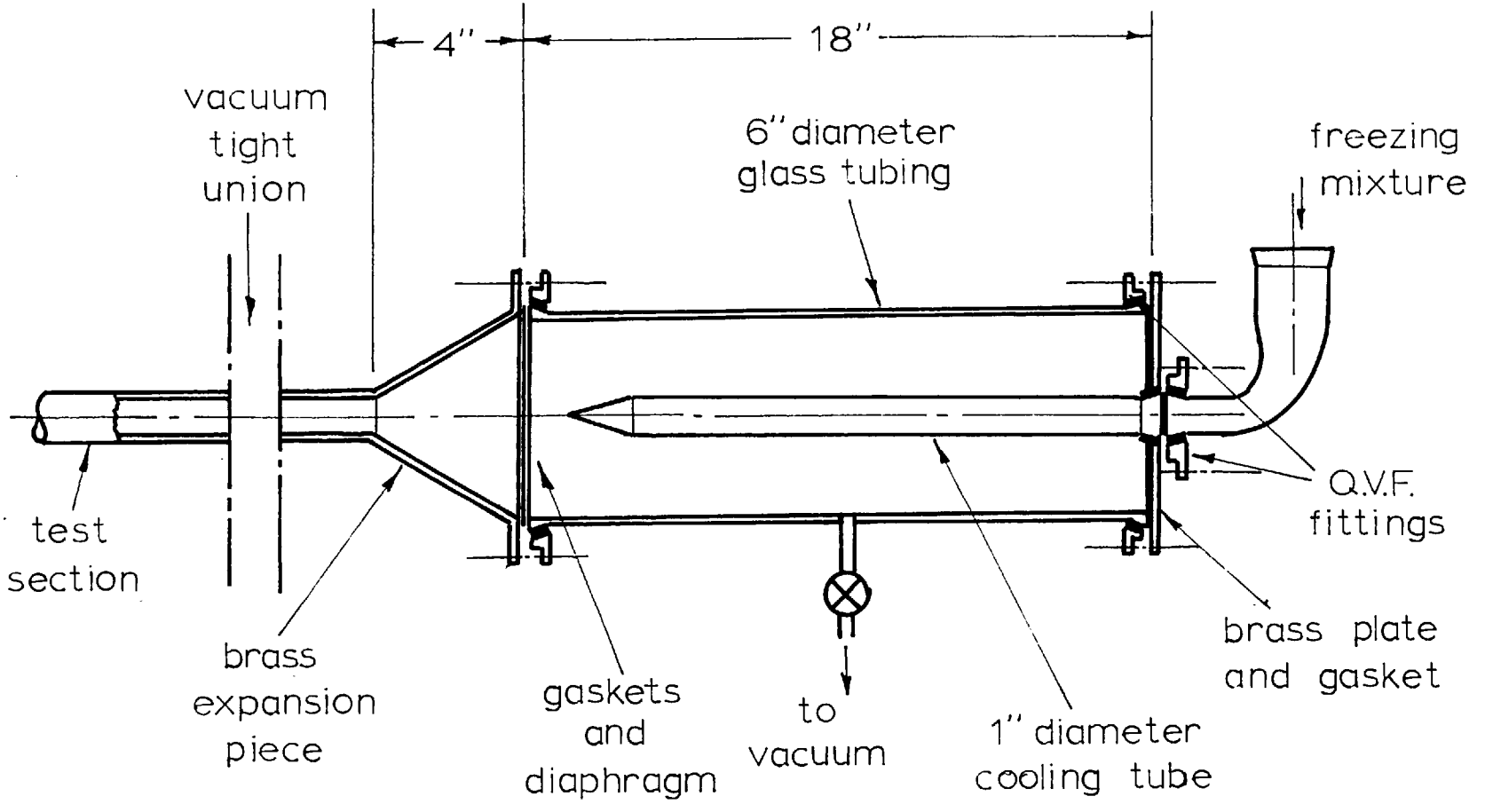

Figure 5.2. Cooled vessel for collection of detonation products.

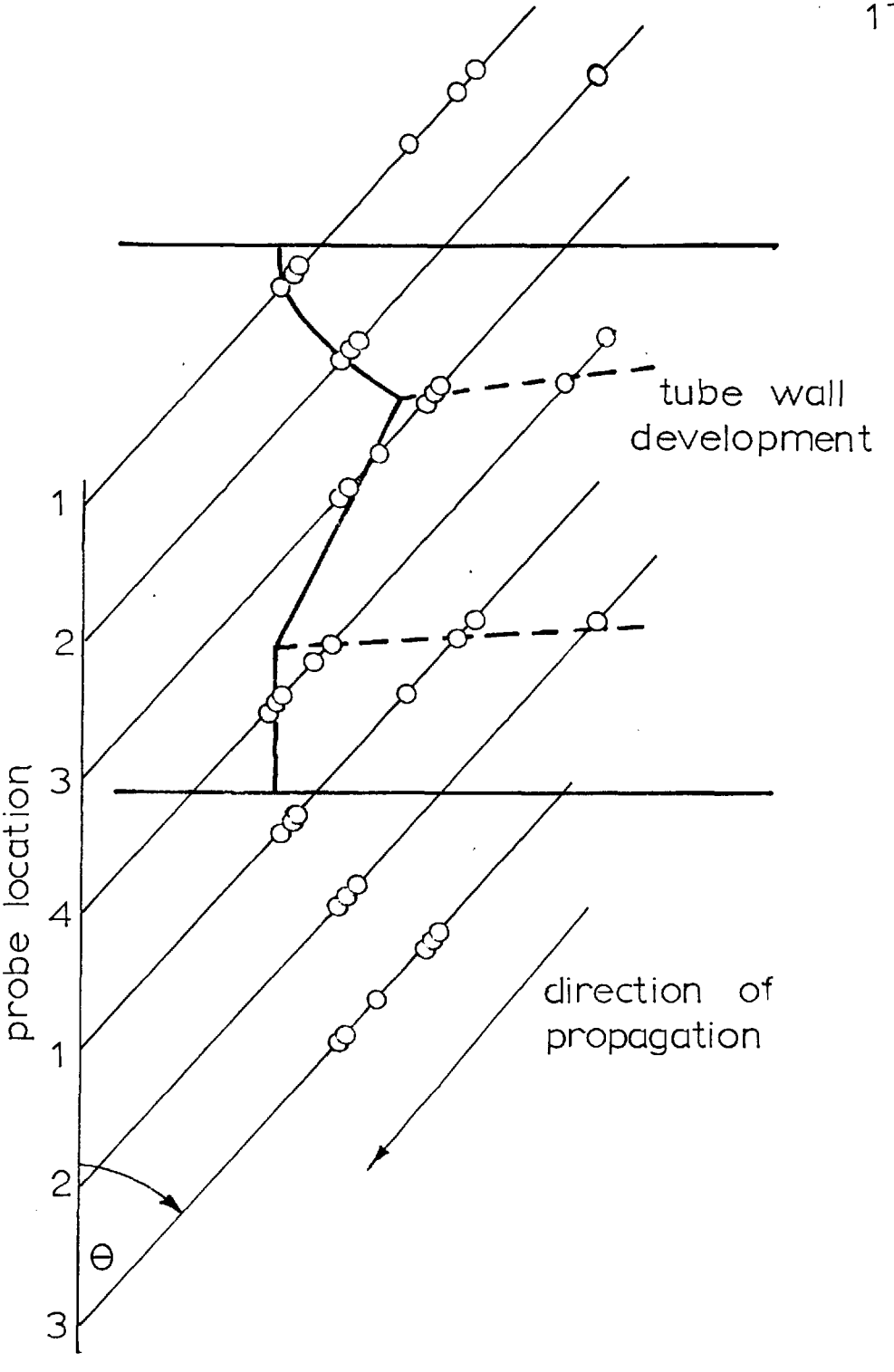

Figure 5.3 Ionisation front profile for three consecutive determinations in the system S_H+A, 90.00 % dilution. Drawn true size. N.B. The direction of spin rotation is uncertain.

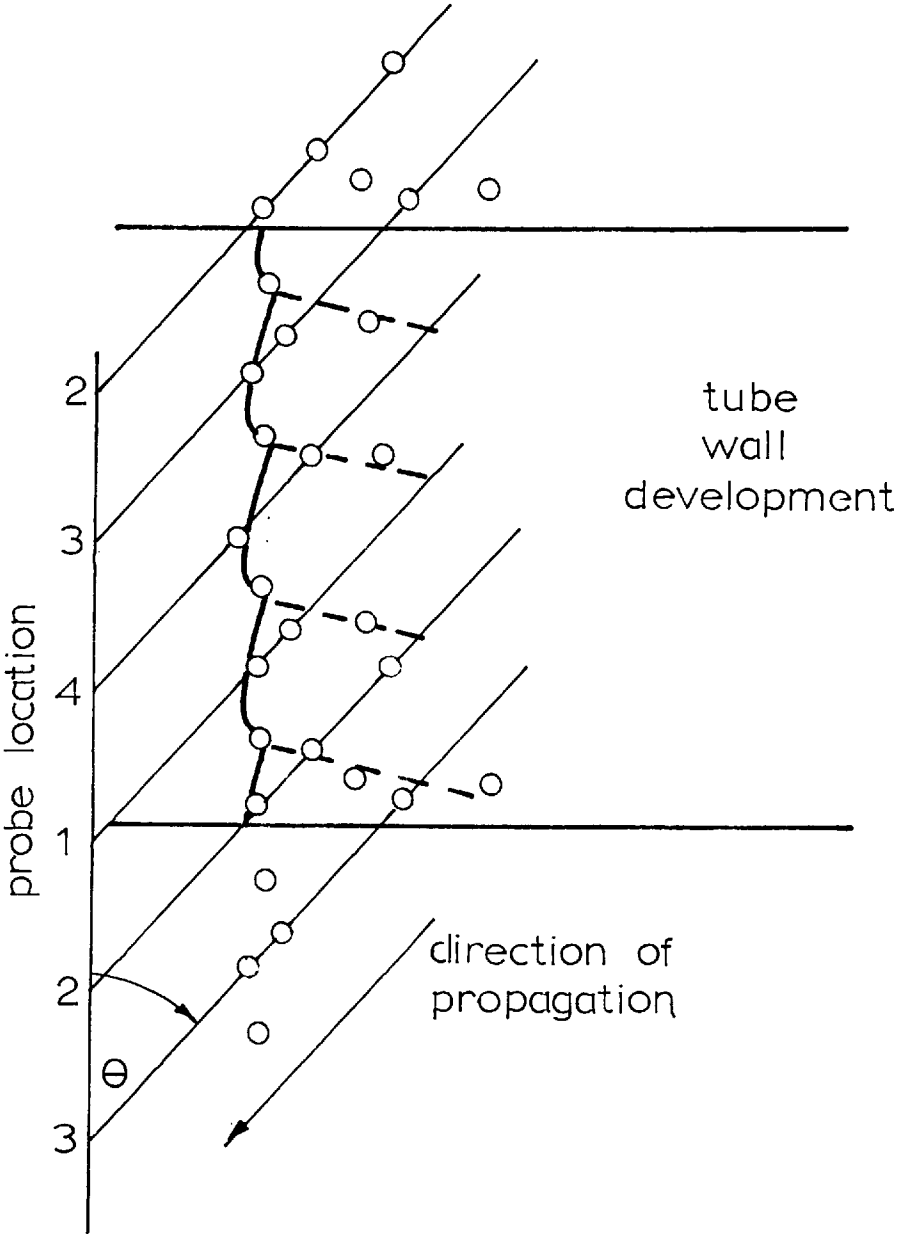

Figure 5.4.1. Ionisation front profile for the system S_H+A, 88.00 % dilution. Drawn true size.

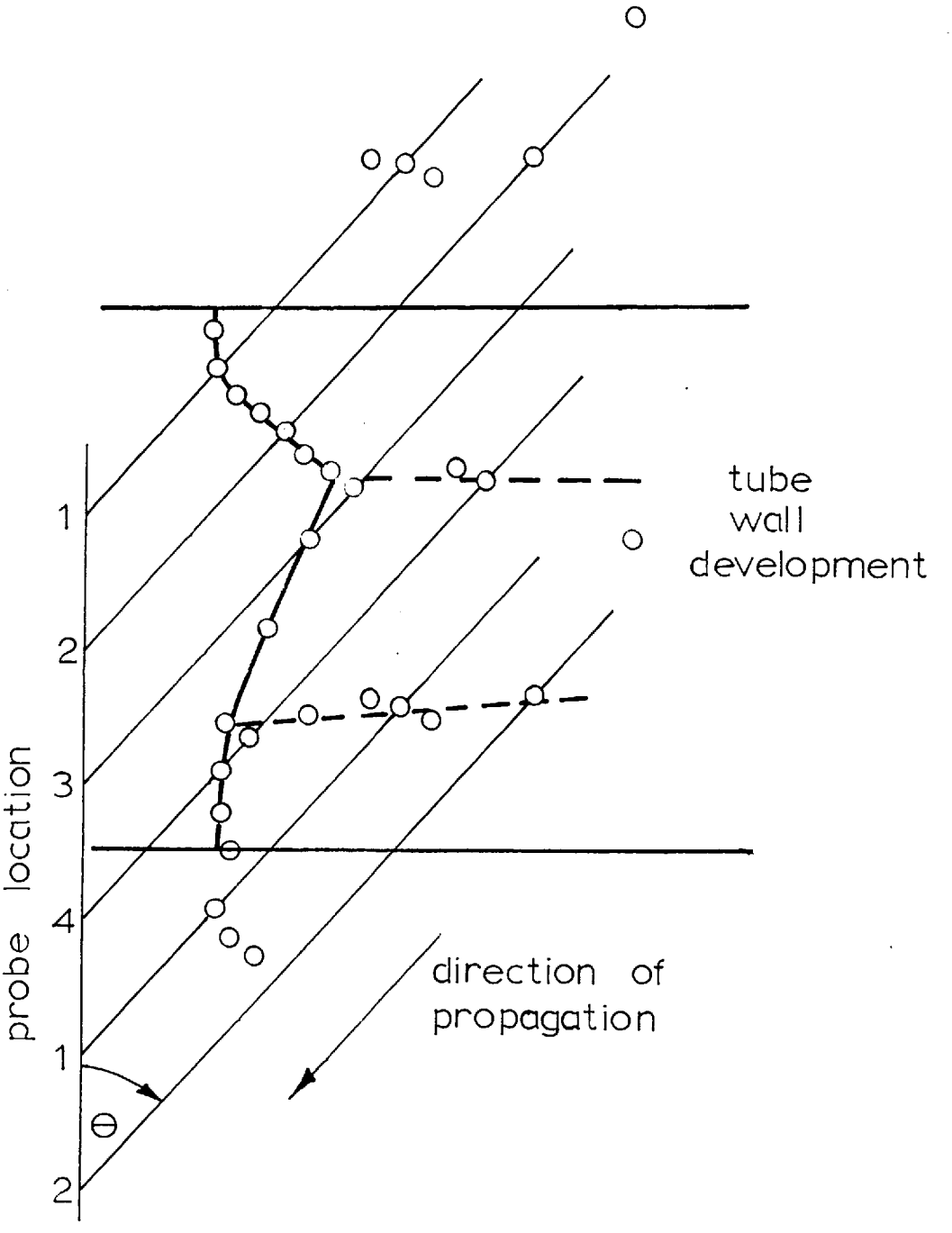

Figure 5.4.2. Ionisation front profile for the system S_H+A, 89.17 % dilution. Drawn true size.

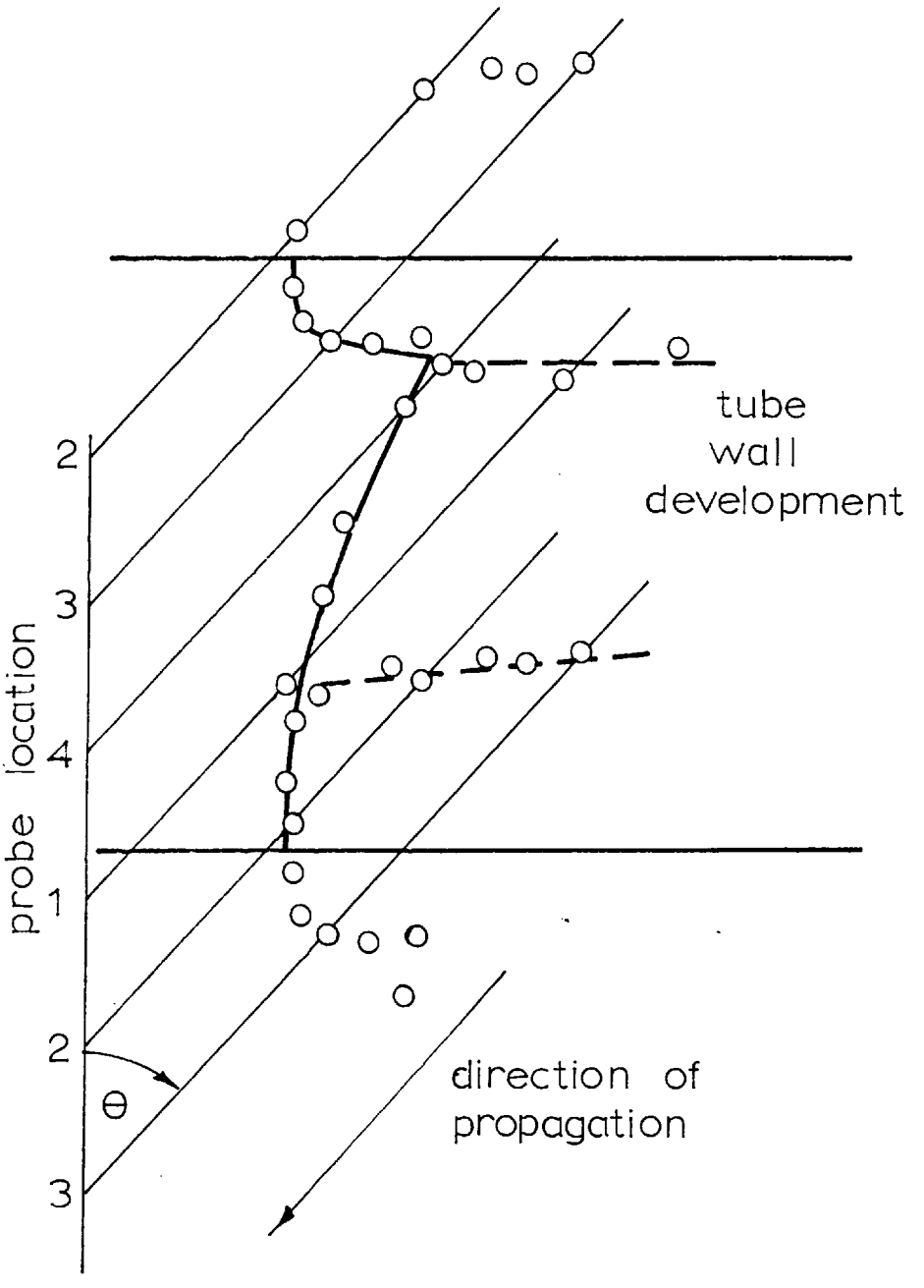

Figure 5.4.3. Ionisation front profile for the system S_H+A, 89.86% dilution. Drawn true size.

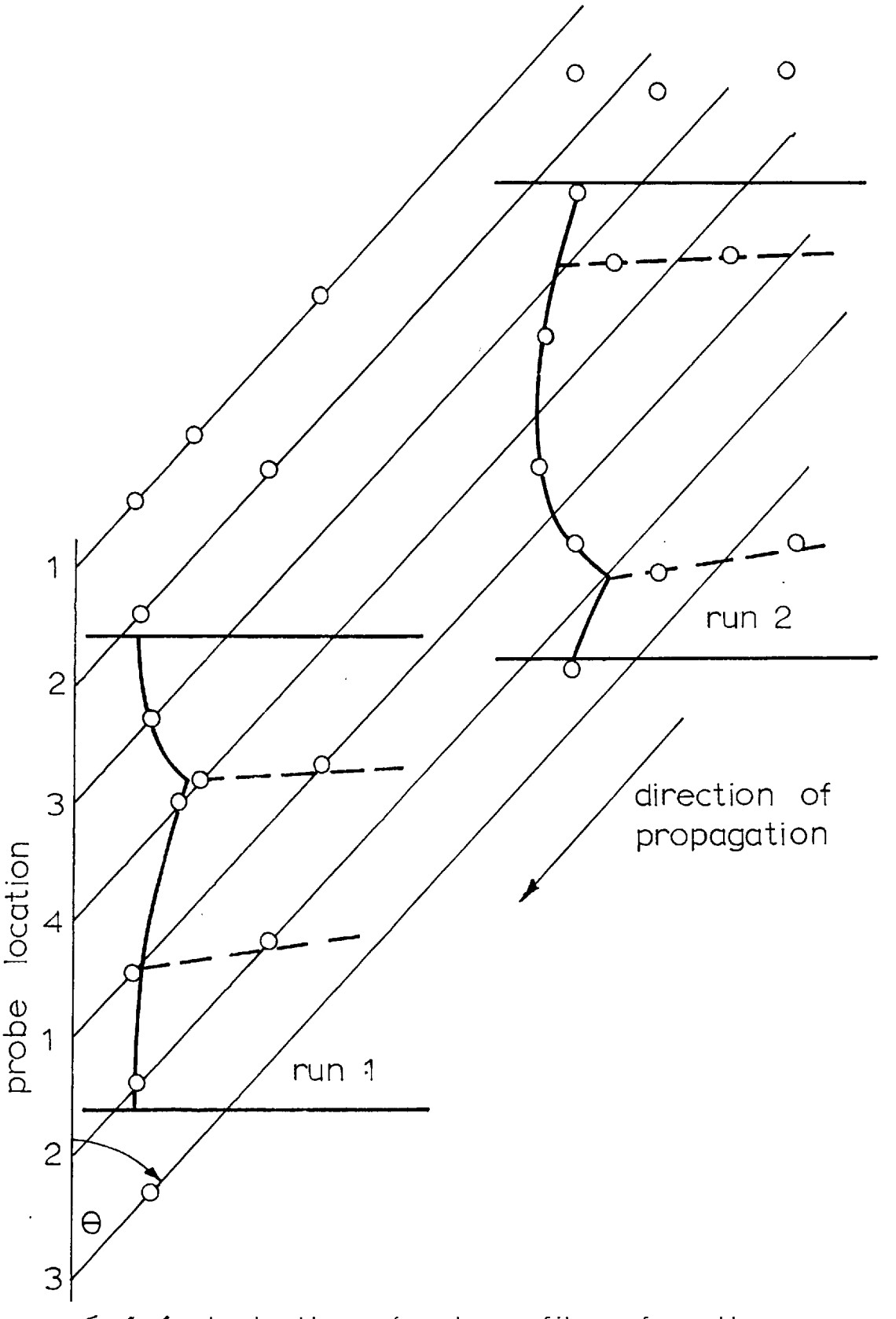

Figure 5.4.4. Ionisation front profiles for the system S_H+A, 91.21% dilution. Drawn true size.

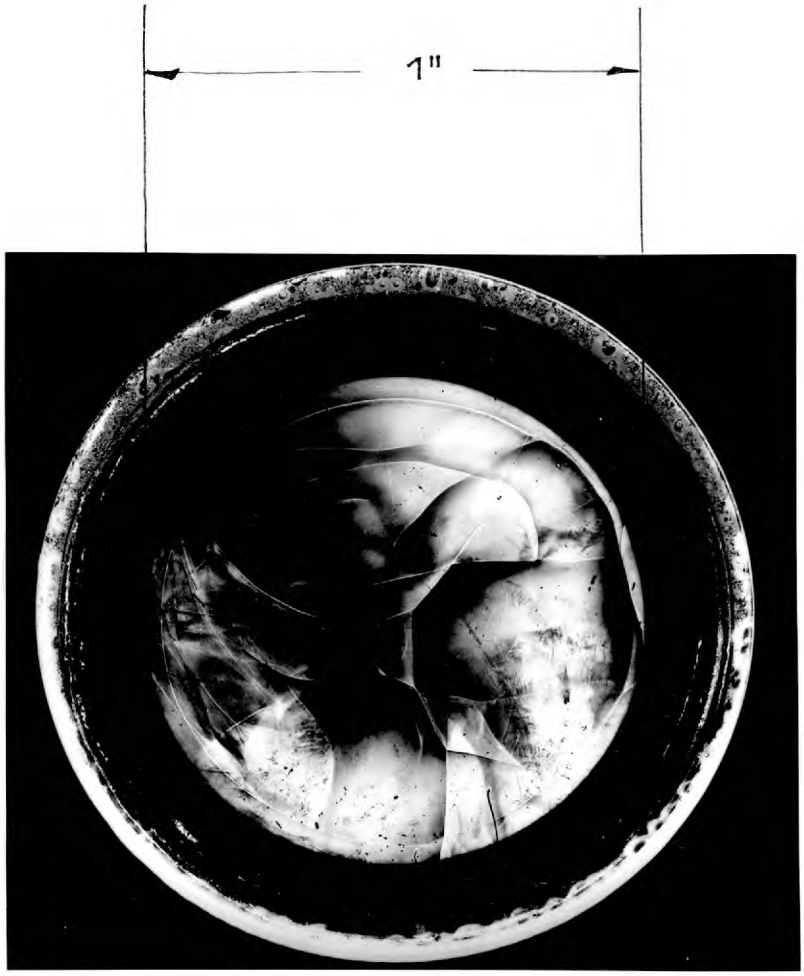

Figure 5.5.1. End-plate soot pattern for the system S_H + A, 88.00% dilution.

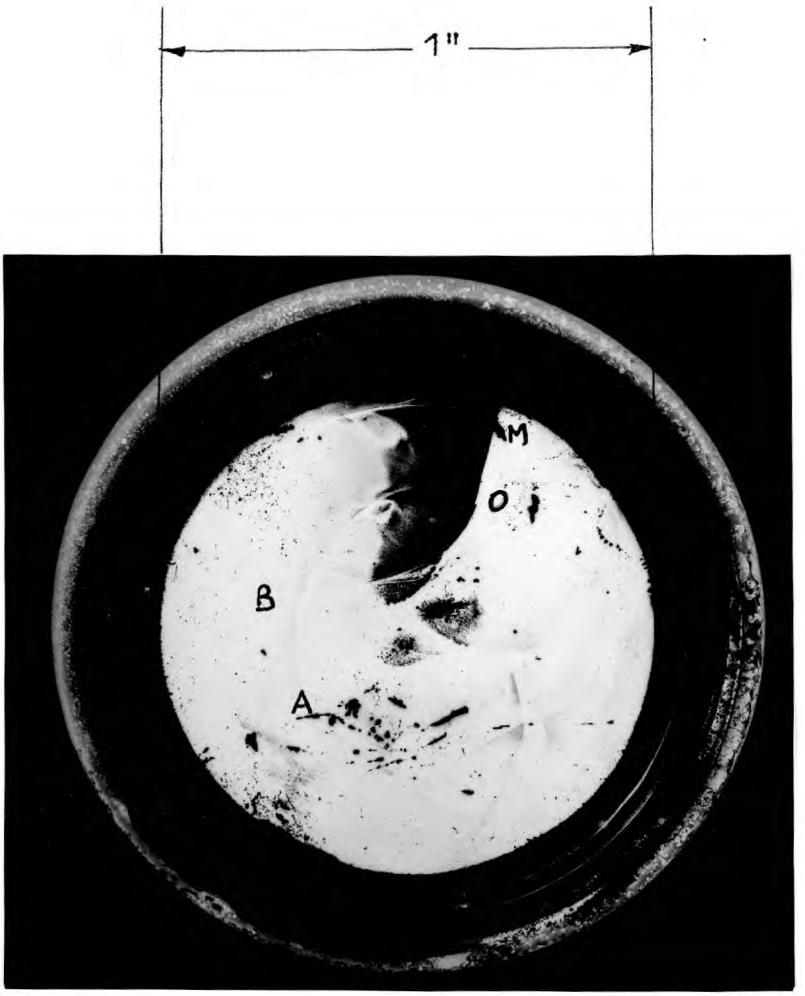

Figure 5.5.2. End-plate soot patterns for the system S_H + A, 89.17% dilution.

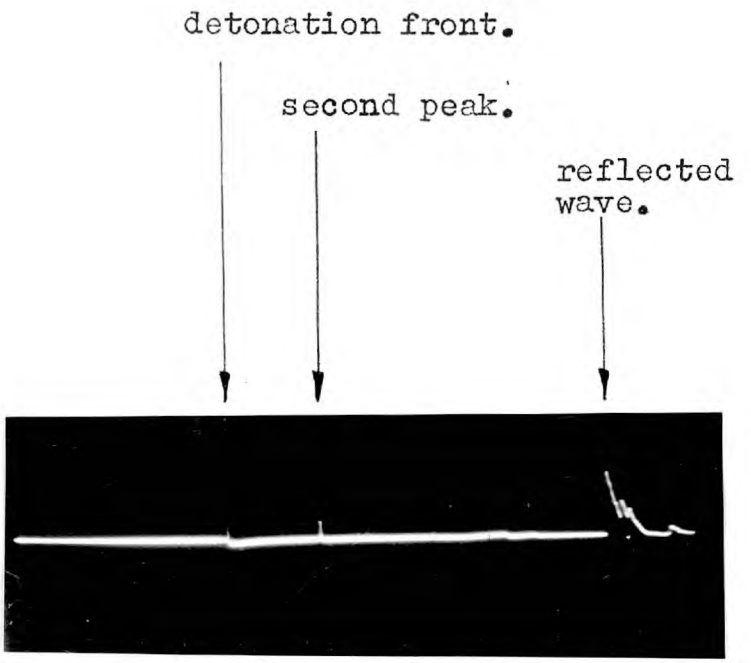

Figure 5.6. Oscilloscope trace indicating the existence of two detonation waves. Signal from first probe only.

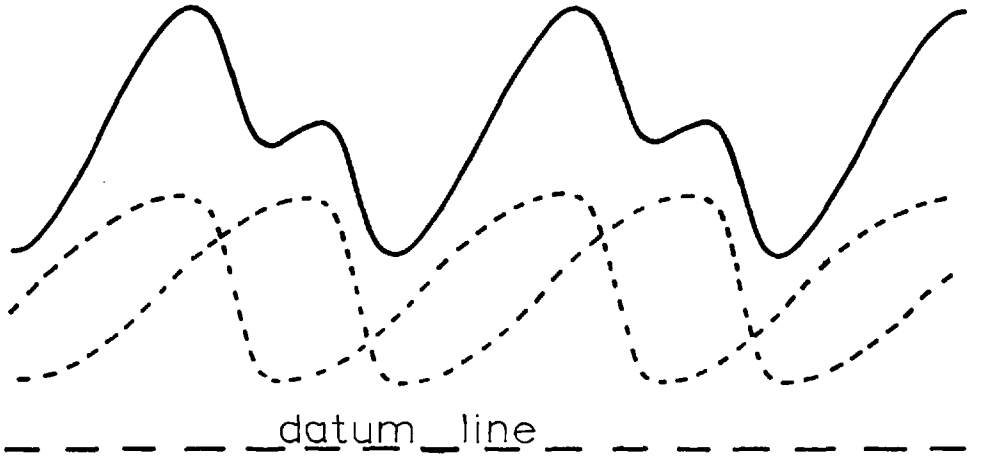

Figure 5.7. Addition of time displacements to give distorted sinusoidal fluctuations. ----, individual displacements; ——, overall displacement.

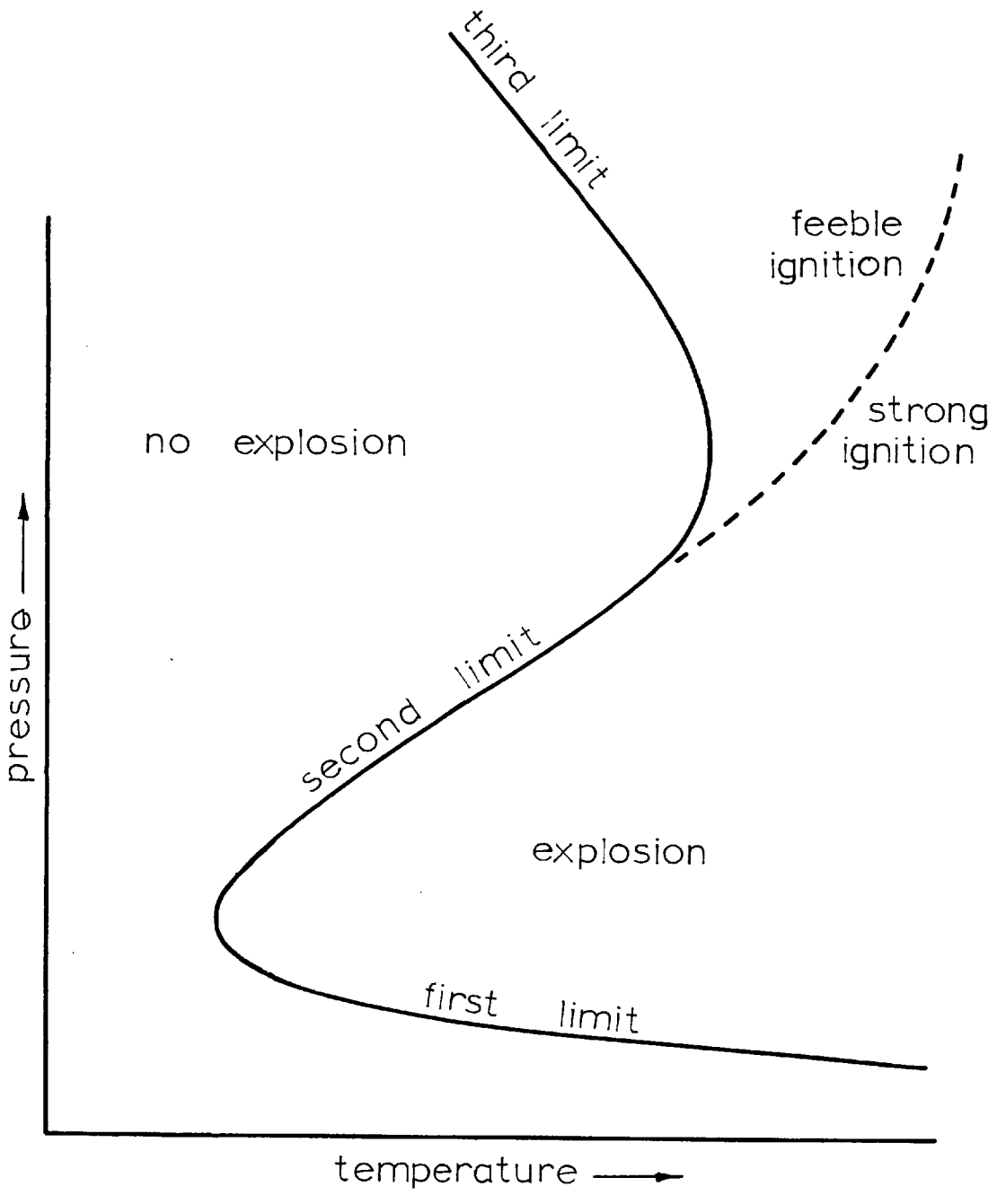

Figure 5.8, The line of demarcation between strong and feeble ignition in shock heated gases (after Voevodsky & Soloukhin).——, isothermal reaction; ----, shock compression.

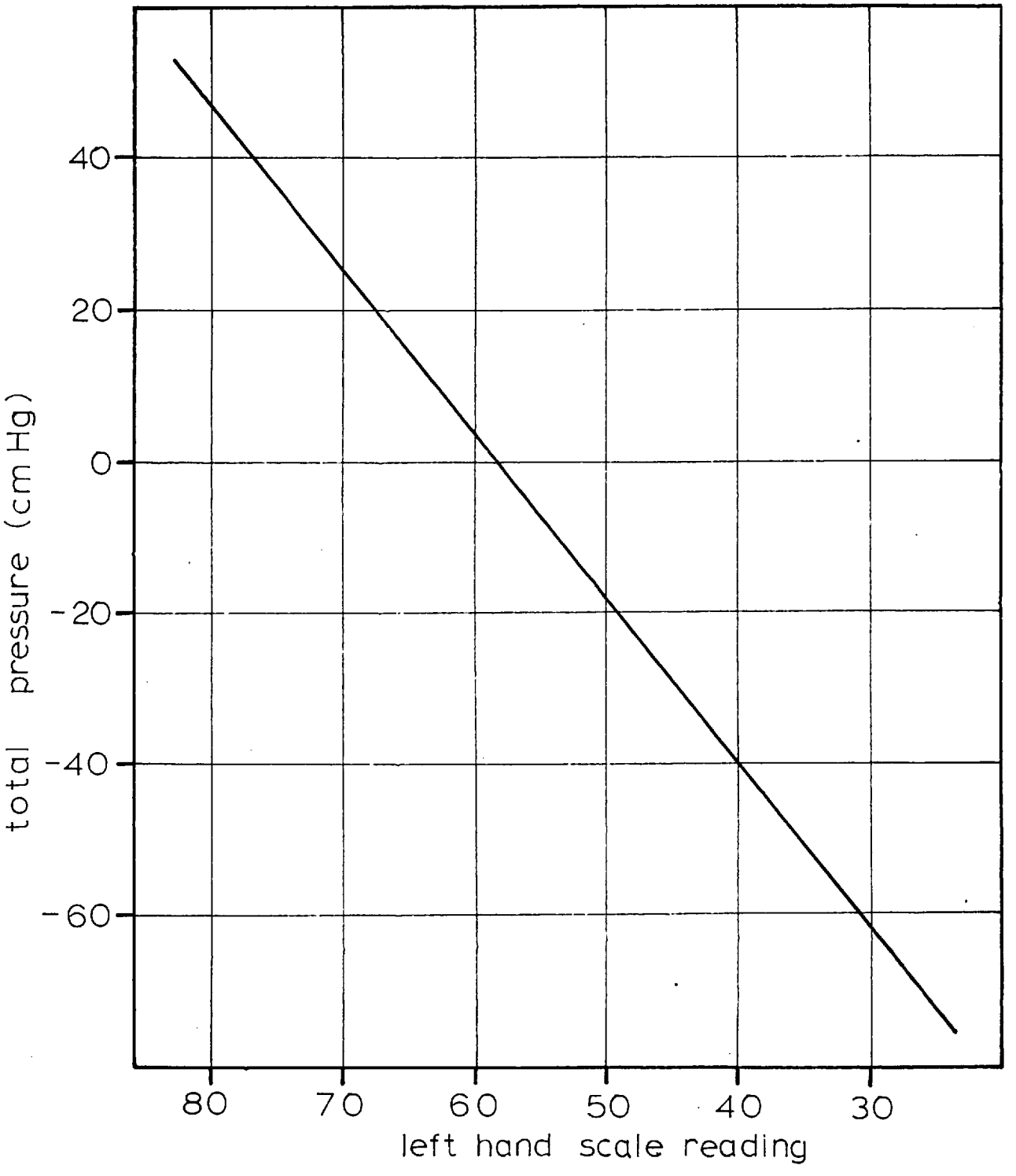

Figure A.1.1. Calibration curve for manometer M_1.

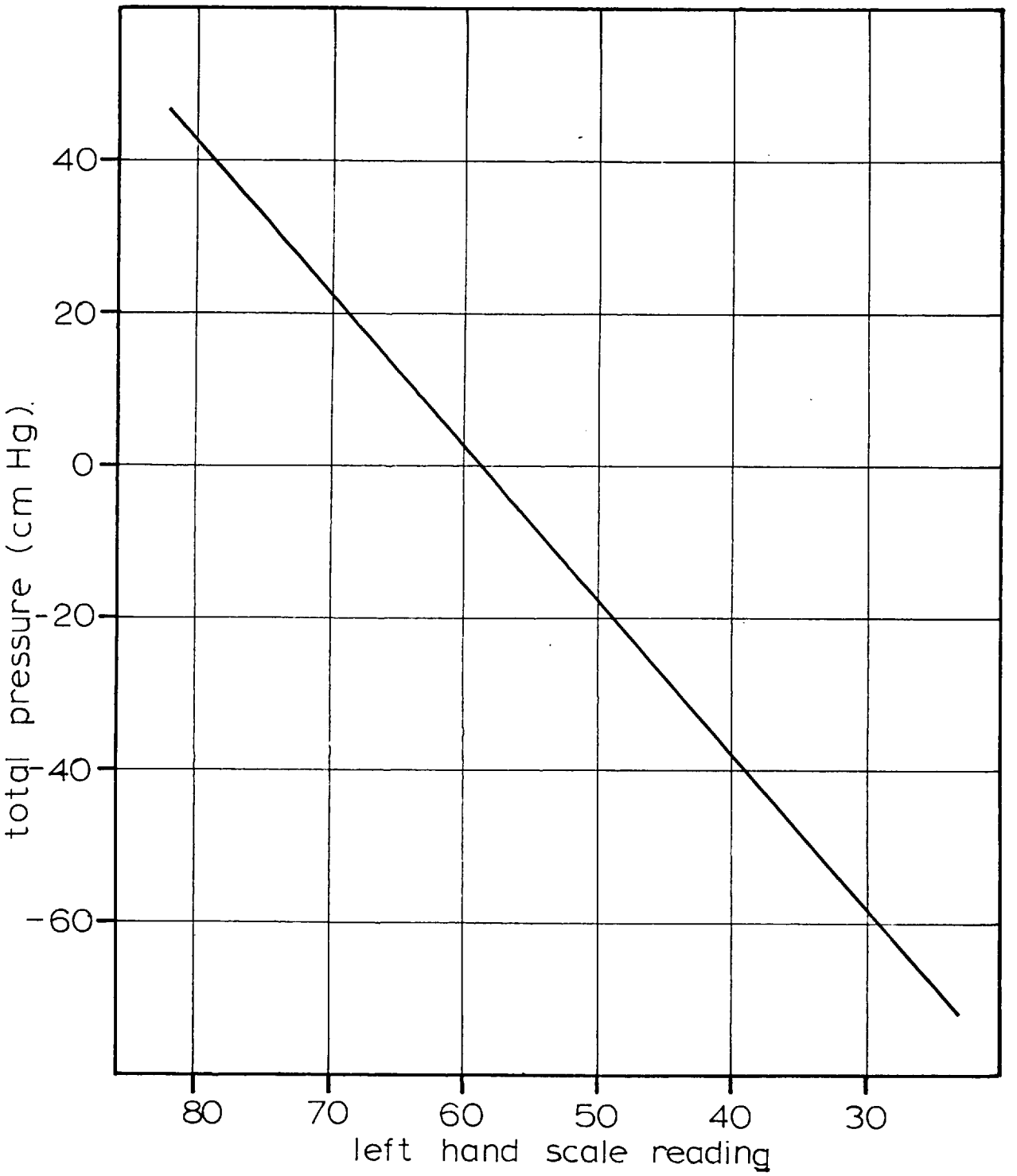

Figure A.1.2. Calibration curve for manometer M_2.

APPENDICES.

A.1. SAMPLE VELOCITY-COMPOSITION DETERMINATION.

For series 1, run B; stoichiometric hydrogen-oxygen diluted with oxygen. Desired composition: 52.5% reactive base, 47.5% diluent. This the same as the binary mixture: 35% hydrogen, 65% oxygen.

A.1.1. Priming mixture :

Initial readings on the manometer M_1 for full vacuum were :

L.H.S.	96.10
R.H.S.	20.55
	- 75.55 cm Hg

For a total gas pressure of 150 cm Hg, the required partial pressure of hydrogen was

$$\frac{66.67 \times 150}{100} = 100 \text{ cm Hg}$$

Therefore the pressure in the vessel after the addition of hydrogen should be 100 - 75.55 = 24.45 cm Hg. From the calibration curve given in figure A.1.1. this corresponded to a L.H.S. reading of 48.2 cm.

After filling the vessel and allowing the gas temperature to return to ambient (no further change in the reading), the manometer readings were:

L.H.S.	48.25
R.H.S.	72.50
	24.25 cm Hg

This means that the pressure of the hydrogen in the vessel was 75.55 + 24.25 = 99.80 cm Hg.

The required partial pressure of the oxygen was therefore 99.80 x 0.5 = 49.90 cm Hg, and the final pressure after the addition of oxygen 24.25 + 49.90 = 74.15 cm Hg. From figure A.1.1. this corresponded to a L.H.S. reading of 24.5 cm. After the addition of the oxygen the manometer readings were:

L.H.S.	24.55
R.H.S.	98.70
	74.15 cm Hg

Therefore the partial pressure of oxygen was 74.15 - 24.25 = 49.90 cm Hg.

The percentage of hydrogen in the mixture was therefore

$$\frac{99.80}{99.80 + 49.90} = 66.7\%$$

A.1.2. Test mixtures :

The same method was employed, using the calibration curve shown in figure A.1.2 to predict the manometer readings.

The % hydrogen in the test mixture was found to be

$$\frac{52.15}{52.15 + 96.95} = 35.45\%$$

This is equivalent to 53.18% reactive base, 46.82% diluent.

A.1.3. Filling detonation tube :

After the mixtures had been stirred for 45 minutes they were admitted to the tube. To ensure that the same initial pressure existed in both sections for all velocity determinations, the tube was always filled so that the right arm of the manometer M_3 was adjacent to a fixed point on the manometer scale. This corresponded to a pressure of 75.10 cm Hg.

A.1.4. Oscilloscope settings :

From published data and previous experiments, the expected detonation velocity was about 1980 metres/second. The distance between the trigger probe and the last detecting probe was slightly less than four metres. A time span of about two m. seconds was therefore required to show all signals on the oscilloscope traces. As the traces were 10 cm long, the time base was set on 0.2 m. sec./cm.

Previous experiments had also shown that probe signals of about 5 and 0.3 volts were transmitted to the oscilloscope from the ionisation and light probes respectively. The plug-in unit sensitivities were set at 2 and 0.1 volts/cm so as to give easily readable peaks on the traces.

A.1.5. Time interval measurement and velocity determination :

The distances between the peaks on the traces were found to be :

ionisation	0.664 cm
light, first set	0.666 cm
second set	0.661 cm

The average of two previous calibration determinations had shown that 1.280 cm on the film corresponded to one m. second. Therefore 0.664 cm corresponded to

$$\frac{0.664}{1.280} \text{ m. seconds}$$

The distance between the ionisation probes was 1.000 metres, thus the average velocity between the probes was

$$\frac{1.280}{0.664} \times 10^3$$

$$= 1943 \text{ metres/second.}$$

The velocities between the two sets of light probes were calculated in the same way, the only difference being that the distance between the probes was 1.005 metres. The velocities were found to be 1946 and 1962 metres/second.

Three such determinations were made with the same mixture, and the velocities for each set of probes found to be:

	1	2	3	ave.
ionisation	1943	1949	1943	1945
light (i)	1946	1959	1953	1953
(ii)	1962	1958	1956	1959
overall average				1953 m/sec.

As there was no significant difference between the velocities determined between the first and second set of light probes, the velocities obtained were taken as being the steady state values. The scatter of 19 metres/second ($\pm$ 0.45%) over the nine values shows the high degree of reproducibility of the velocity determinations.

A.2. VELOCITY-COMPOSITION RELATIONSHIPS FOR THE SYSTEMS STUDIED IN THE STAINLESS STEEL TUBE.

Owing to the similarity of the results obtained from the ionisation and light probes, only the overall average velocities are given in each case.

A.2.1. Stoichiometric hydrogen-oxygen diluted with hydrogen:

Run No.	% diluent from partial pressures	% diluent from oxygen analyser	detonation velocity (m/sec.)	Mach product γM^2
1 L	0.10		2815	
1 M	25.36		3156	
8 A	55.60		3602	33.72
8 B	61.60		3642	31.26
8 C	67.00		3664	28.71
8 D	70.00		3658	27.00
8 E	72.70		3636	25.23
8 F	75.10		3596	23.43
8 G	76.00		3576	22.71
9 A	76.66	76.66	3540	
8 H	76.75		3542	21.90
8 N	76.96		3523	21.56
9 B	77.02	77.05	3510	
			(1919)	(6.39)
8 J	77.11		3500	21.20
9 C	77.14	77.14	3524	
			(1867)	(6.03)
8 L	77.20		3534	21.57
9 D	77.26	77.23	3541	
			(1940)	(6.49)
8 K 1	77.29		3537	21.57
8 K 2	77.38		3537	21.52
9 E	77.53	77.47	3522	
			(1900)	(6.19)
8 M	77.59		3507	21.05
8 O	77.74		3482	20.68
9 F	77.74	77.71	(1896)	(5.96)
9 G	77.77	77.74	3477	
8 Q	77.95		3463	20.35
9 H	78.04	78.10	3451	
			(1906)	(6.15)

Run No.	% diluent from partial pressures	% diluent from oxygen analyser	detonation velocity (m/sec.)	Mach product γM^2
8 P	78.13		3455	20.17
9 J	78.28	78.34	3452	
			(1379)	(5.94)
8 R	78.43		3456	20.04
9 L	78.61	78.70	3445	
			(1894)	(5.99)
8 T	78.73		3435	19.65
9 M	78.76	78.82	(1943)	(6.28)
8 S	79.03		(2000)	
9 N	80.50		(1901)	(5.76)

N.B. The values given in parentheses are for the second velocity regime.

A. 2.2. Stoichiometric hydrogen-oxygen diluted with oxygen:

Run No.	% diluent from partial pressures	detonation velocity (m/sec.)	Mach product γM^2
1 A	25.52	2315	
1 B	46.82	1953	
1 C	61.81	1748	
7 A	69.55	1560	25.45
7 B	72.55	1480	23.43
7 D	74.35	1434	22.29
7 E	75.25	1405	21.55
		(1005)	(11.03)
7 F	75.70	1395	21.31
7 G	76.00	1378	20.84
		(993)	(10.82)
7 H	76.22	1370	20.64
		(989)	(10.75)
7 J	76.38	(980)	(10.57)
7 K	76.74	1245	17.11
		(945)	(9.86)
7 L	76.98	(663)	(4.86)

N.B. The values given in parentheses are for the second velocity regime.

A. 2.3. Stoichiometric hydrogen-oxygen diluted with helium:

Run No.	% diluent from partial pressures	detonation velocity (m/sec.)	Mach product γM^2
13 B	20.16	3046	
13 A	39.95	3300	
13 C	59.30	3564	
13 D	69.58	3647	
13 E	74.70	3684	32.99
13 F	78.26	3690	31.53
13 G	80.68	3627	29.44
13 H	82.75	3568	27.64
13 J	83.55	3517	26.53
13 K	85.00	3442	24.86
13 L	86.93	3340	22.72
13 Q	87.60	3271	21.55
13 R	87.97	3221	20.78
13 M	88.14	3181	20.21
13 T	88.28	3047	18.50
13 P	88.48	2946	17.24
13 U	88.72	2877	16.37
13 X	88.96	2897	16.54
13 N	89.00	2946	17.09
13 W	89.10	2879	16.30

A.2.4. Stoichiometric hydrogen-oxygen diluted with argon:

Run No.	% diluent from partial pressures	detonation velocity (m/sec.)	Mach product γM^2
15 A	20.12	2362 (8)	
15 B	40.16	2065 (41)	
15 C	60.06	1807 (29)	
15 D	74.96	1603 (12)	
15 E	79.99	1490 (5)	30.82
15 F	82.98	1419 (0)	28.82
15 G	85.96	1331 (20)	25.79
15 H	87.50	1266 (27)	23.61
15 J	88.19	1237 (8)	22.66
15 K	88.69	1193 (10)	21.15
15 P	88.84	1195 (27)	21.25
15 L	88.96	1210 (6)	21.81
15 Q	89.04	1208 (6)	21.74

Run No.	% diluent from partial pressures	detonation velocity (m/sec.)	Mach product γM^2
15 M	89.10	1185 (19)	20.93
15 N	89.21	1179 (10)	20.74
15 R	89.29	1187 (12)	21.04
15 S	89.35	1199 (9)	21.48
15 T	89.44	1178 (2)	20.75
15 U	89.50	1170 (5)	20.44
15 V	89.59	1178 (8)	20.77
15 W	89.69	1151 (4)	19.84
15 X	89.80	1138 (16)	19.41
15 Y	89.89	1143 (28)	19.59
15 Z	90.20	1117 (27)	18.76
15 AA	90.39	1076 (20)	17.44
15 AB	90.50	1081 (36)	17.62
15 AC	90.58	1047 (19)	16.52
15 AD	90.70	1032 (44)	16.07
15 AE	90.99	1037 (13)	16.26
15 AM	91.10	1032	16.12
15 AN	91.26	1030	16.08
15 AF	91.51	1012	15.55
15 AH	91.81	992 (17)	14.97
15 AK	91.90	975	14.47

N.B. The values given in parentheses are the variations over three separate determinations.

A.2.5. Stoichiometric hydrogen-oxygen diluted with carbon dioxide:

Run No.	% diluent from partial pressures.	detonation velocity (m/sec.)
16 A	20.00	2102
16 B	30.32	1880
16 Q	36.08	1759
16 G	37.69	1723
16 P	38.50	1498
16 N	38.97	1313 (1055)
16 H	39.39	1306 (1023)

Run No.	% diluent from partial pressures.	detonation velocity (m/sec.)
16 L	39.46	1308 (1026)
16 K	39.53	1532 (976)
16 M	39.71	1605
16 J	39.80	1319 (996)
16 C	39.98	1297 (1031)
16 R	40.18	(1059)
16 E	42.00	(868)
16 D	45.18	(752)
16 F	47.41	(745)
16 S	49.97	(711)
16 T	50.83	(724)
16 U	51.47	(716)
16 V	52.17	(657)
16 W	52.63	(690)

N.B. The values given in parentheses are for the second velocity regime.

A.2.6. Stoichiometric hydrogen-oxygen diluted with ammonia.

Run No.	% diluent from partial pressures.	detonation velocity (m/sec.)
14 A	15.26	2819
14 B	25.26	2839
14 C	32.83	2789
14 D	35.16	2753
14 U	36.91	2734
14 E	37.57	2702
14 J	38.13	2762
14 H	38.51	2840
14 K	38.86	2870
14 L	39.48	2802
14 F	39.80	2745
14 M	39.97	2677
14 P	40.15	2680

Run No.	% diluent from partial pressures.	detonation velocity (m/sec.)
14 N	40.48	2669
14 R	40.60	2664
14 Q	41.06	2664
14 T	41.19	failed

A.2.7. Stoichiometric deuterium-oxygen diluted with deuterium:

Run No.	% diluent from partial pressures	detonation velocity (m/sec.)	Mach product γ_M^2
25 B	66.91	3116	27.77
25 C	68.53	3086	26.66
25 D	69.37	3054	25.81
25 L	69.76	3009	24.93
25 E	70.33	3024	24.98
25 M	70.60	3039	25.14
25 N	70.90	3031	24.90
25 F	71.17	3002	24.33
25 G	71.68	3010	24.29
25 H	71.83	3031	24.58
25 J	72.10	2988	23.79
25 K	72.22	failed	

A.2.8. Stoichiometric deuterium-oxygen diluted with oxygen:

Run No.	% diluent from partial pressures	detonation velocity (m/sec.)	Mach product γ_M^2
27 A	69.56	1528	24.80
27 B	72.98	1439	22.53
27 F	73.72	1411	21.77
27 M	73.99	1300	18.51
27 Q	74.06	(563)	(3.47)
27 R	74.20	1391	21.22
		(556)	(3.39)
27 P	74.29	1383	21.00
27 K	74.47	(552)	(3.35)

Run No.	% diluent from partial pressures	detonation velocity (m/sec.)	Mach product γM^2
27 D	74.48	1368	20.57
27 L	74.57	(546)	(3.28)
27 G	74.65	(486)	(2.60)

N.B. the values given in parentheses are for the second velocity regime.

A.2.9. Stoichiometric deuterium-oxygen diluted with helium:

Run No.	% diluent from partial pressures	detonation velocity (m/sec.)	Mach product γM^2
22 A	79.61	3534	29.75
22 B	83.98	3404	25.69
22 C	86.99	3278	22.61
22 D	87.99	3097	19.82
22 G	88.25	2635	14.28
22 H	88.35	2533	13.17
22 E	88.48	2546	13.28
22 J	88.67	2512	12.88
22 F	87.76	2365	11.40

A.2.10. Stoichiometric deuterium-oxygen diluted with argon:

Run No.	% diluent from partial pressures	detonation velocity (m/sec.)	Mach product γM^2
23 A	85.63	1335	25.89
23 B	87.49	1239	22.71
23 G	88.34	1211	21.84
23 C	88.50	1195	21.28
23 E	88.74	1211	21.90
23 H	88.86	1194	21.31
23 D	89.01	1186	21.05
23 J	89.12	1198	21.48
23 F	89.25	1172	20.59
23 L	90.29	1073	17.38
23 K	90.40	1050	16.67

Run No.	% diluent from partial pressures	detonation velocity (m/sec.)	Mach product γM^2
23 M	90.51	1033	16:13
23 N	91:00	1014	15:60
23 Q	91:42	1000	15:22
23 P	91.50	840	10.74

A.2.11. Stoichiometric cyanogen-oxygen diluted with cyanogen:

Run No.	% diluent from partial pressures	detonation velocity (m/sec.)	Mach product γM^2
28 A	0:00	2755	128:6
28 B	20.10	2228	88:09
28 C	29:96	1976	70.90
28 D	39.86	1930	69:13
28 E	43.84	1992	74:27
28 F	46.04	1953	71:72
28 G	48.94	1879	66:82
28 J	50.90	1865	66.09
28 H	51.94	668	-

A.2.12. Stoichiometric cyanogen-oxygen diluted with oxygen:

Run No.	% diluent from partial pressures	detonation velocity (m/sec.)	Mach product γM^2
29 A	20.18	2529	103:19
29 B	29:54	2398	90:61
29 C	39.10	2264	78:79
29 E	43.76	2240	76:18
29 D	48:74	2223	74:05
29 F	51.88	2204	72:16
29 G	54.84	2194	70:95
29 H	59.50	2066	62.09
29 J	60.88	2075	62:40
29 K	62:56	2084	62:64
29 L	63:94	2024	58:88
29 M	64.82	2000	57.34
29 N	65.82	2033	59.08

Run No.	% diluent from partial pressures	detonation velocity (m/sec.)	Mach product γM^2
29 P	69:06	1984	55:74
29 R	71:78	1930	52:34
29 Q	72.06	1586	35.31

A.2.13. Stoichiometric cyanogen-oxygen diluted with helium:

Run No.	% diluent from partial pressures	detonation velocity (m/sec.)	Mach product γM^2
31 A	69:89	3443	73:84
31 B	75:91	3493	64.74
31 F	80:96	3474	54:70
31 C	82:13	3452	51.90
31 G	82.28	failed	

A.2.14. Stoichiometric cyanogen-oxygen diluted with argon:

Run No.	% diluent from partial pressures	detonation velocity (m/sec.)	Mach product γM^2
30 A	19:47	2636	116:67
30 B	39:92	2524	105:93
30 C	58:73	2289	86:34
30 D	64:88	2185	78:41
30 E	70:96	2080	70:84
30 F	75:91	1992	64:82
30 G	80:66	1831	54:65
30 H	85:82	1638	43:61
30 J	88:11	1514	37:22
30 K	90:01	1399	31.75
30 M	90.52	failed	

A.3. VELOCITY-COMPOSITION RELATIONSHIPS FOR THE SYSTEMS STUDIED IN THE COATED TUBE.

A.3.1. Stoichiometric hydrogen-oxygen diluted with hydrogen:

Run No.	% diluent from partial pressures	detonation velocity (m/sec.)
18 A	38.68	3384
18 B	55.09	3611
18 C	68.14	3664
18 D	69.94	3658
18 E	73.30	3631
18 F	76.21	3572
18 G	76.78	3549
18 H	77.38	(2165)
18 J	77.71	(2261)
18 K	78.04	(2167)
18 L	79.03	(2193)

Higher fuel concentrations were not attempted as the probe signals were too small.

N.B. The values given in parentheses are for the second velocity regime.

A.3.2. Stoichiometric hydrogen-oxygen diluted with oxygen:

Run No.	% diluent from partial pressures	detonation velocity (m/sec.)
19 A	70.20	1576
19 B	73.12	1468
19 D	74.17	1428
19 C	74.38	1395
19 M	74.41	1304
19 P	74.47	1401
19 E	74.50	1002
19 L	74.57	1410

Run No.	% diluent from partial pressures	detonation velocity (m/sec.)
19 J	74.63	1401
19 F	75.22	1403
19 G	75.88	1382
19 H	76.60	1334
		(960)
19 N	76.96	(810)

N.B. The values given in parentheses are for the second velocity regime.

A.3.3. Stoichiometric hydrogen-oxygen diluted with carbon dioxide.

Run No.	% diluent from partial pressures	detonation velocity (m/sec.)
20 A	37.94	1649
20 B	38.61	1528
20 C	39.07	1286
20 D	39.59	1423
		1644
20 E	39.79	1660
20 F	40.04	1482
20 G	40.27	1447
20 H	40.57	(1030)
20 J	40.65	1448
		(1003)
20 K	40.98	1407
		(947)
20 M	41.52	(882)
20 N	44.96	(771)
20 P	47.98	(745)
20 Q	49.00	(716)
20 R	49.93	(706)
20 S	50.88	(730)
20 T	52.29	(605)
20 U	52.61	(715)
20 V	52.71	(610)
20 W	52.79	(450)

N.B. The values given in parentheses are for the second velocity regime.

A. 3.4. Stoichiometric hydrogen-oxygen diluted with ammonia:

Run No.	% diluent from partial pressures	detonation velocity (m/sec.)
21 A	35.04	2772
21 B	37.46	2738
21 C	37.99	2722
21 D	38.85	2694
21 E	39.56	2679
21 F	40.13	2681
21 G	40.57	2675

A.4. RESIDUAL GAS PRESSURE AFTER DETONATION IN A FIXED VOLUME.

A.4.1. Sample calculated values :

For a mixture of 92.5% hydrogen, 7.5% oxygen, initially at 20.5°C and 75.1 cm Hg pressure:

If all of the oxygen combined with hydrogen to form water i.e.

$$0.925\ H_2 + 0.075\ O_2 = 0.775\ H_2 + 0.15\ H_2O$$

then the partial pressures of the product gases for an initial pressure of 75.1 cm Hg would be:

hydrogen	58.20 cm Hg
water	11.27 cm Hg.

Assuming that the product gas returned to ambient temperature, then some of the water vapour would condense, the condensate causing a negligible change in the volume of the container. The partial pressure of water would then be its vapour pressure, and the partial pressures of the products would be:

hydrogen	58.20 cm Hg
water	1.81 cm Hg (from tables)
total pressure	60.01 cm Hg.

If, however, all of the oxygen combined with hydrogen to form hydrogen peroxide which subsequently decomposed to water and oxygen, the overall reaction would be:

$$0.925\ H_2 + 0.075\ O_2 = 0.850\ H_2 + 0.0375\ O_2 + 0.075\ H_2O$$

In the same way as above, the partial pressures of the product gases would be:

hydrogen	63.84
oxygen	2,82
water	1.81
total pressure	68.47 cm Hg

It would therefore be expected that the end pressure of the detonation products could be a sensitive test for whether water is formed directly, or via hydrogen peroxide.

A.4.2. Experimental values :

The residual pressures were determined by measuring the overall pressure in the detonation tube after detonation with a mercury manometer. The relationship between the overall pressure in the entire detonation tube and manometer arm and the residual pressure in the test section was found by using the normal detonation procedure with the test section filled with argon. The relationship, averaged over three separate determinations, was found to be:

$$p' = \frac{R - 0.2504\ vp}{0.750}$$

where p' is the residual pressure, R is the overall pressure, and vp is the vapour pressure of water at atmospheric temperature.

Using the calibration relationship, the following results were obtained for hydrogen-oxygen mixtures:

Measured residual pressures after detonation

Run No.	velocity regime	% hydrogen	p' (expl.)	p' (water)	p' (hydrogen peroxide)
12 C 1	upper	92.61	59.35	59.54	
12 C 2	lower	92.61	65.99		68.59
12 C 3	upper	92.61	59.79	59.54	
12 D 1	upper	92.63	59.88	59.53	
12 D 2	upper	92.63	59.74	59.53	
12 D 3	lower	92.63	65.74		68.58
12 E 1	lower	15.70	58.75	59.36	59.36
12 E 3	upper	15.70	58.75	59.36	59.36
12 F 3	upper	15.76	58.80	59.40	59.40
12 G 1	lower	15.70	58.68	59.41	59.41
12 G 2	upper	15.70	58.81	59.41	59.41
12 G 3	lower	15.70	58.81	59.41	59.41

A.5. CALCULATED STEADY STATE DETONATION VELOCITIES.

A.5.1. Sample calculation:

For a mixture of 90% H_2 + 10% O_2, initially at 25°C and one atmosphere pressure:

The overall reaction can be written as

$$0.9\ H_2 + 0.1\ O_2 = a\ H_2 + b\ H + c\ O_2 + d\ H_2O + e\ O + f\ OH + g\ HO_2$$

The equilibrium constants at the temperatures involved (about 2500°K) showed that the radicals O, OH and HO_2 are present in such low concentrations at equilibrium that the only two chemical reactions that need be considered are

$$2H_2 + O_2 \overset{k_1}{=} 2H_2O$$

and

$$H_2 \overset{k_2}{=} 2H.$$

Therefore

$$k_1 = \frac{d^2}{a^2\ c\phi} \quad . \ . \ . \ . \quad (1)$$

and

$$k_2 = \frac{b^2\ \phi}{a} \quad . \ . \ . \ . \quad (2)$$

where $\phi = p/n$; p = pressure at equilibrium and n = number of moles of product gas per mole of reactant gas.

Hydrogen mole balance:

$$0.9 = a + \frac{b}{2} + d \quad . \ . \ . \ . \ . \quad (3)$$

Oxygen mole balance:

$$0.1 = c + \frac{d}{2} \quad . \ . \ . \ . \ . \ . \quad (4)$$

From (2), $$a = \frac{b^2 \phi}{k_2} \quad . \quad . \quad . \quad . \quad . \quad . \quad (5)$$

From (1) and (5), $$c = \frac{d^2}{k_1 a^2 \phi} = \frac{d^2 k_2^2}{k_1 b^4 \phi^3} \quad . \quad . \quad (6)$$

Substituting (5) into (3) gives

$$0.9 = \frac{b^2 \phi}{k_2} + \frac{b}{2} + d \quad . \quad . \quad . \quad (7)$$

Substituting (5) and (6) into (4) gives

$$0.1 = \frac{d^2 k_2^2}{k_1 b^4 \phi^3} + \frac{d}{2} \quad . \quad . \quad . \quad . \quad (8)$$

But, from preliminary investigations, at the temperatures incurred, $k_1 \doteqdot 10^4$, $k_2 \doteqdot 10^{-5}$, $\phi \doteqdot 10$, $b \doteqdot 10^{-3}$, and $d \doteqdot 10^{-1}$.

$$\therefore \quad \frac{d^2 k_2^2}{k_1 b^4 \phi^3} \doteqdot 10^{-7}$$

which is insignificant, i.e. equation (6) reduces to

$$c = 0 \quad . \quad . \quad . \quad . \quad (9)$$

and therefore, from (4)

$$d = 0.2 \quad . \quad . \quad . \quad . \quad (10)$$

b can then be found from (7), and subsequently, a can be found from (3)

Assuming values for T_2 and v of 2250°K and 0.6 respectively:

$$\theta = 7.550$$

$$\phi = \frac{p}{n} = \frac{\theta}{v} = 12.583$$

From NBS circular 500, the value of k_2 for this temperature is 5.489×10^{-5}.

∴ Substituting this value into (7),

$$2.292 \times 10^{5}\, b^2 + 0.5\, b - 0.7 = 0$$

i.e. $$b^2 + 2.182 \times 10^{-6}\, b - 3.054 \times 10^{-6} = 0$$

i.e. $$b = -1.091 \times 10^{-6} + (1.190 \times 10^{-12} + 3.054 \times 10^{-6})^{2}$$

$$= 0.0017$$

Substituting into (3),

$$a = 0.9 - 0.2 - 0.00085$$

$$= 0.69915$$

The composition of the product gases at 2250°K was therefore

H_2	0.69915
H	0.0017
H_2O	0.2
	0.90085 = n

∴ m = 1.1101

p = nφ = 11.335

By definition,

$$c = \frac{2M_1 \Delta H}{R \Delta T}$$

From thermodynamic tables given in NBS circular 500,

$$\begin{aligned} \Delta H &= 0.69915 \times 15573 = 10888 \\ &+ 0.0017 \times 9697 = 16 \\ &+ 0.2 \times 20423 = 4085 \\ & \qquad\qquad 14989 \text{ cals} \end{aligned}$$

$$\therefore \quad c = \frac{2 \times 14989}{1.987 \times 1952} = 7.729$$

By definition, $q = \frac{2M_1 Q}{RT_1}$

Now $Q = \sum n_i \Delta H^{o}_{fi}$

$$\begin{aligned} &= 0.2 \times 57798 = 11560 \\ &+ 0.0017 \times -52089 = - 89 \\ & \qquad\qquad 11471 \text{ cals} \end{aligned}$$

$$\therefore \quad q = \frac{2 \times 11471}{1.987 \times 298} = 38.747$$

Now the equation for the R-H curve is

$$c\,(\theta - 1) = (v + 1)\,(p - 1) + q$$

or

$$\theta = \frac{(v + 1)\,(p - 1) + q}{c} + 1$$

$$= \frac{1.6 \times 10.335 + 38.747}{7.729} + 1$$

$$= 8.153$$

$$\therefore \quad T_2 = 2430^{o}K.$$

This was not in agreement with the originally assumed value of 2250°K, so a second value for T_2 had to be assumed, and 2430°K was chosen as the second approximation. The process was then repeated until the assumed and calculated values of θ corresponded. This occurred at $\theta = 8.496$, the corresponding value of p being 12.789.

$\therefore$ $v = 0.6$, $p = 12.789$ is a point on the R-H curve. For this point, the slope of the Rayleigh line

$$= \frac{p - 1}{1 - v} = \frac{11.789}{0.4}$$

$$= 29.473$$

Similar calculations were conducted for other values of v, and the slope of the Rayleigh line calculated for each. The minimum slope of 29.345 was found to occur when $v = 0.578$, $p = 12.384$.

$$\therefore \quad \gamma M^2 = 29.345.$$

Now the detonation velocity $= (RT_1 \gamma M^2 / M_1)^{\frac{1}{2}}$

$$= \left[\frac{8.314 \times 10^7 \times 298 \times 29.345}{0.9 \times 2.016 + 0.1 \times 32}\right]^{\frac{1}{2}} \text{ cm/sec.}$$

$$= 3813 \text{ m/sec.}$$

A.5.2. Calculated values:

TABLE A.5.1.

Steady state detonation velocities for various detonable gas mixtures initially at 25°C and one atmosphere pressure :

Reacting system	calculated γM^2	calculated velocity (m/sec.)
0.9 H_2 + 0.1 O_2 (forming H_2O)	29.345 ± 0.005	3813 ± 0.5
0.9 D_2 + 0.1 O_2 (forming D_2O)	28.385 ± 0.005	3170 ± 0.5
0.925 H_2 + 0.075 O_2 (forming H_2O)	24.770 ± 0.005	3800 ± 0.5
0.925 H_2 + 0.075 O_2 (forming H_2O_2)	8.675 ± 0.005	2245 ± 1.0

The calculated velocity values for the system 0.925% H_2 + 0.075% O_2 are compared with the experimentally determined values in Table 5.2, p. 104.